



**The Weather  
and Climate**

Emergent Laws and Multifractal Cascades

SHAUN LOVEJOY and DANIEL SCHERTZER

CAMBRIDGE

# Rocks, clouds, anisotropic multifractals and the unity of geophysics

Multifractal Analysis: From Theory to Applications and Back,  
Banff, Alberta, Feb, 25, 2014

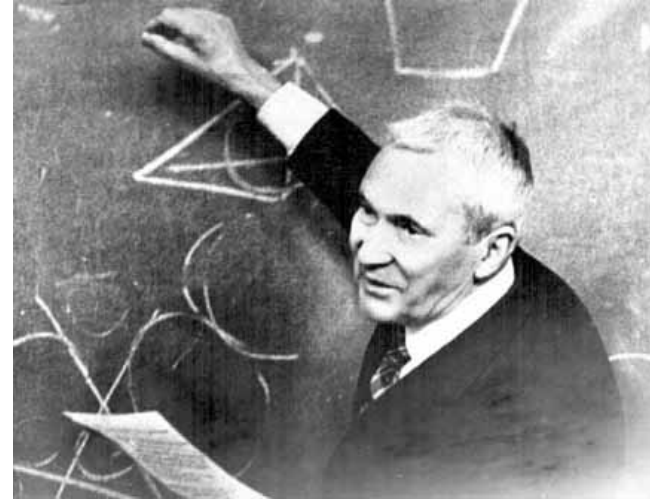
**S. Lovejoy McGill, Montreal**

# Pioneers of turbulence

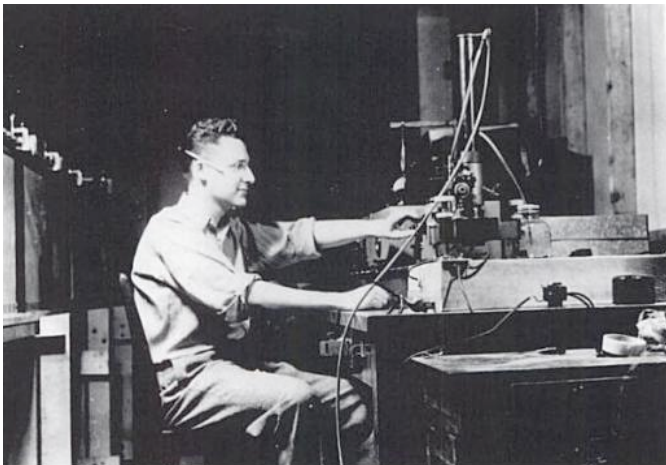
Richardson  
1881 - 1953



Kolmogorov  
1903 - 1987



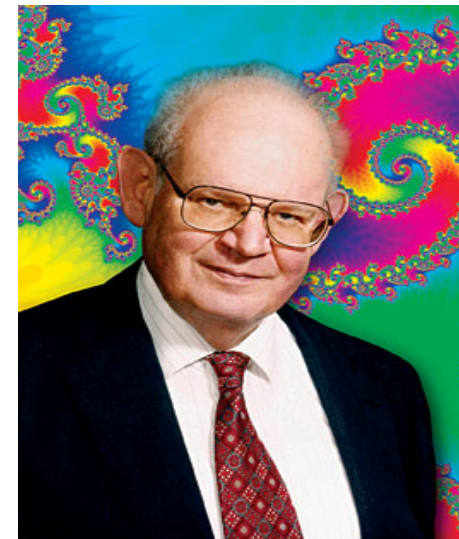
Corrsin  
1920 - 1986



Obukhov  
1918 - 1989



Mandelbrot  
1924-2010



# The emergence of atmospheric dynamics

Continuum mechanics

deterministic

Low level  
(fundamental)

Large Re



Laws of turbulence

Classical:

Richardson, Kolmogorov,  
Corrsin, Obukhov, Bolgiano

High level

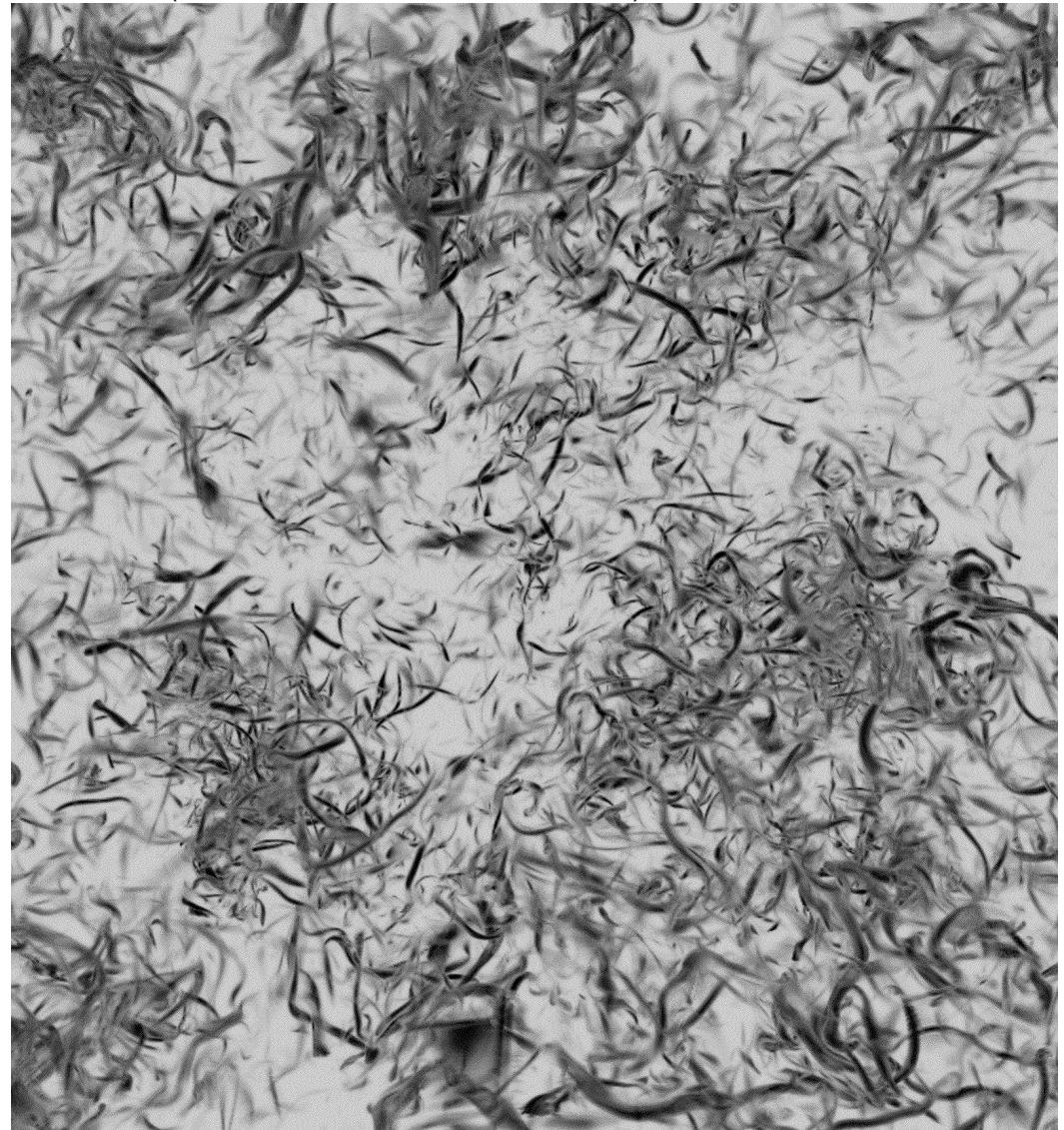
stochastic

$$\Delta v(\underline{\Delta r}) = \varphi |\underline{\Delta r}|^H$$

e.g. Kolmogorov  $\varphi = \varepsilon^{1/3}$ ,  $H = 1/3$

## Vortices in strongly turbulent fluid

(M. Wiczek, numerical simulation, 2010)



a)  $|\underline{\Delta r}| \ll 100m$     b) isotropic

c)  $\varphi \approx \text{constant}$ , quasi Gaussian

# Emergent Turbulence laws

$$\text{Fluctuations} \approx (\text{turbulent flux}) \times (\text{scale})^H$$

Differences,  
tendencies,  
wavelet  
coefficients

Cascading  
Turbulent flux

Anisotropic  
Space-time  
Scale function

Fluctuation  
exponent

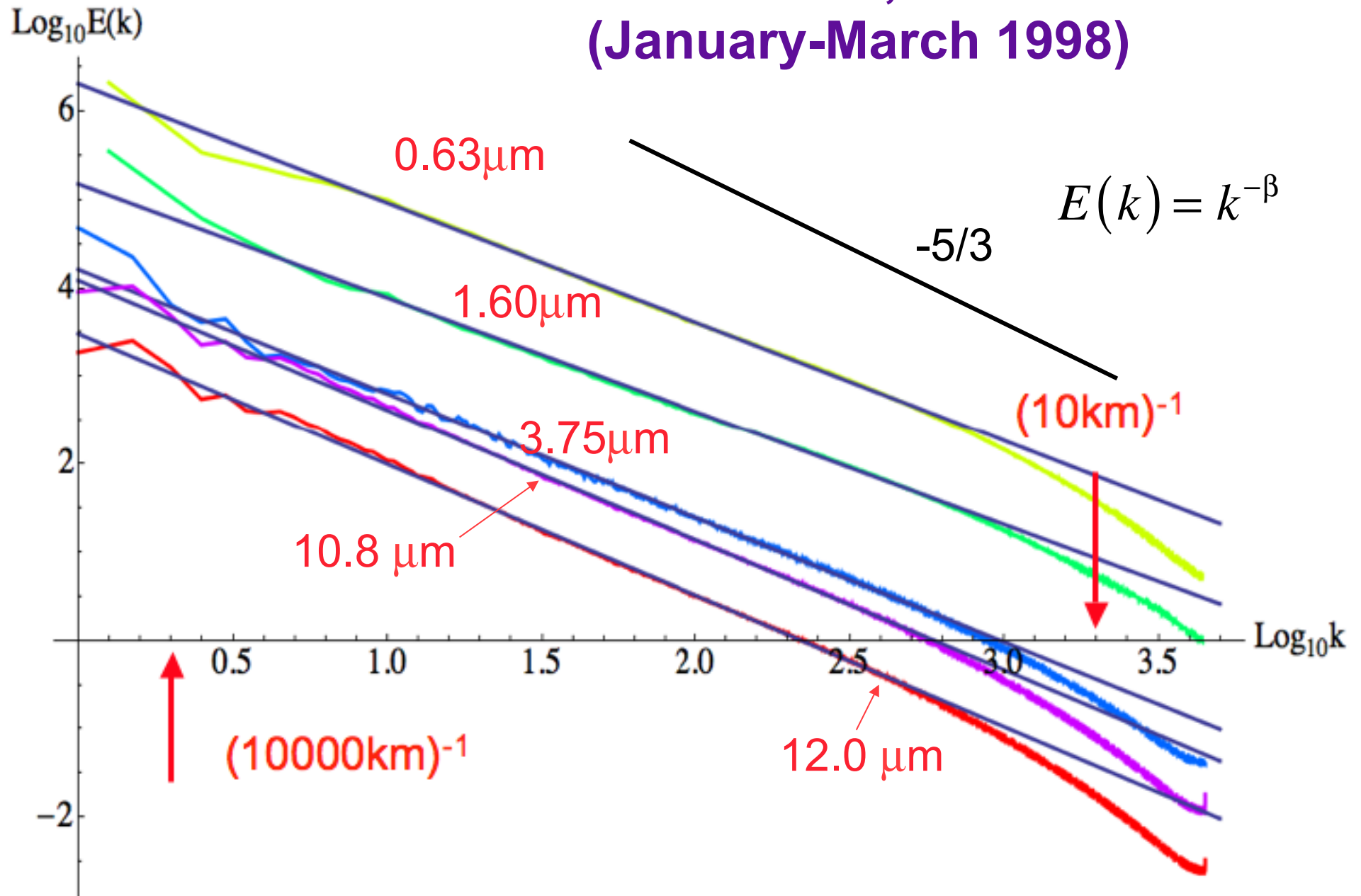


The unity of clouds  
and rocks:

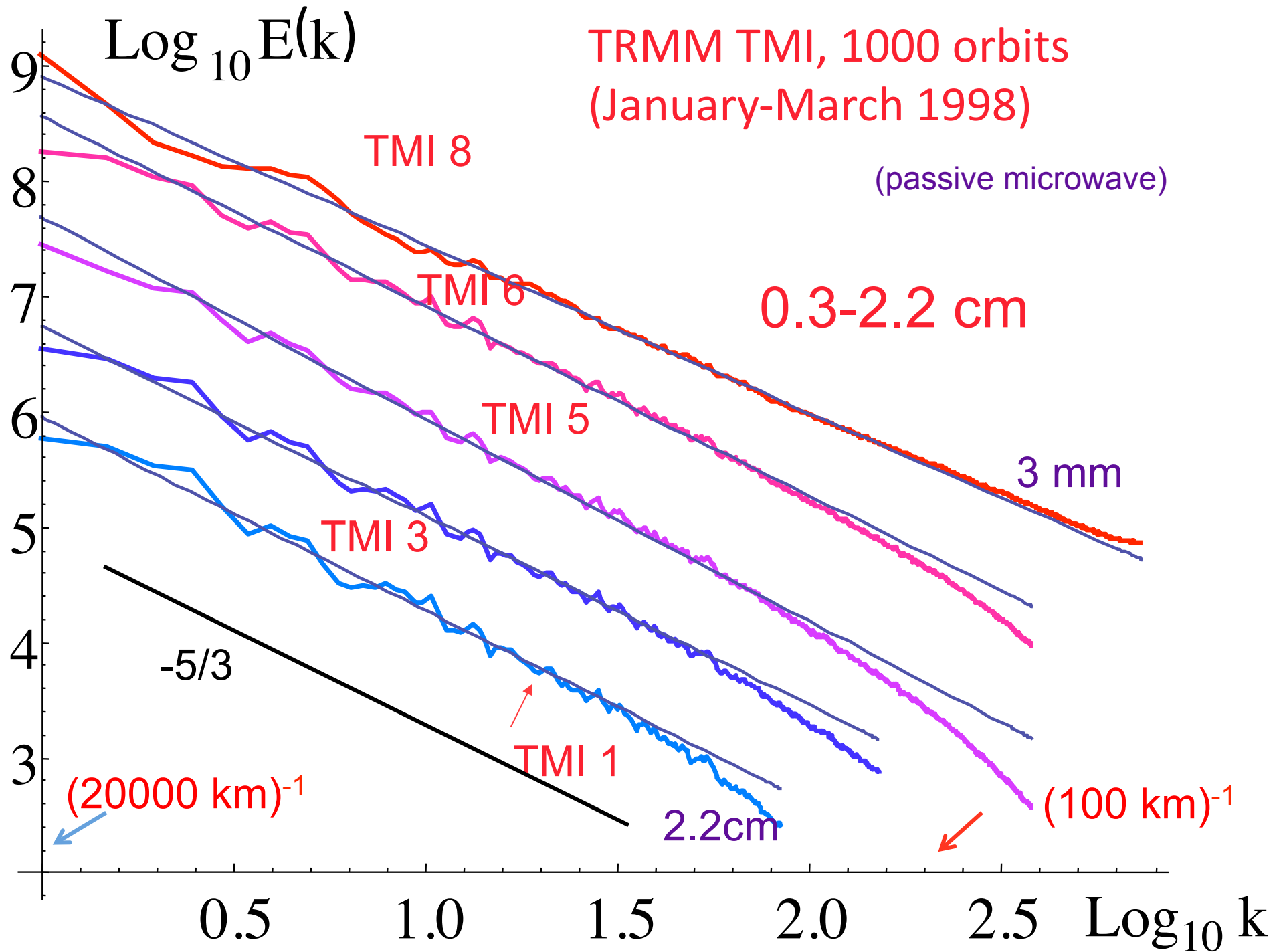
Scaling

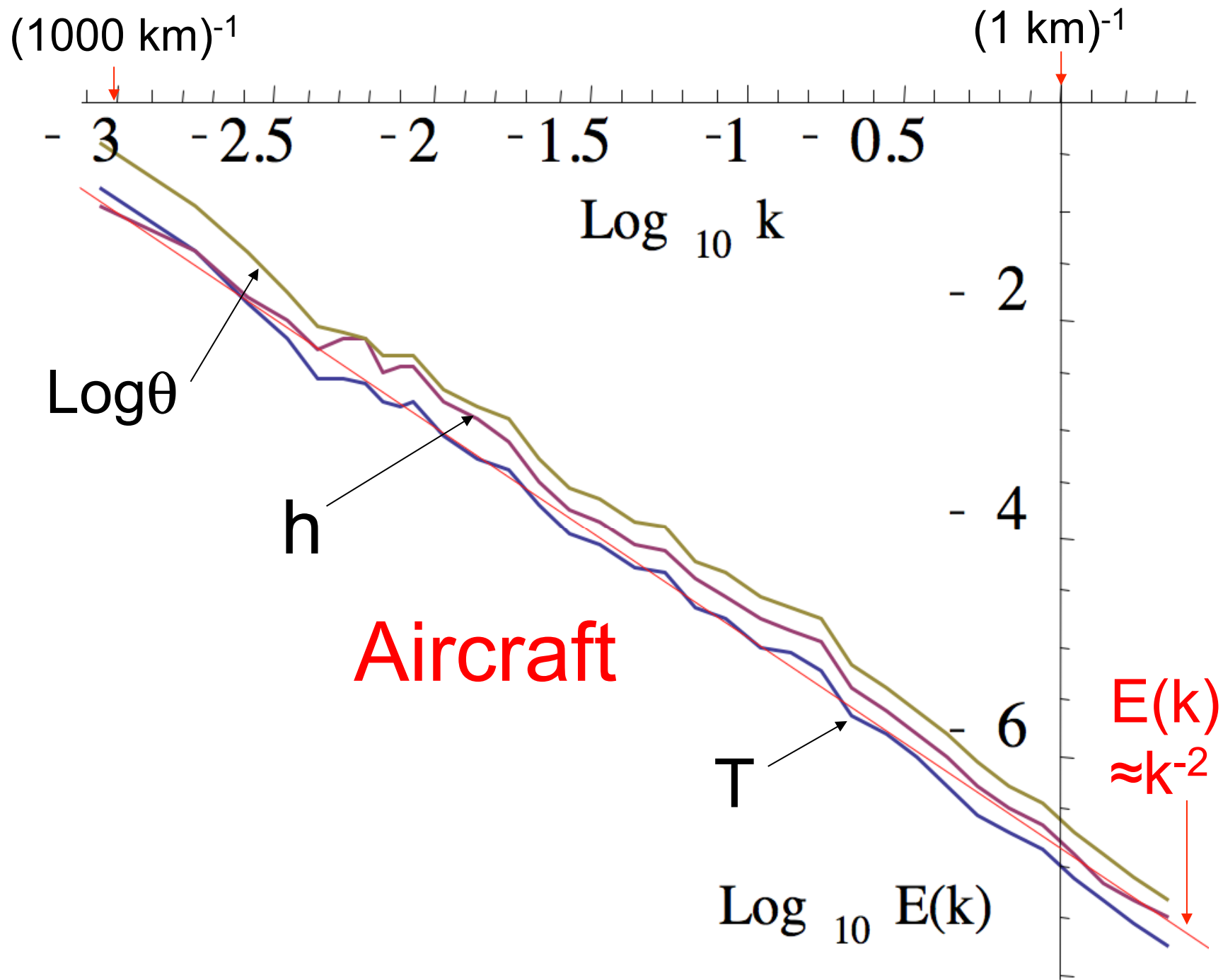
Multifractal simulation

# TRMM VIRS, 1000 orbits (January-March 1998)



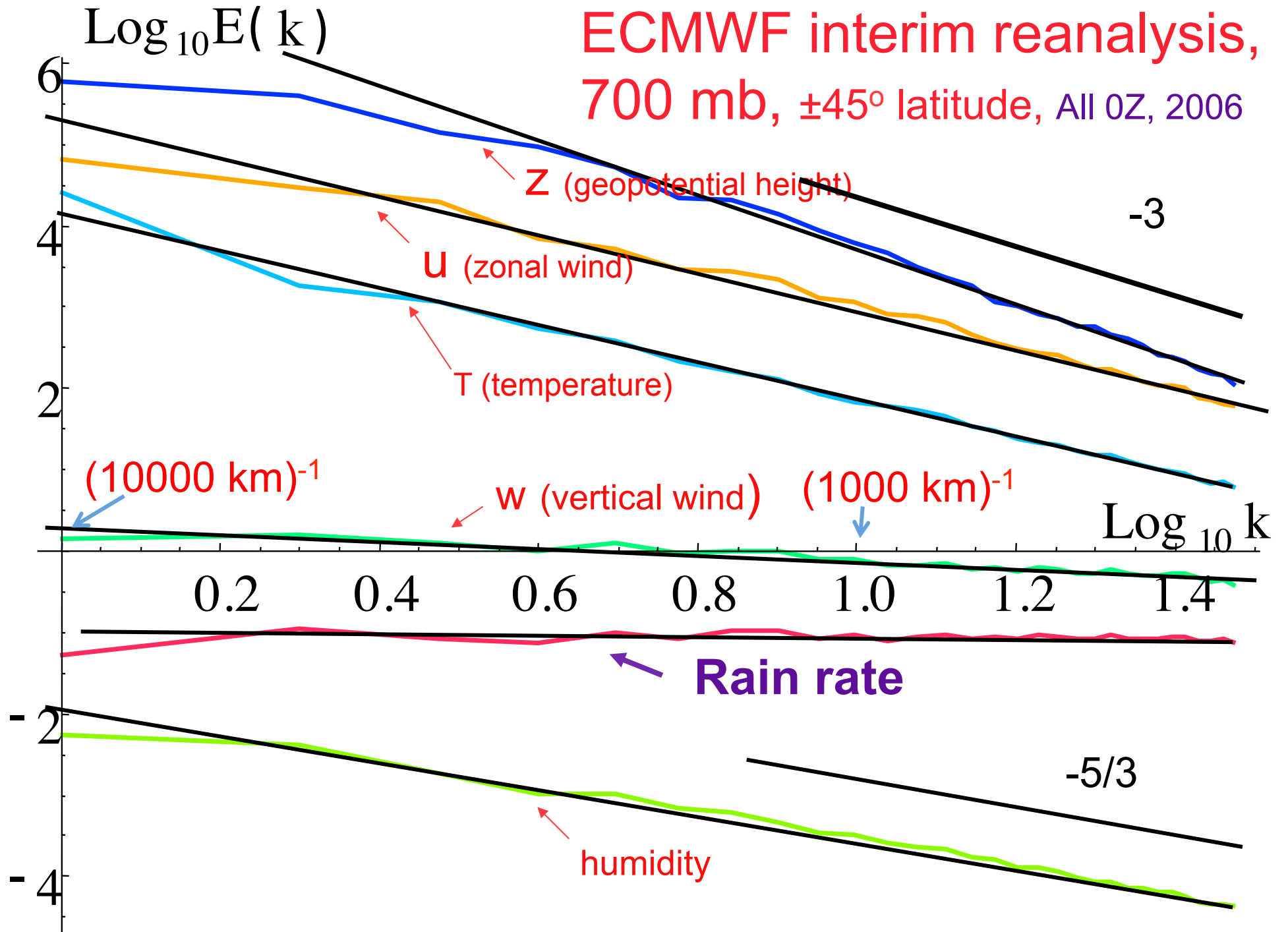
Visible, near infra red, thermal infra red



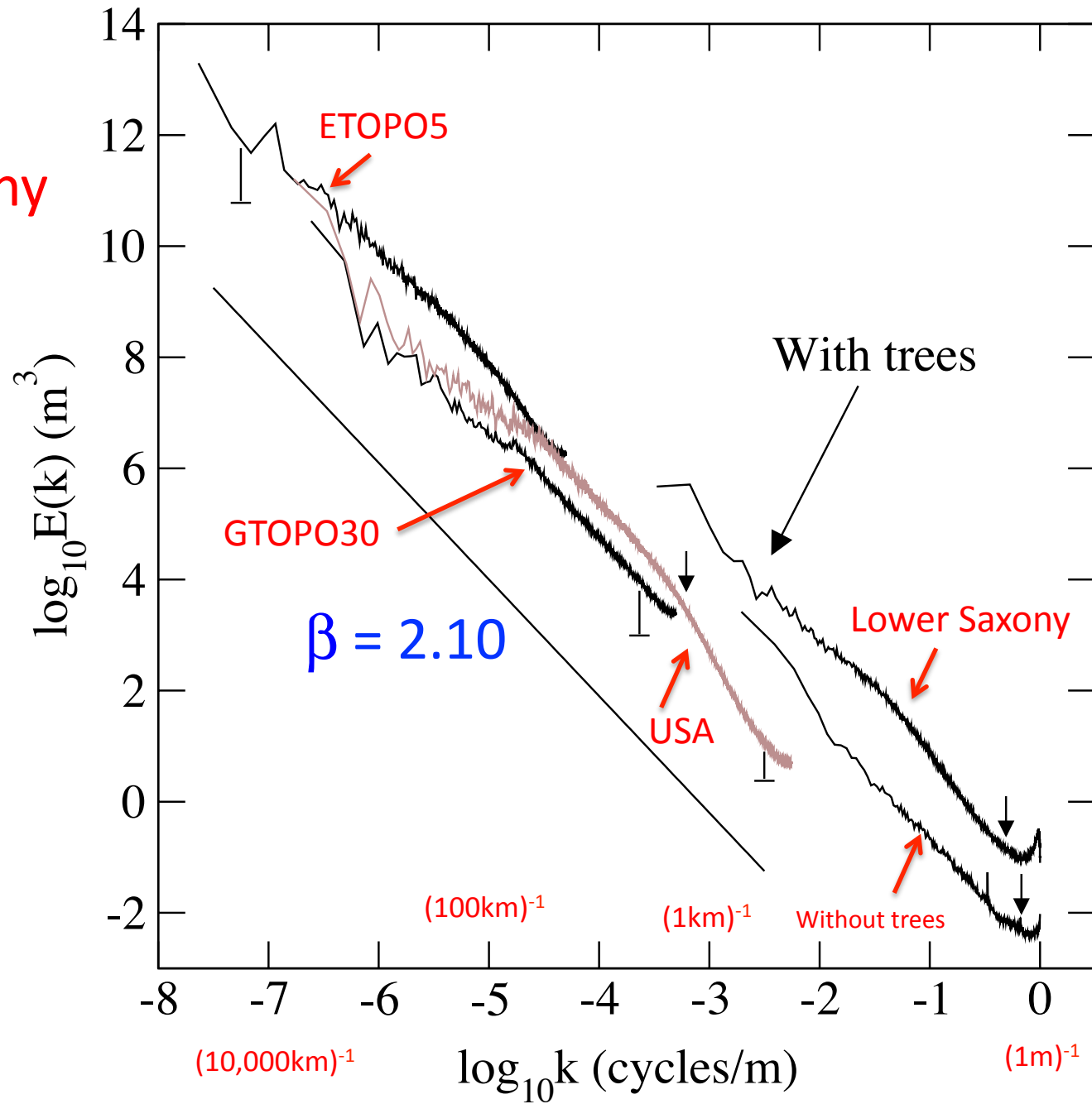




ECMWF interim reanalysis,  
700 mb,  $\pm 45^\circ$  latitude, All OZ, 2006

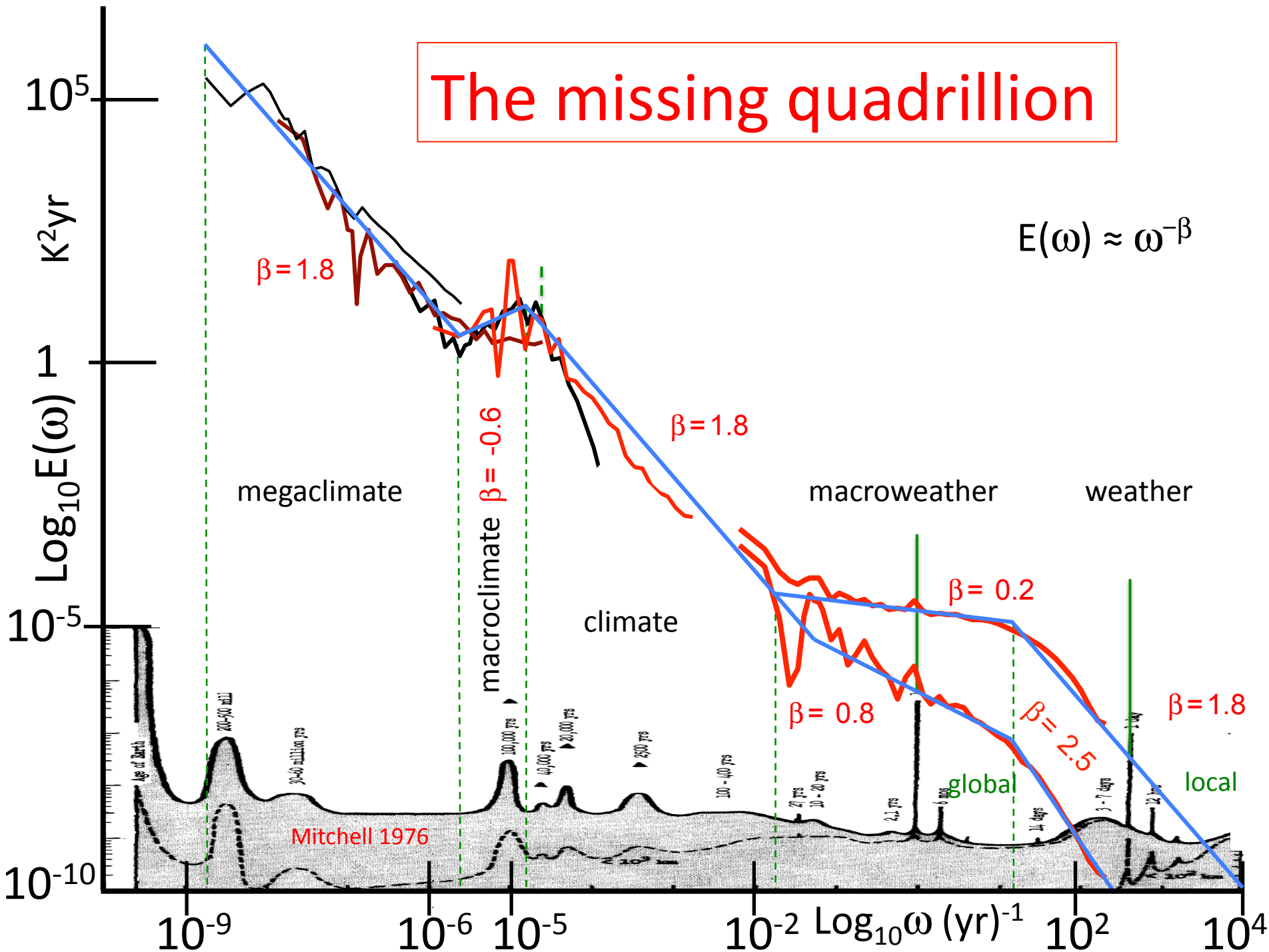


# Topography



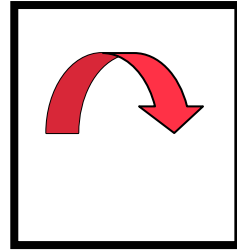
# Temporal scaling

# The missing quadrillion



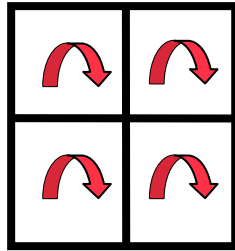
# CASCADES

(isotropic)

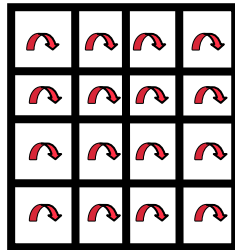


Parent eddy

Homogeneous

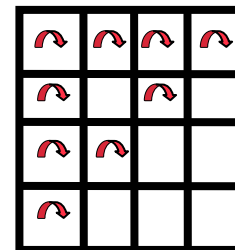
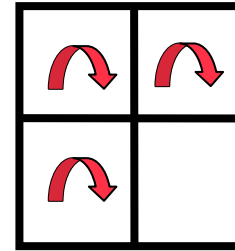


Daughter eddies



Grand-daughter eddies

Intermittent



# Multiplicative Cascades

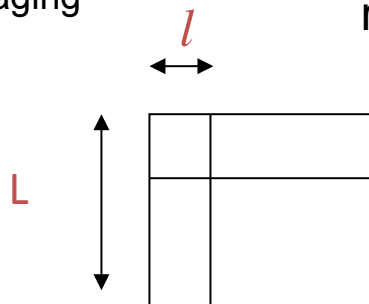
Generic statistical behaviour:

scaling Scale invariant

$$\langle \varepsilon_\lambda^q \rangle \approx \lambda^{K(q)}$$

Statistical averaging

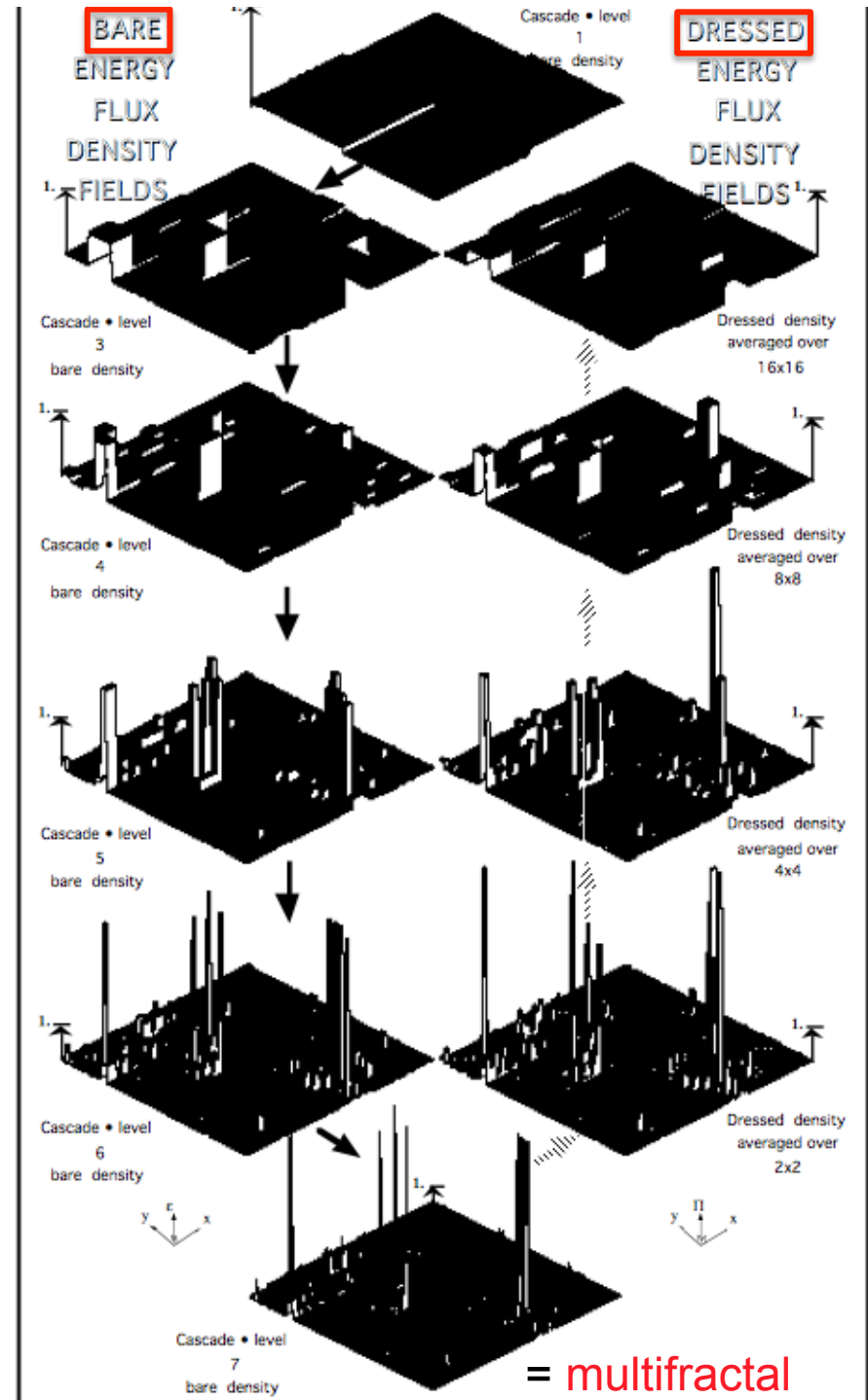
Resolution: ratio  $\lambda=L/l$



Probabilities:

$$\Pr(\varepsilon_\lambda > \lambda^\gamma) \approx \lambda^{-c(\lambda)}$$

No pointwise convergence - no Hölder exponents (hence bare-dressed)



# Codimension and dimension multifractal formalisms

## Codimension

(densities of measures, stochastic)

### Singularities

$$\varepsilon_\lambda = \lambda^\gamma$$

## Dimension

(measures, deterministic)  $l = \lambda^{-1}$   $vol(B_\lambda) = \lambda^{-d}$

$$\Pi_\lambda = \int_{B_\lambda} \varepsilon_\lambda d^d \underline{x} = \lambda^{-\alpha_d}$$

$$\Pi_\lambda = \varepsilon_\lambda vol(B_\lambda) = \lambda^{\gamma-d}$$

$$\alpha_d = d - \gamma$$

### Probabilities

$$\Pr(\varepsilon_\lambda = \lambda^\gamma) \approx \lambda^{-c(\gamma)}$$

( $c \geq 0$ )

Probabilistic  
definition

$$Number(\Pi_\lambda = \lambda^{-\alpha_d}) = \lambda^{f_d(\alpha_d)}$$

$$Number = \lambda^d \Pr$$

( $d \geq f_d \geq 0$ )

$$f_d(\alpha_d) = d - c(\gamma)$$

### Statistical Moments

$$\langle \varepsilon_\lambda^q \rangle = \lambda^{K(q)}$$

$$\sum_{i=1}^{\lambda^d} \Pi_{\lambda,i}^q = \lambda^{-\tau_d(q)}$$

$$\sum_{i=1}^{\lambda^d} \Pi_{\lambda,i}^q = \left\langle \sum_{i=1}^{\lambda^d} (\lambda^{-d} \varepsilon_\lambda)^q \right\rangle = \lambda^{d(q-1)} \langle \varepsilon_\lambda^q \rangle = \lambda^{K(q)-d(q-1)}$$

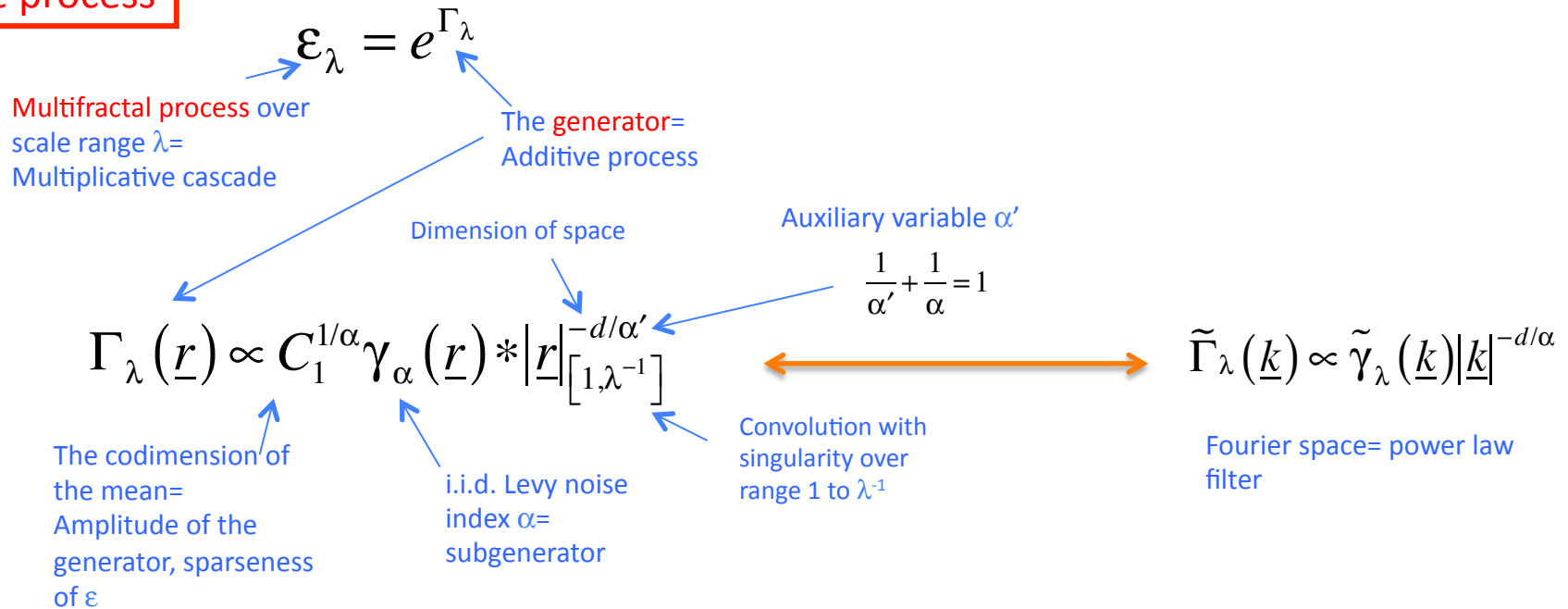
$$\tau_d(\alpha_d) = d(q-1) - K(q)$$

$$c(\gamma) \stackrel{L.T.}{\leftrightarrow} K(q); \quad f_d(\alpha_d) \stackrel{L.T.}{\leftrightarrow} \tau(q)$$

# Multiplicative cascade processes

## The process

(canonical conservation of flux)



## The statistics

$$\langle \varepsilon_\lambda^q \rangle = \lambda^{K(q)}$$

General multifractal statistics, convex  $K(q)$

$$K(q) = \frac{C_1}{\alpha - 1} (q^\alpha - q)$$

$$q < q_D \quad 0 \leq \alpha \leq 2$$

Universal multifractals ("multiplicative central limit theorem", Schertzer Lovejoy 1987)

$$\Pr(\varepsilon_\lambda > s) \approx s^{-q_D}$$

$$s \gg 1$$

Extremes: "Fat tails"  
Mandelbrot 1974



# Fractionally Integrated Flux

(FIF) model (both additive and multiplicative)

## The process

$$I(\underline{r}) = \varepsilon_\lambda(\underline{r}) * |\underline{r}|^{-(d-H)} \longleftrightarrow \tilde{I}(\underline{k}) = \tilde{\varepsilon}_\lambda(\underline{k}) |\underline{k}|^{-H}$$

Convolution=  
fractional integration  
order H

Fourier space= power  
law filter

## The statistics

$$S_q(\underline{\Delta r}) = \langle \Delta I(\underline{\Delta r})^q \rangle = \langle \varepsilon_\lambda^q \rangle |\underline{\Delta r}|^{qH} = |\underline{\Delta r}|^{\xi(q)} \quad \xi(q) = qH - K(q)$$

q<sup>th</sup> order  
structure  
function

fluctuation

Note:

$$\lambda = L / |\underline{\Delta r}|$$

$$\langle \varepsilon_\lambda^q \rangle = \lambda^{K(q)}$$

structure  
function  
exponent



The unity of clouds and  
rocks:

Multifractality

Multifractal simulation

# Early evidence of cascades: Precipitation 1987

(70 Radar Scans, Montreal, horizontal 3 weeks of rain data)

$$M = \frac{\langle Z_\lambda^q \rangle}{\langle Z \rangle^q}$$

Schertzer and Lovejoy 1987



Large scales

?

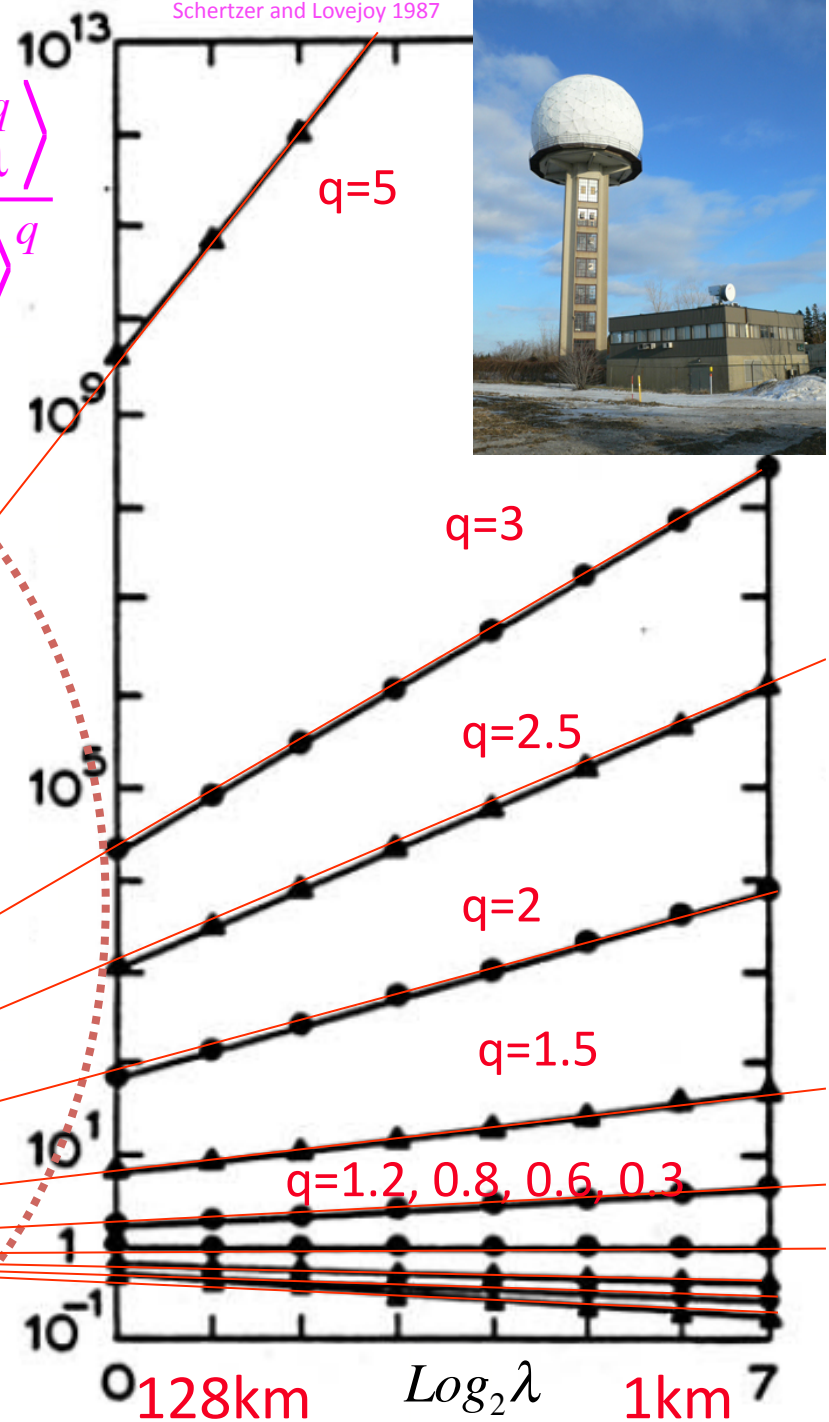
?

32,000km

Cascade prediction:

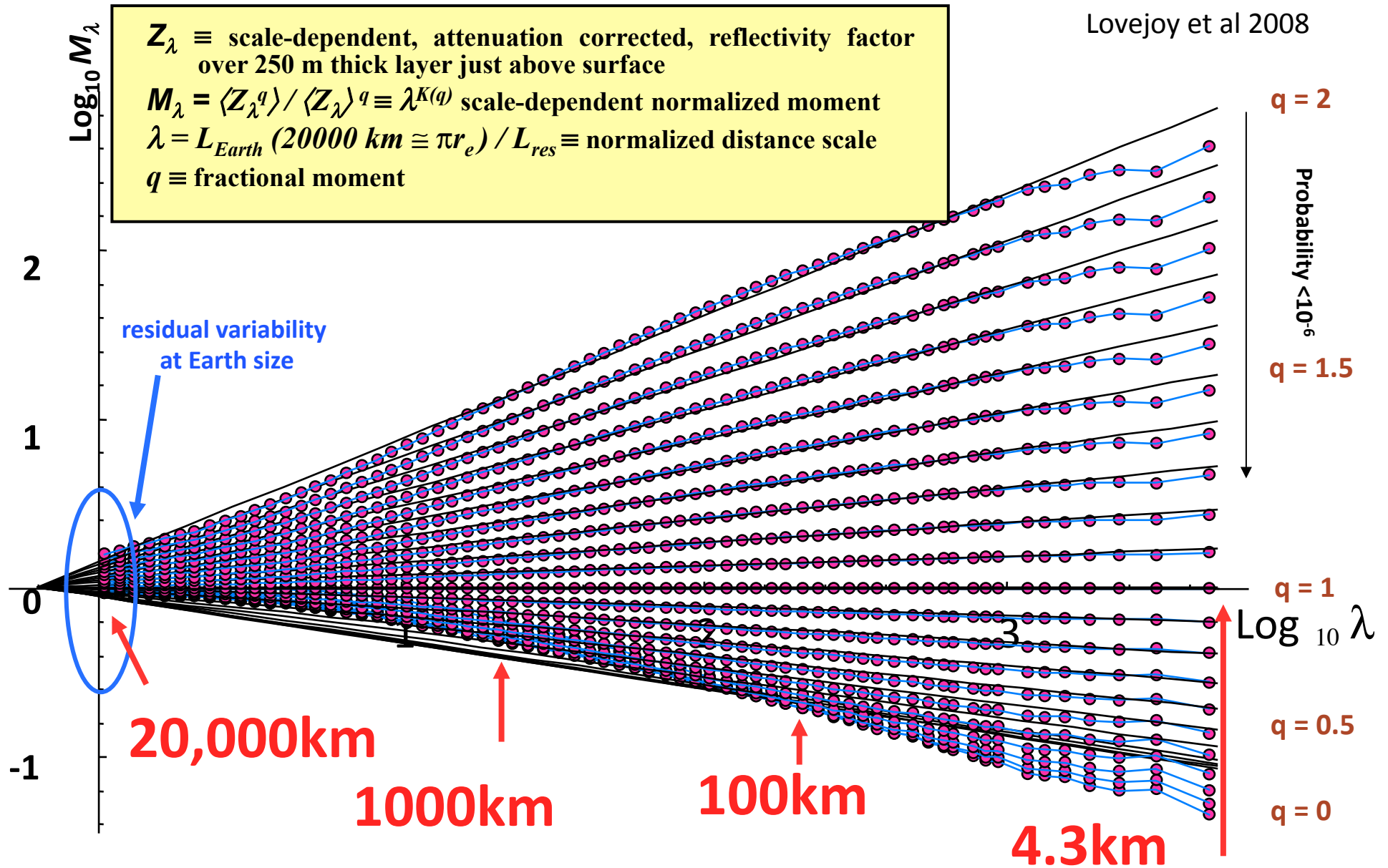
$$\langle Z_\lambda^q \rangle / \langle Z_1 \rangle^q = \lambda^{K(q)}$$

$$\lambda = L_{\text{eff}} / L_{\text{res}}$$



# Scale-dependent TRMM PR Attenuation Corrected Reflectivity Factor [ $Z_\lambda$ ] (1176 consecutive orbits -- ~70 days)

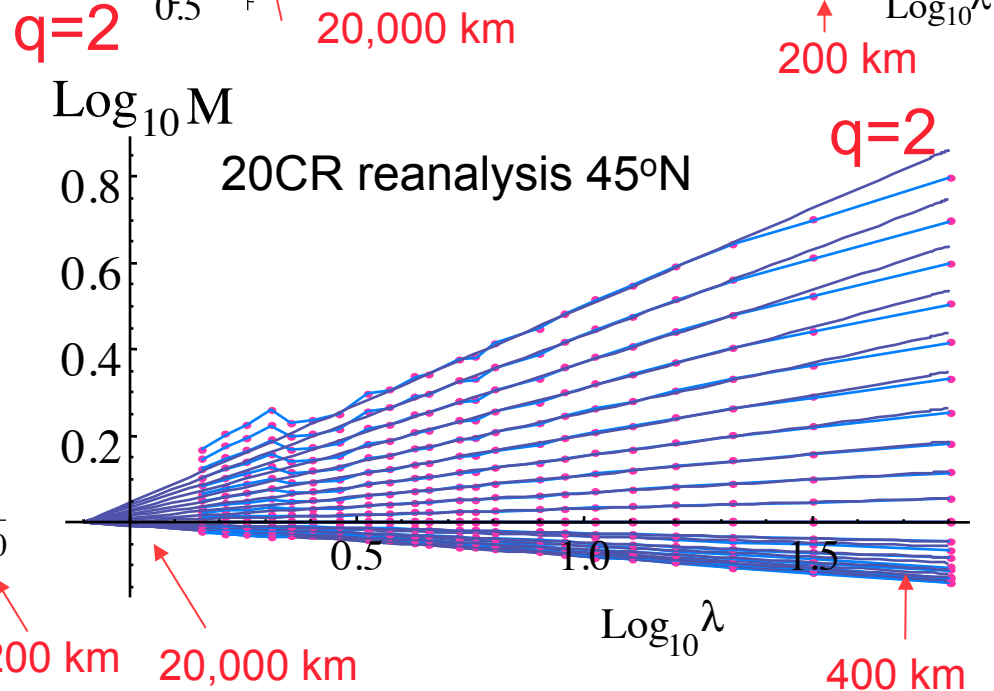
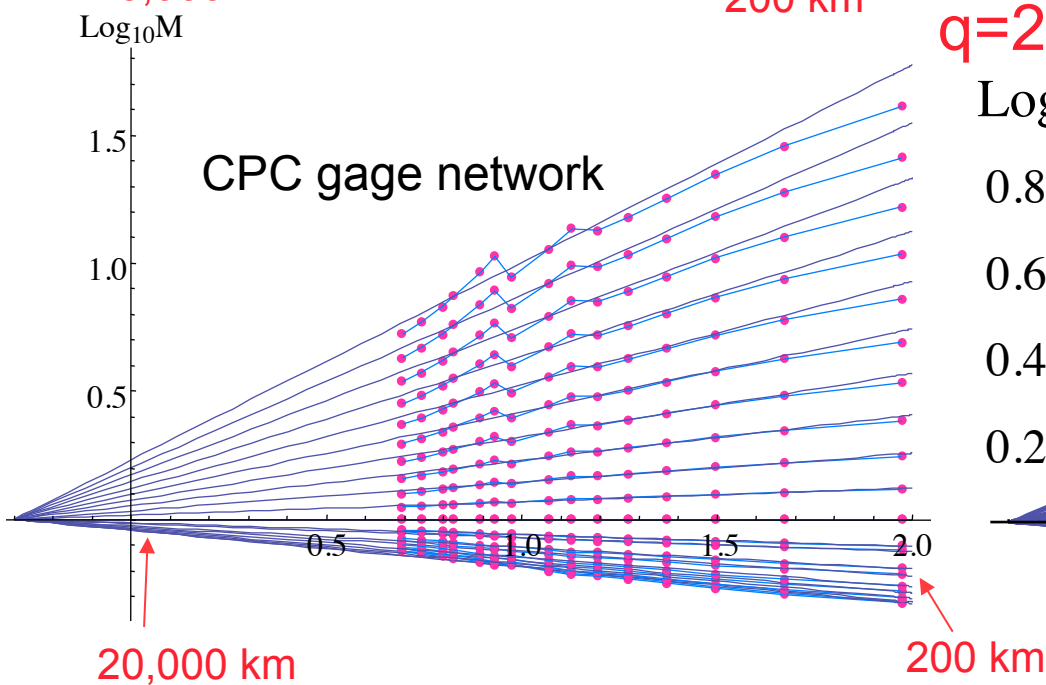
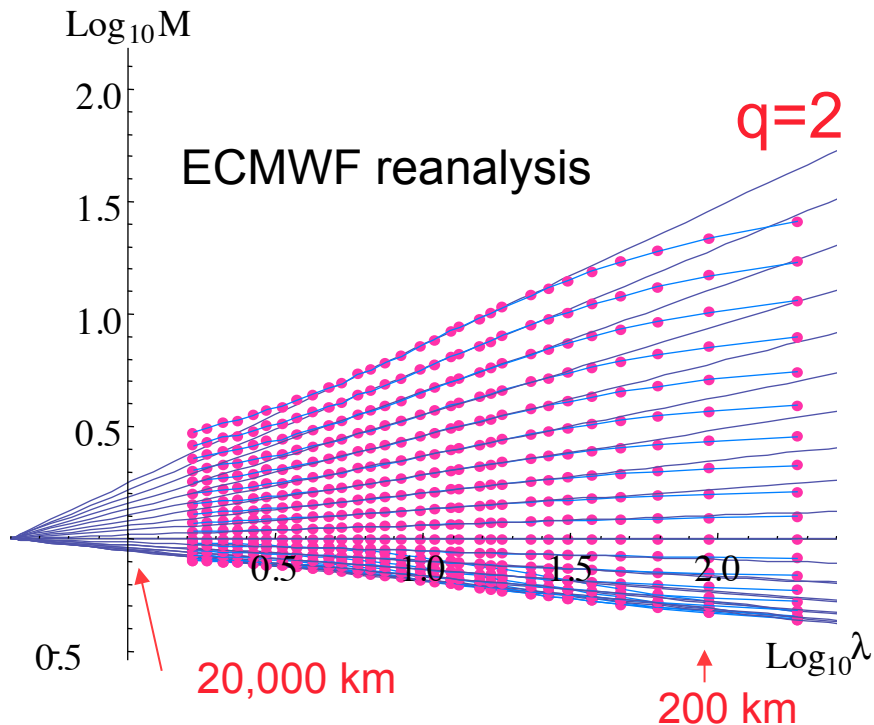
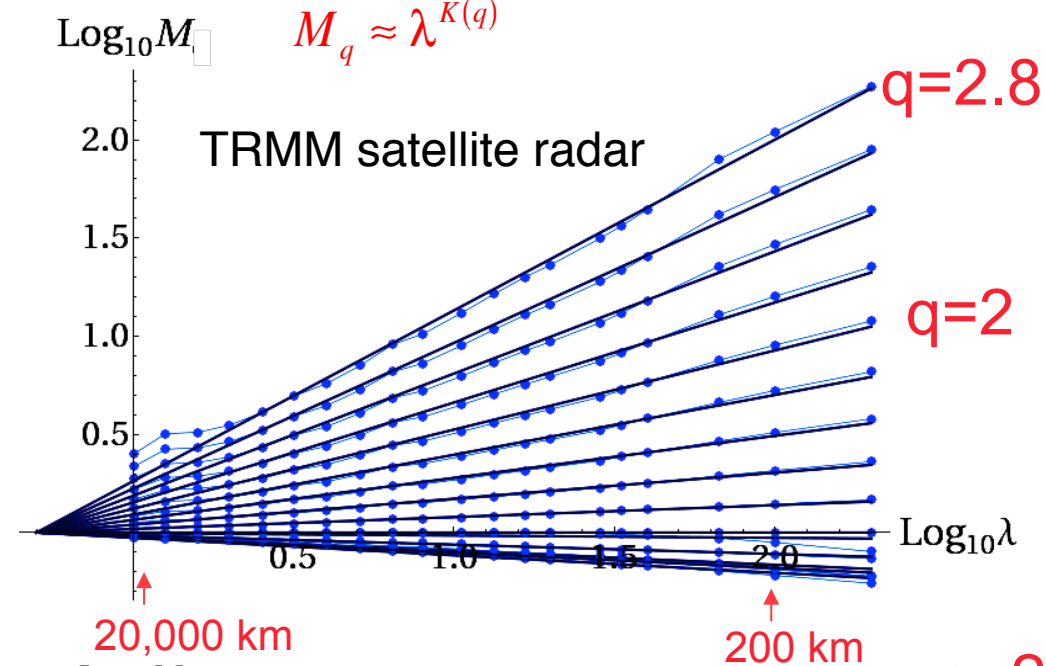
Lovejoy et al 2008



# Rainrates East-West

$$M = \langle \phi_\lambda^q \rangle / \langle \phi \rangle^q$$

$$M_q \approx \lambda^{K(q)}$$



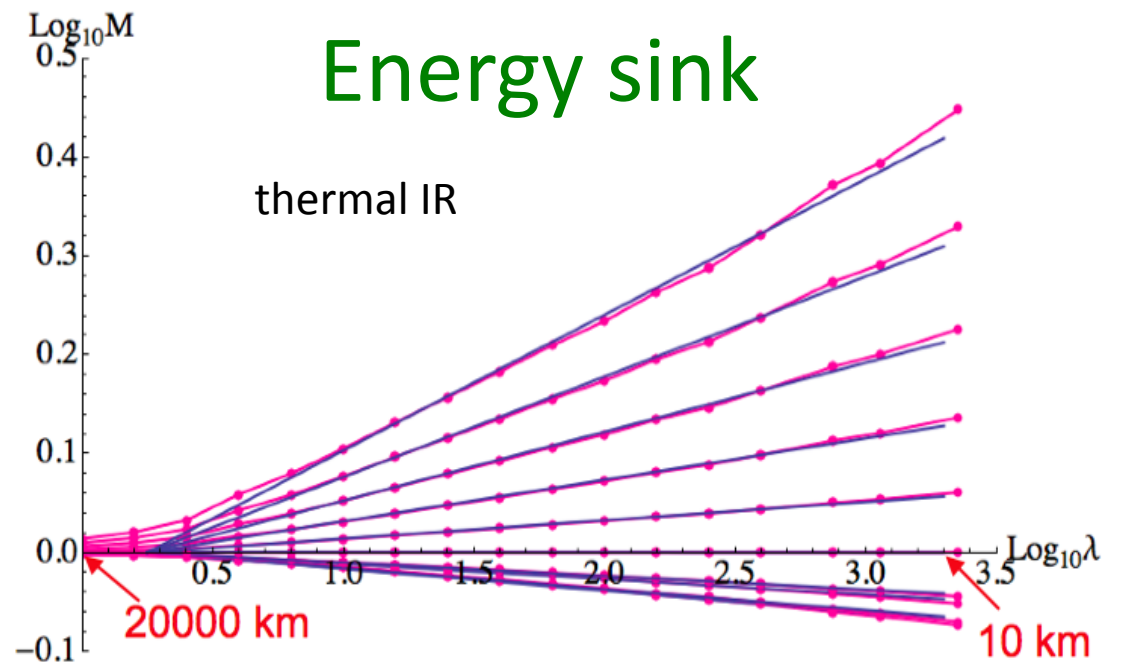
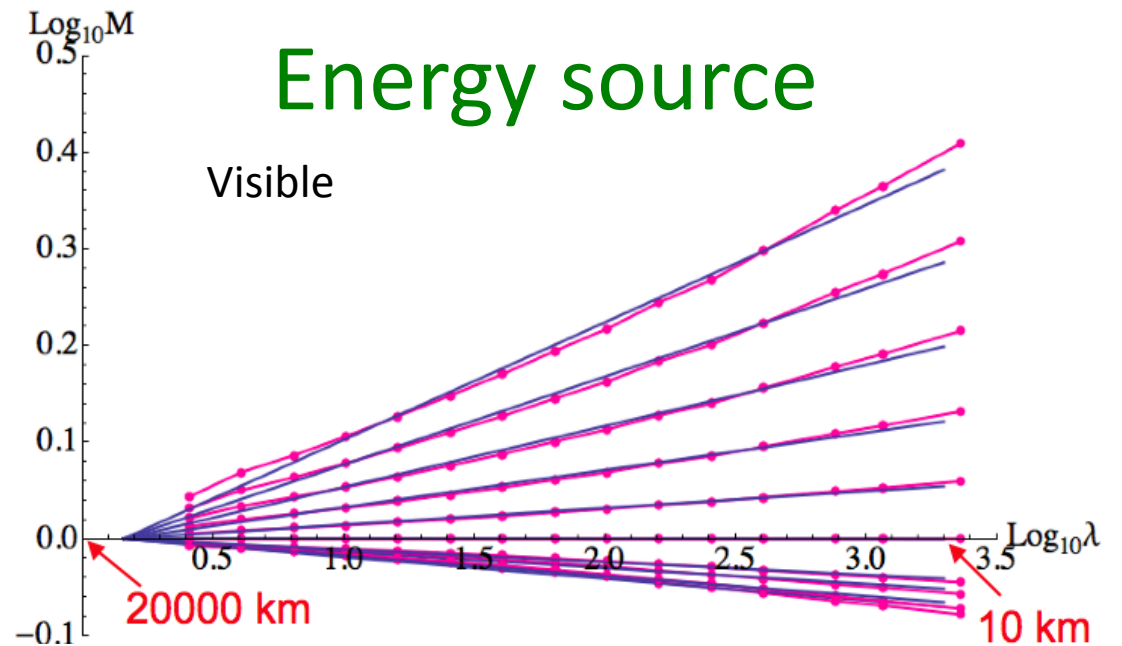
# Satellite radiances:

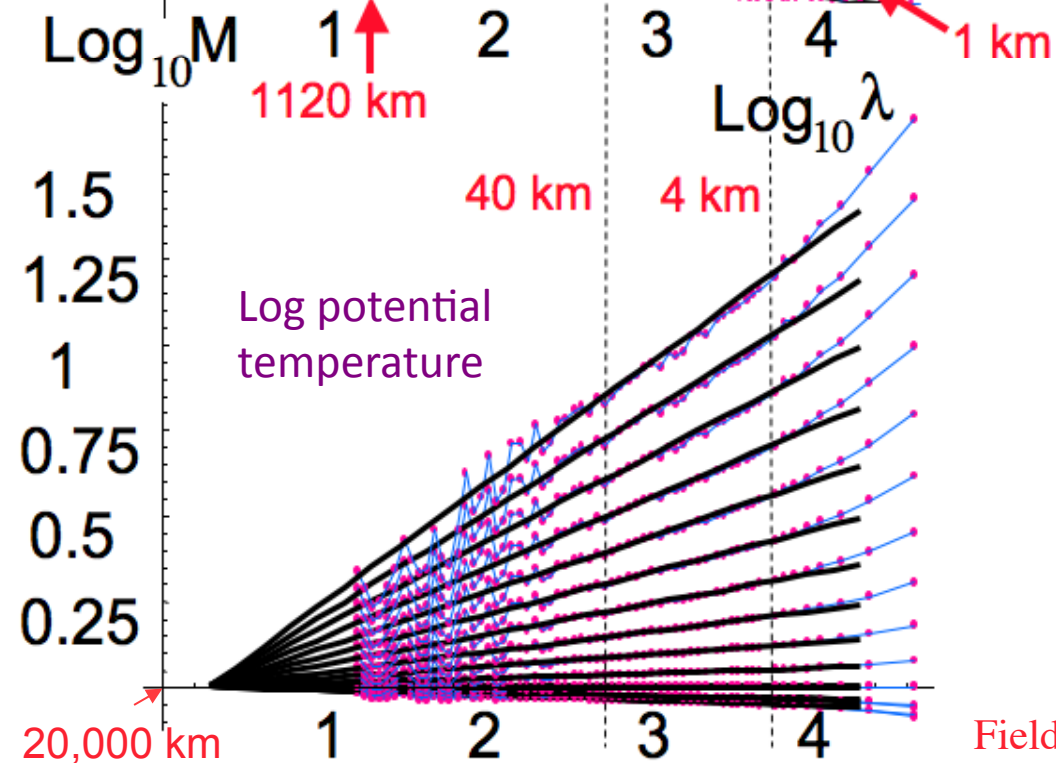
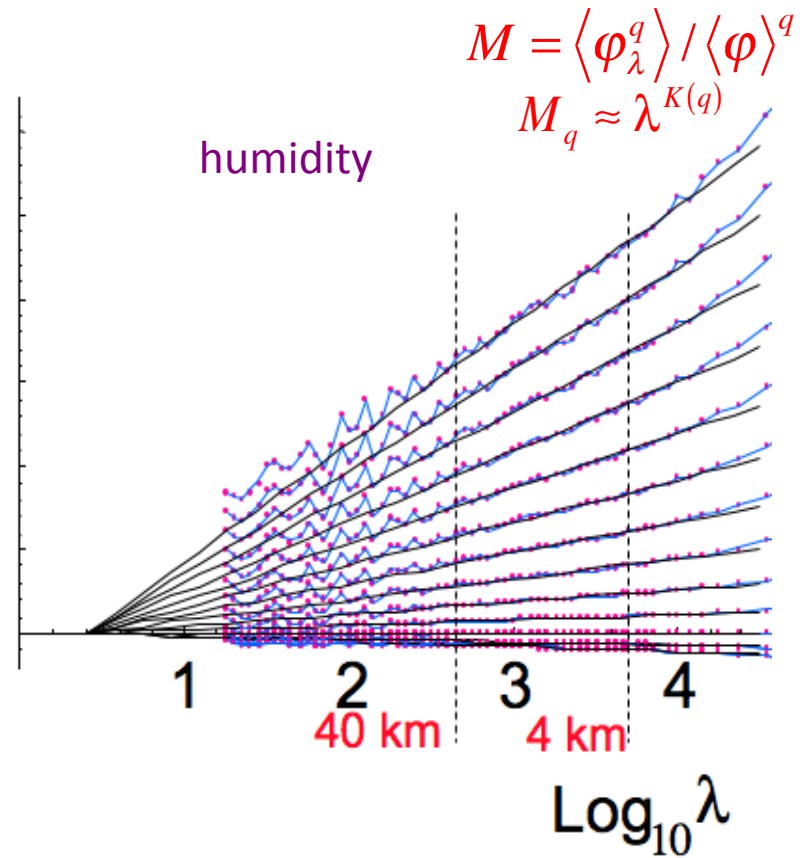
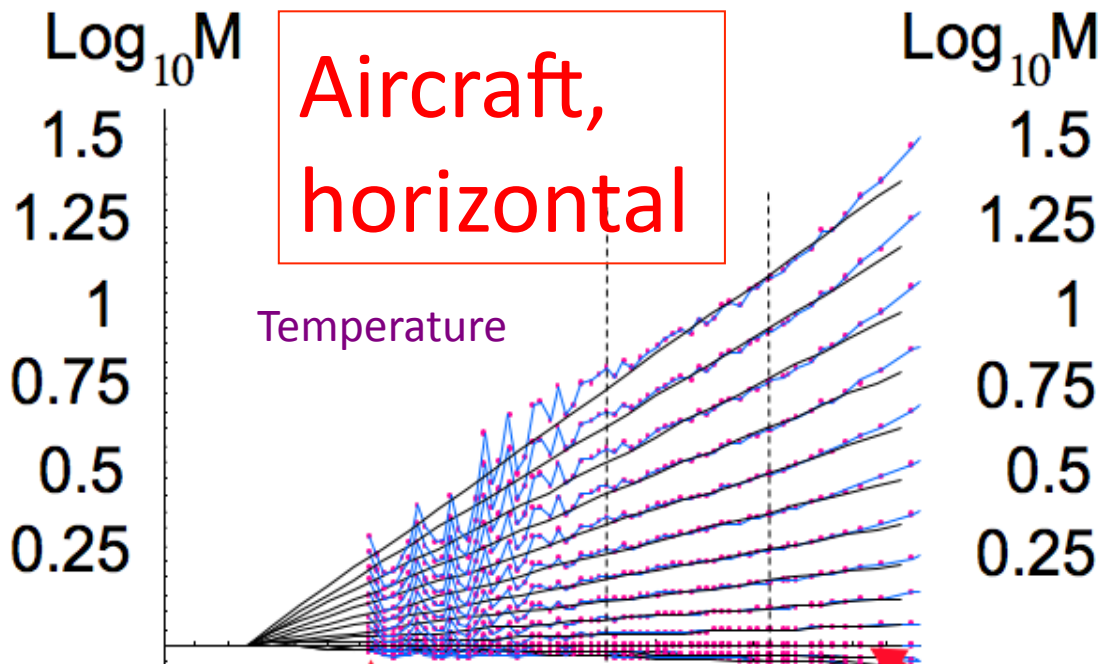
## Energy budget

TRMM satellite data,  $\approx 1000$   
orbits

$$M = \langle \varphi_\lambda^q \rangle / \langle \varphi \rangle^q$$
$$M_q \approx \lambda^{K(q)}$$

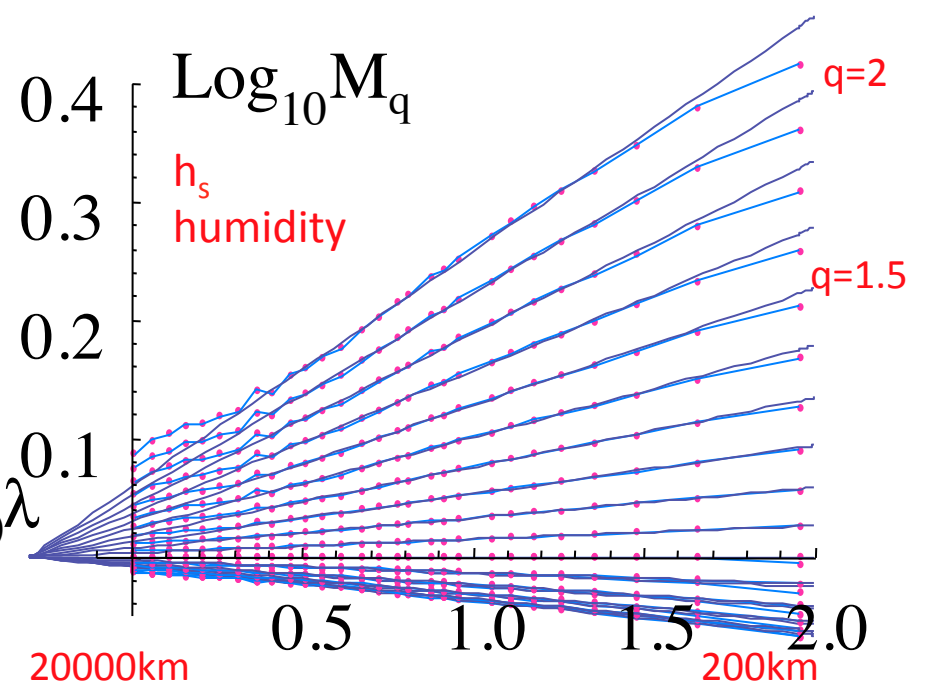
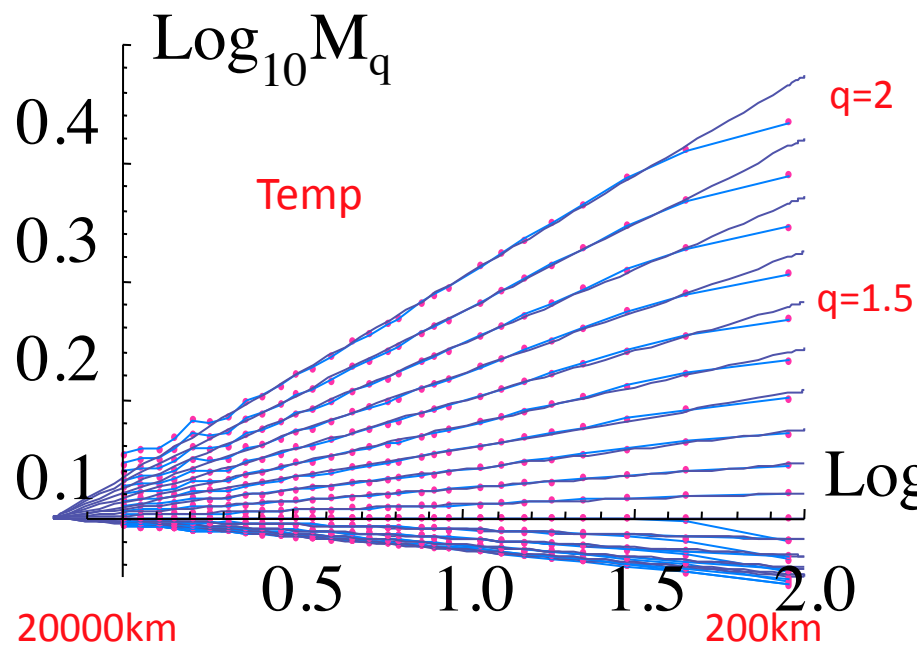
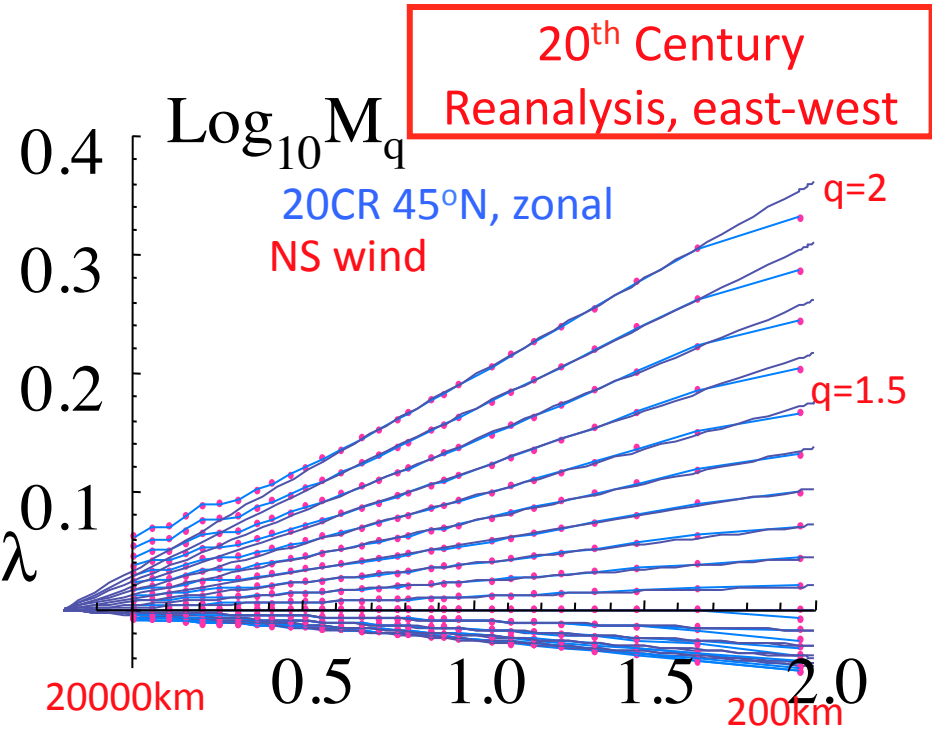
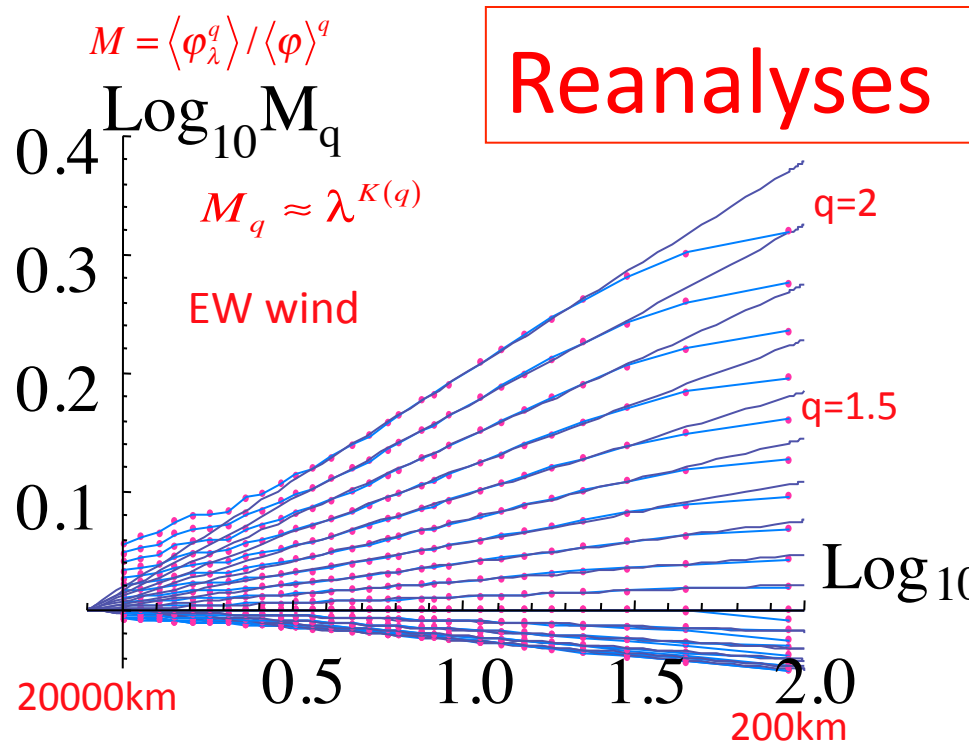
Lovejoy et al 2009





From 24 aircraft legs (altitude 11-13km)

Fields that are relatively unaffected by the trajectories





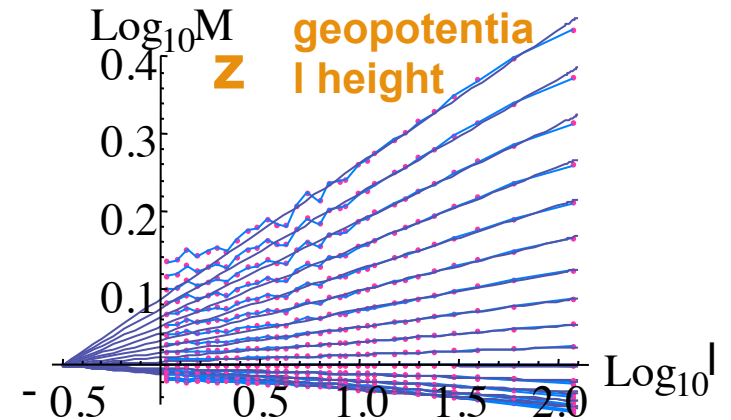
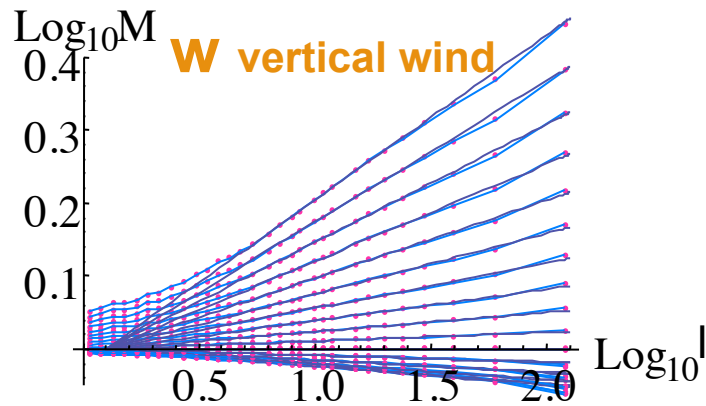
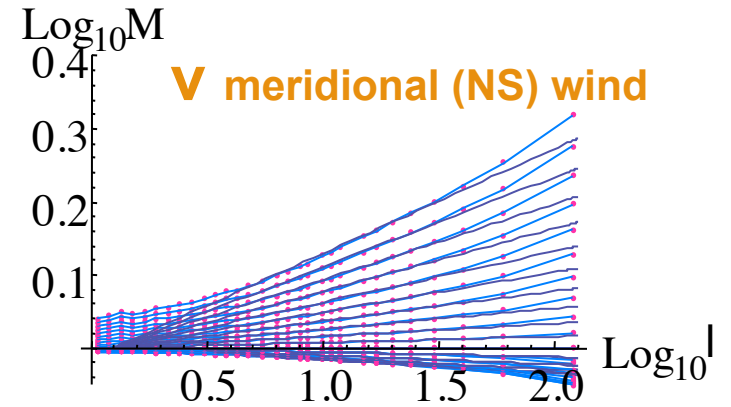
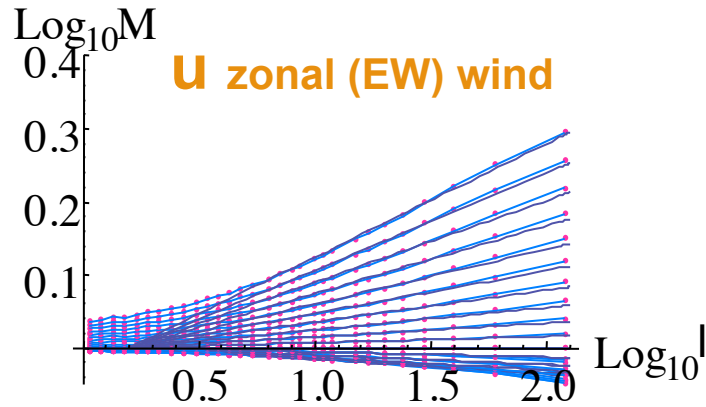
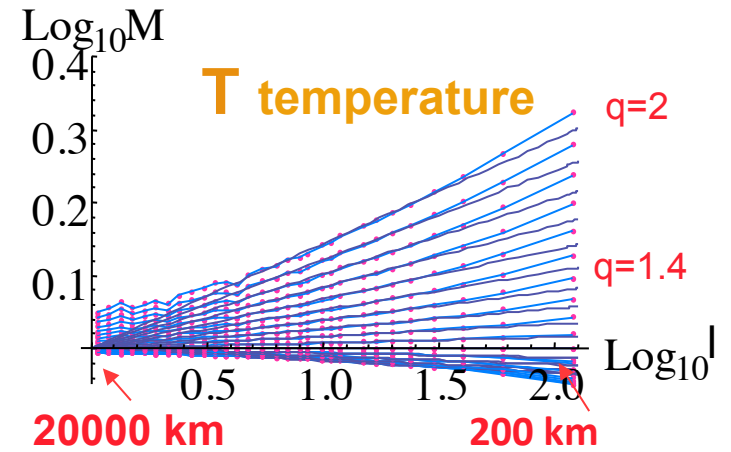
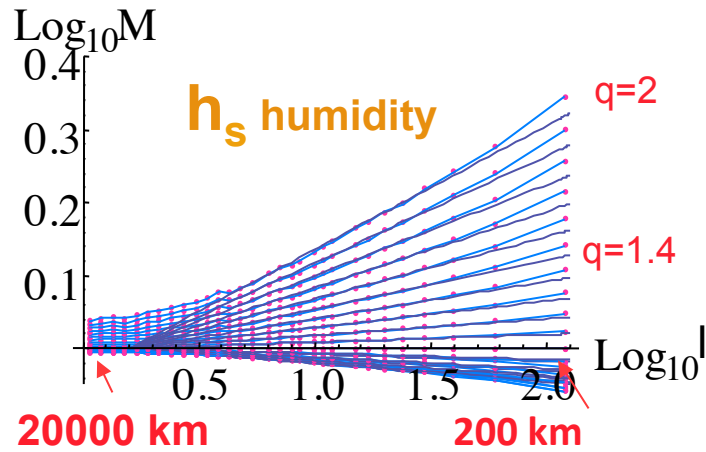
# Reanalyses

ECMWF  
reanalysis

East-West  
(2006, OZ, 700 mb)

$$M = \langle \varphi_{\lambda}^q \rangle / \langle \varphi \rangle^q$$

$$M_q \approx \lambda^{K(q)}$$



# Weather models:

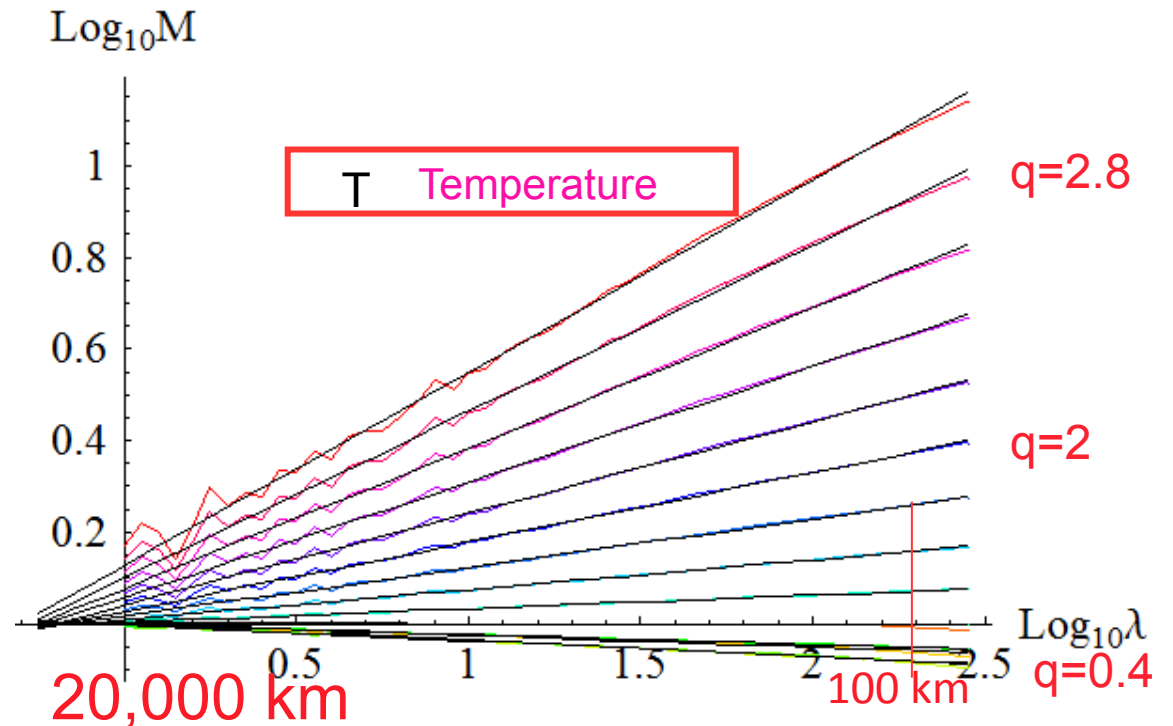
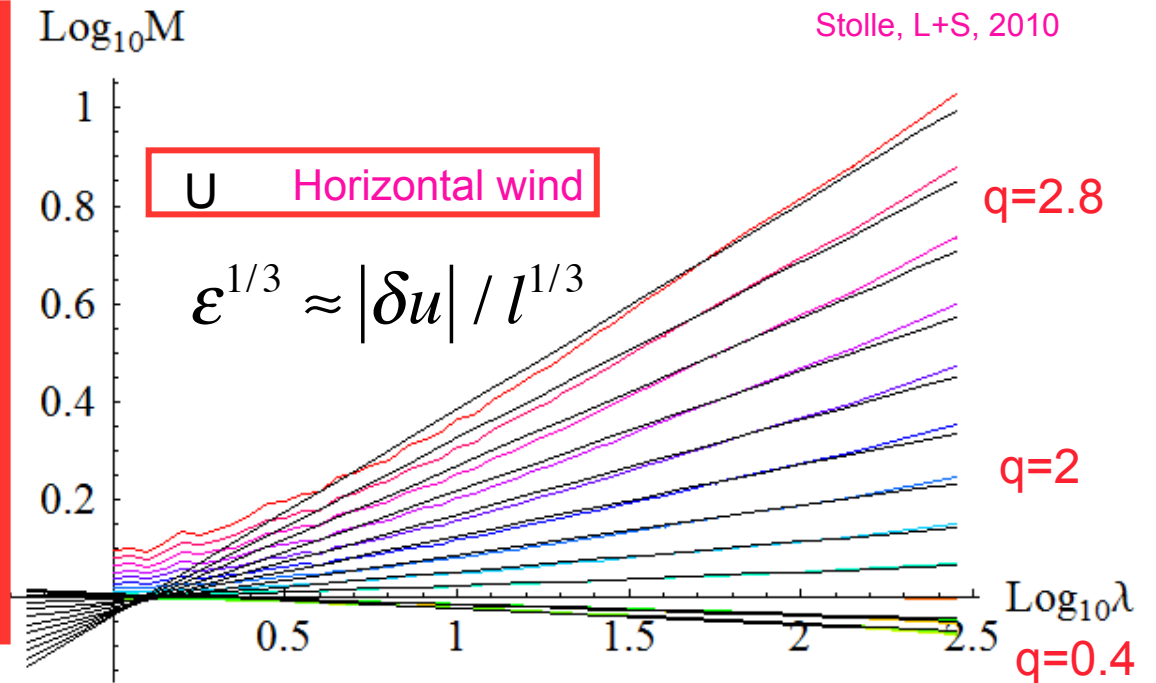
## Global GEMS Model 00h

Analysis of four months U,T at 1000 mb

(48 h forecasts are almost the same)

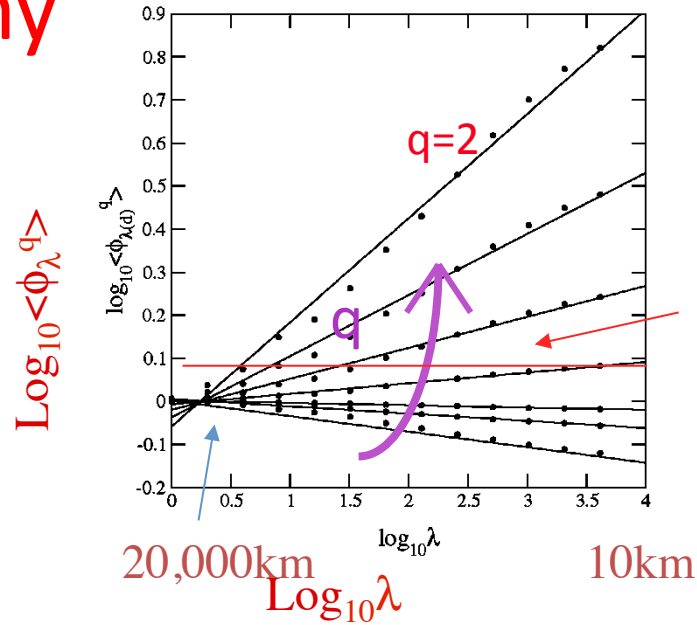
$$M = \langle \varphi_\lambda^q \rangle / \langle \varphi \rangle^q$$

$$M_q \approx \lambda^{K(q)}$$

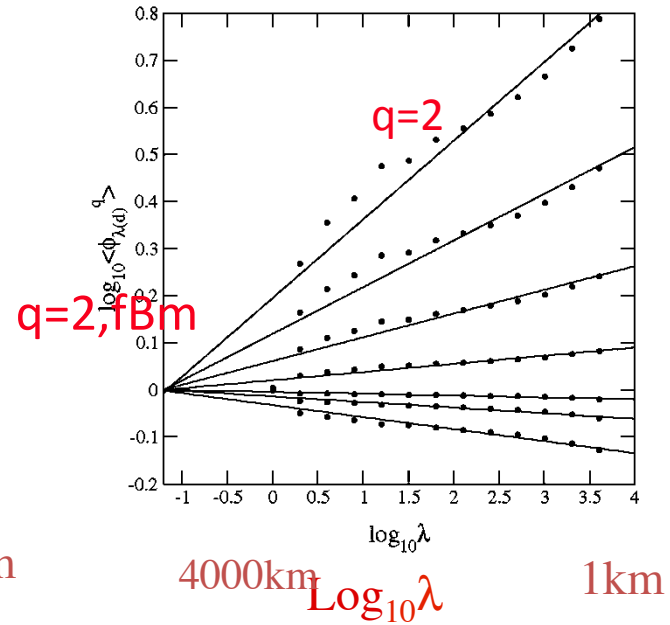


# Topography

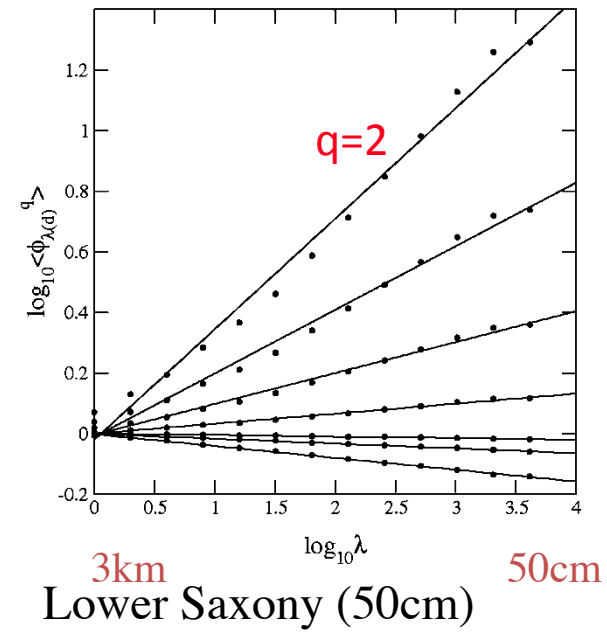
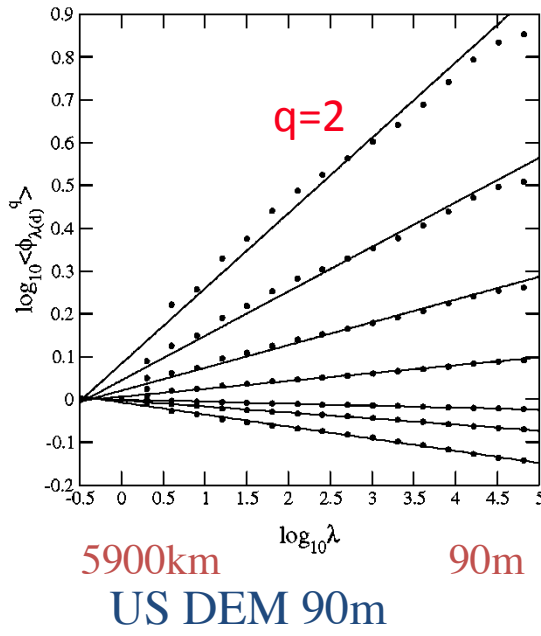
ETOPO5 (strip; 10km)



GTOPO30 1km



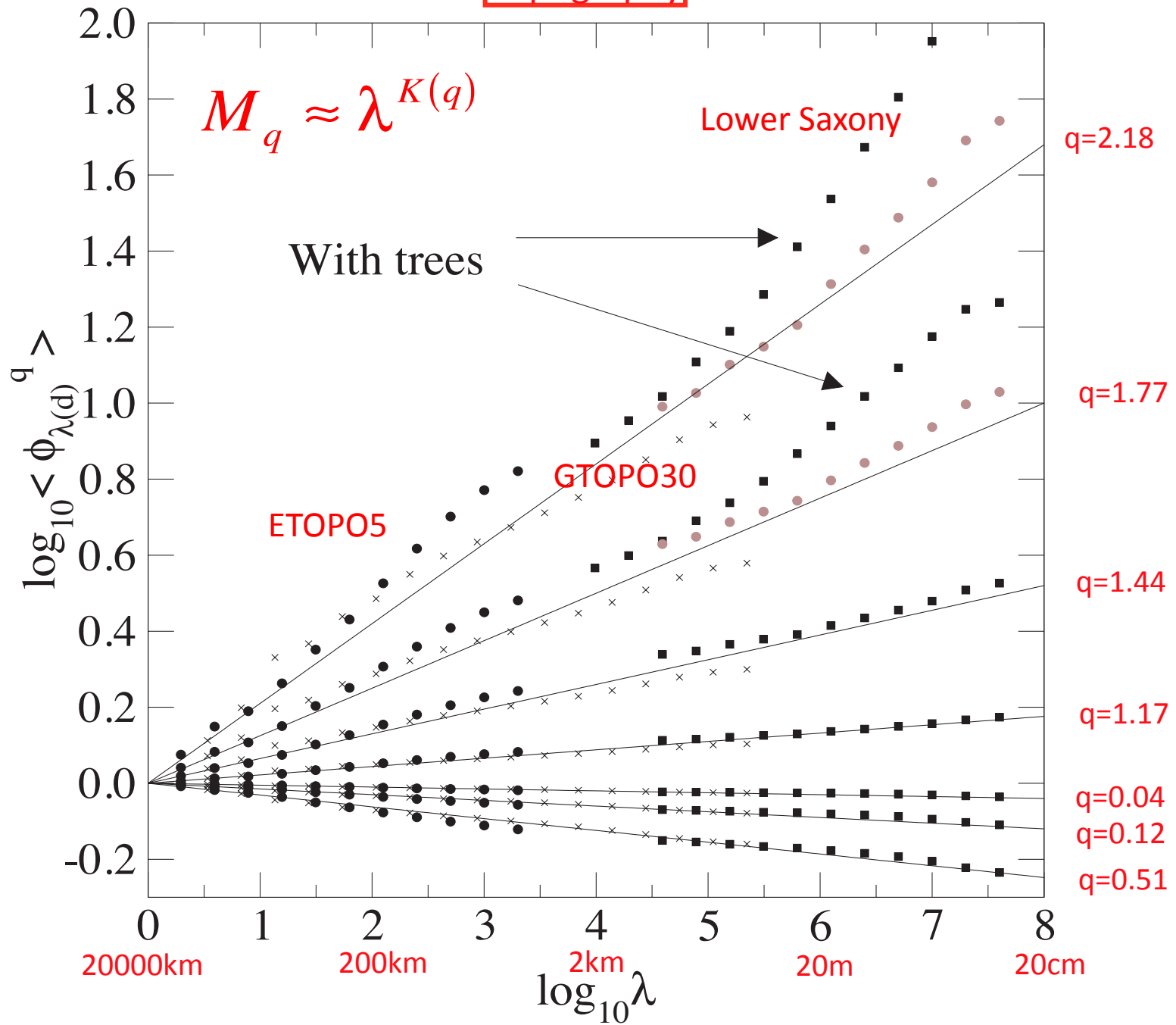
$\text{Log}_{10} \langle \phi_{\lambda}^q \rangle$



$$\phi_{\lambda} = |\Delta h_{\lambda}|$$

$$\langle \phi_{\lambda}^q \rangle = \lambda^{K(q)}$$

Topography



# Multifractal parameters of geophysical fields

$$S_q(\Delta x) = \langle \Delta v(\Delta x)^q \rangle = \langle \Phi_{\Delta x}^q \rangle \Delta x^{qH} \approx \Delta x^{\xi(q)}; \quad \langle \Phi_{\Delta x}^q \rangle = \left( \frac{L_{eff}}{\Delta x} \right)^{K(q)}; \quad \xi(q) = qH - K(q)$$

With universality:  $K(q) = \frac{C_1}{\alpha-1}(q^\alpha - q)$  i.e. we seek  $H, C_1, \alpha$

$$\xi(q) = qH - K(q) = qH - \frac{C_1}{\alpha-1}(q^\alpha - q)$$

		$C_1$	$\alpha$	$H$	$\beta$	$L_{eff}$
<b>State variables</b>	$u, v$	0.09	1.9	1/3, (0.77)	1.6, (2.4)	(14 000)
	$w$	(0.12)	(1.9)	(-0.14)	(0.4)	(15 000)
	$T$	0.11, (0.08)	1.8	0.50, (0.77)	1.9, (2.4)	5000 (19 000)
	$h$	0.09	1.8	0.51	1.9	10 000
	$z$	(0.09)	(1.9)	(1.26)	(3.3)	(60 000)
<b>Precipitation</b>	$R$	0.4	1.5	0.00	0.2	32 000
<b>Passive scalars</b>	Aerosol concentration	0.08	1.8	0.33	1.6	25 000
<b>Radiances</b>	Infrared	0.08	1.5	0.3	1.5	15 000
	Visible	0.08	1.5	0.2	1.5	10 000
	Passive microwave	0.1–0.26	1.5	0.25–0.5	1.3–1.6	5000–15 000
<b>Topography</b>	Altitude	0.12	1.8	0.7	2.1	20 000
<b>Sea surface temperature</b>	SST (see Table 8.2)	0.12	1.9	0.50	1.8	16 000

The unity of clouds and rocks:

Anisotropic scaling,  
scaling stratification

Multifractal simulation

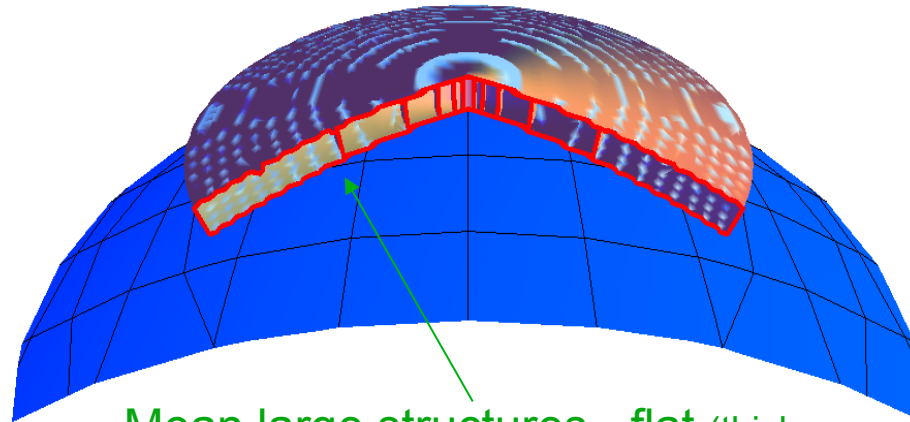
# The Standard (2D/3D) Model

Large scale 2D

“Weather”

Size notion:

$$|(\Delta x, \Delta y)| = (\Delta x^2 + \Delta y^2)^{1/2}$$



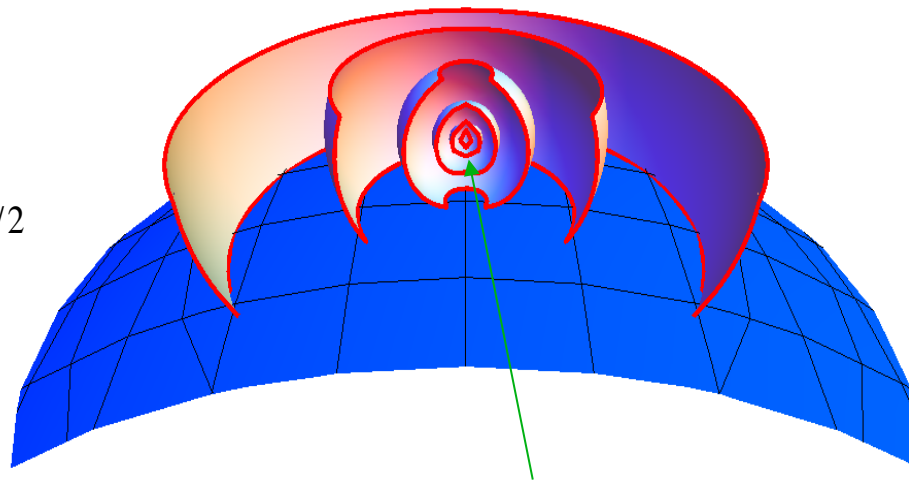
Mean large structures - flat (thickness independent of scale)

Small scale 3D

“Turbulence”

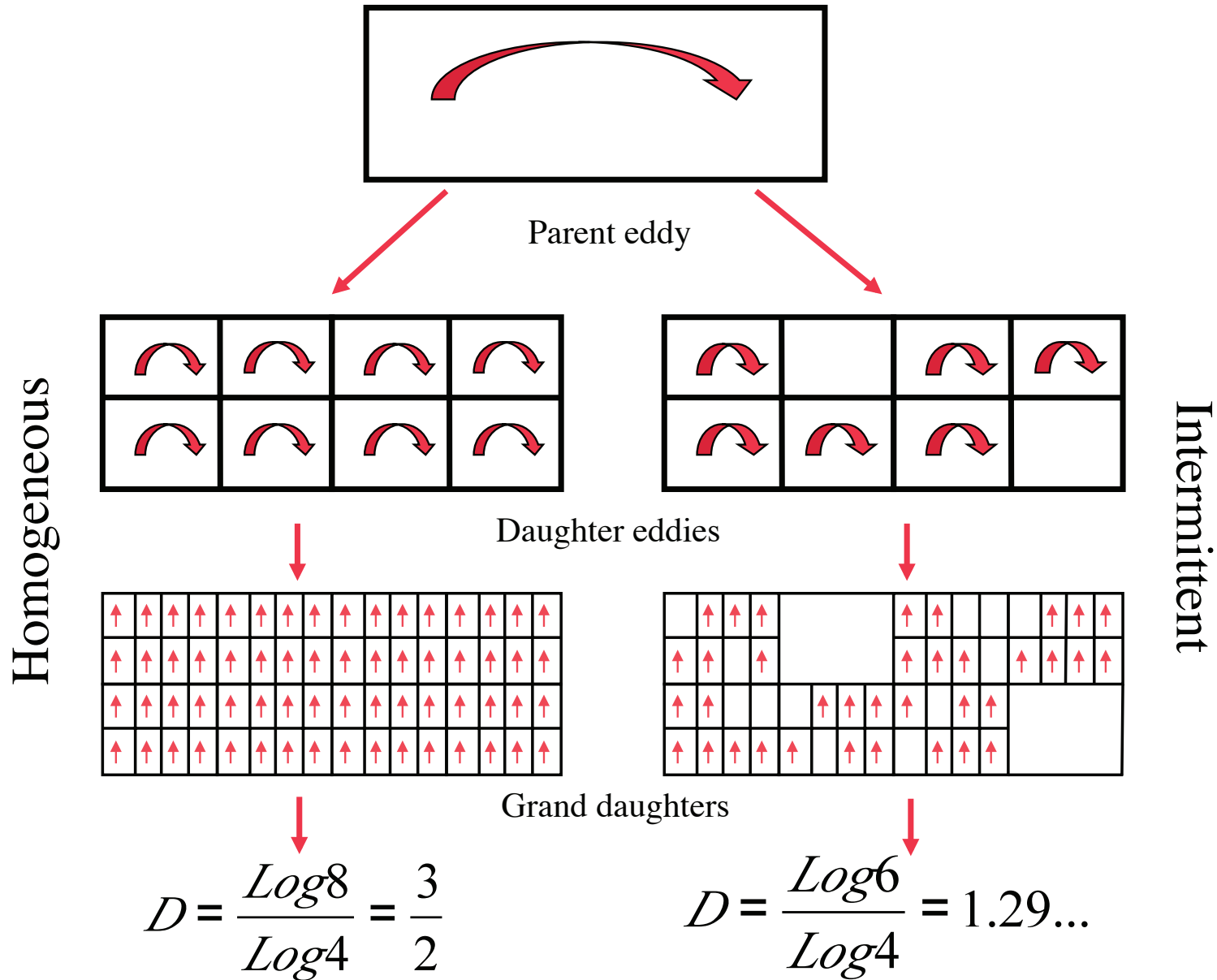
Size notion:

$$|(\Delta x, \Delta y, \Delta z)| = (\Delta x^2 + \Delta y^2 + \Delta z^2)^{1/2}$$



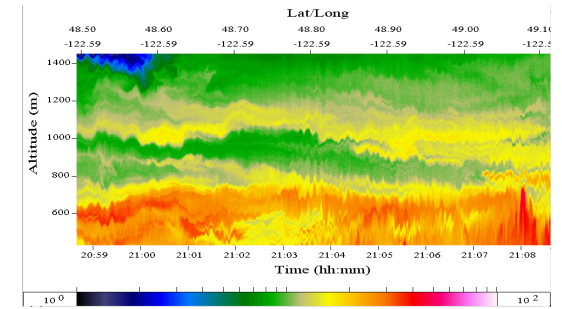
Mean structures - spherical (only small ones are physically possible due to finite thickness)

# Stratified CASCADES



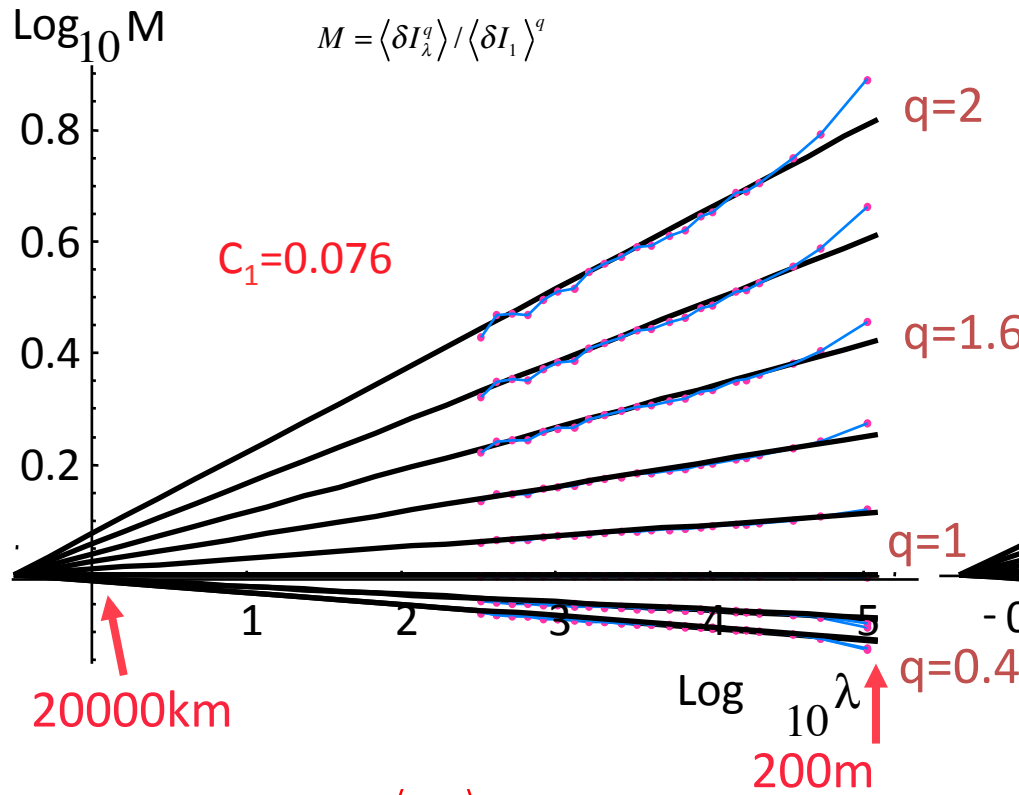


# Vertical cascades: lidar backscatter



From 10 airborne lidar cross-sections near Vancouver B.C.

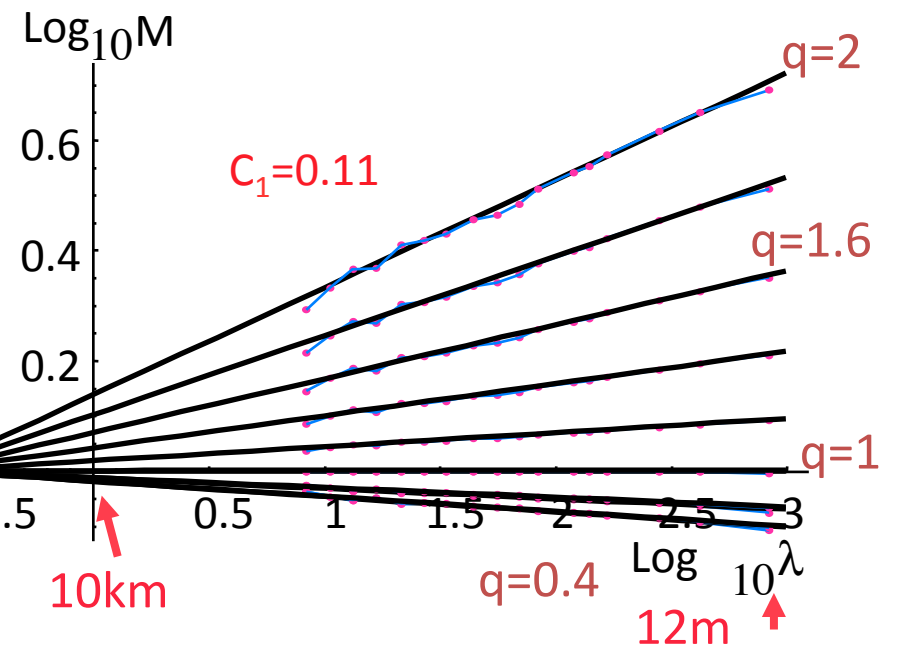
Horizontal cascade



$$M = \langle \varphi_\lambda^q \rangle / \langle \varphi \rangle^q$$

$$M_n \approx \lambda^{K(q)}$$

Vertical cascade

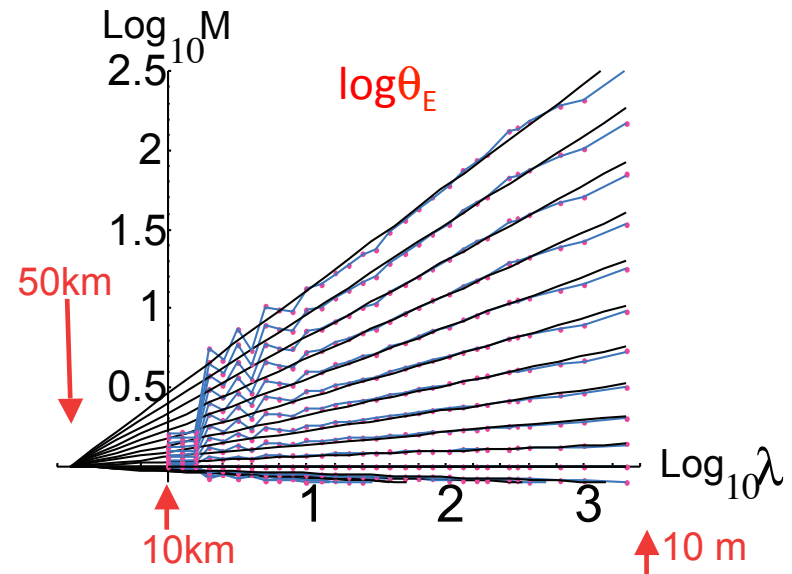
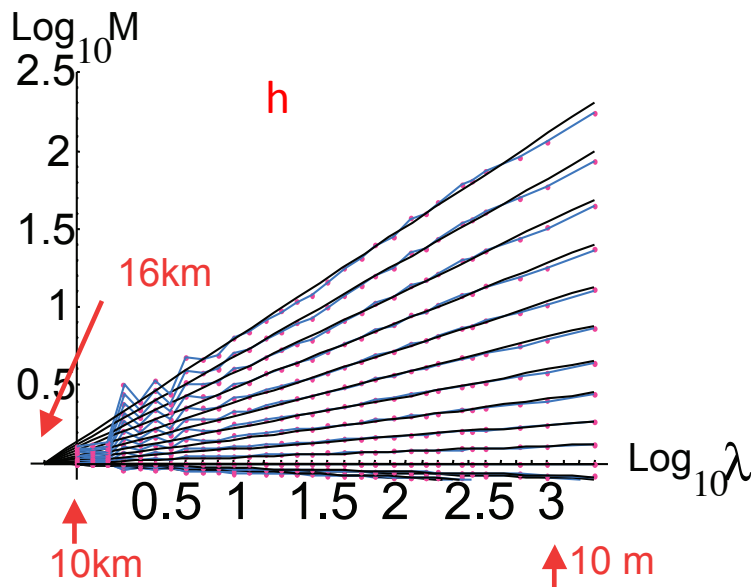
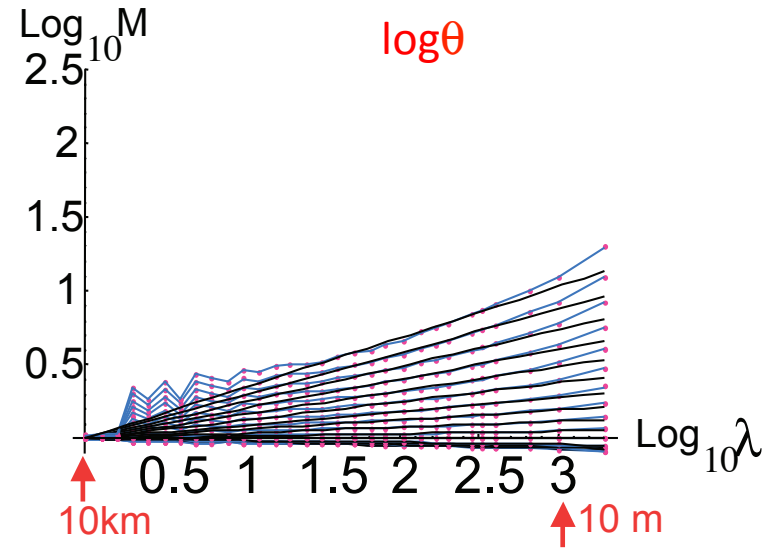
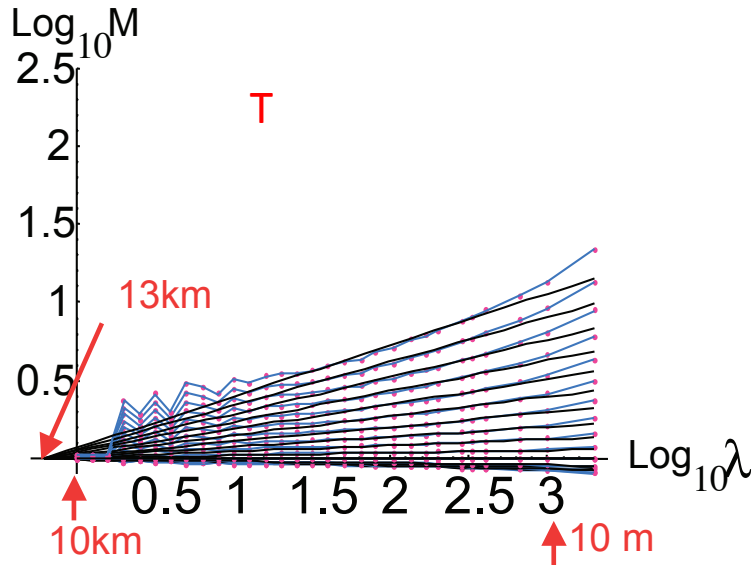


$q=0, 0.2, 0.4, \dots, 2$

# Vertical cascades:

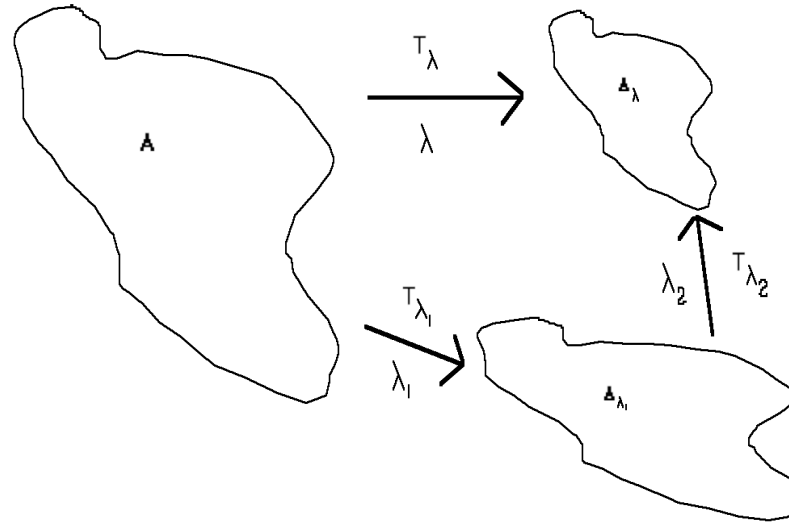
Thermodynamic fields (drop sondes)

$$M = \langle \varphi_\lambda^q \rangle / \langle \varphi \rangle^q$$
$$M_q \approx \lambda^{K(q)}$$



# Generalized Scale Invariance (GSI)

## The scale changing operator $T_\lambda$



$T_\lambda$  is the rule relating the statistical properties at one scale to another and involves only the scale ratio. This implies that  $T_\lambda$  has certain properties. In particular, if and only if  $\lambda_1 \lambda_2 = \lambda$ , then:

$$B_\lambda = T_\lambda B_1 = T_{\lambda_1 \lambda_2} B_1 = T_{\lambda_1} B_{\lambda_2} = T_{\lambda_2} B_{\lambda_1}$$

it is also commutative  $T_\lambda = T_{\lambda_2} T_{\lambda_1} = T_{\lambda_1} T_{\lambda_2}$

This implies that  $T_\lambda$  is a one parameter multiplicative group with parameter  $\lambda$

# The Elements of (GSI)

$T_\lambda$  is a generalized contraction on a vector space  $E$ , it is a one-parameter (semi-) group for the positive real scale ratio  $\lambda$  ( $\lambda \geq 1$  for a semi-group), i.e.:

$$\forall \lambda, \lambda' \in \mathbb{R}^+ : T_{\lambda'} \circ T_\lambda = T_{\lambda'\lambda}$$

hence

$$T_\lambda = \lambda^{-G}$$

and admits a generalized scale denoted  $\|\underline{r}\|$  (double lines to distinguish it from the usual Euclidean metric  $|\underline{r}|$ ), which in addition to being nonnegative, satisfies the following three properties:

i) *Nondegeneracy:*

$$\|\underline{r}\| = 0 \Leftrightarrow \underline{r} = \underline{0}$$

ii) *Linearity with the contraction parameter  $1/\lambda$ :*

$$\forall \underline{x} \in E, \forall \lambda \in \mathbb{R}^+ : T_\lambda \|\underline{r}\| \equiv \|\underline{T}_\lambda \underline{r}\| = \lambda^{-1} \|\underline{r}\|$$

iii) *Strictly decreasing balls: the balls defined by this scale*

$$B_\ell = \{\underline{r} \mid \|\underline{r}\| \leq \ell\} \quad (\text{used to define anisotropic Hausdorff measures})$$

must be strictly decreasing with the contraction:  $\forall L \in \mathbb{R}^+, \forall \lambda > 1 : B_{L/\lambda} \equiv T_\lambda(B_L) \subset B_L$

and therefore:  $\forall L \in \mathbb{R}^+, \forall \lambda' \geq \lambda \geq 1 : B_{L/\lambda'} \subset B_{L/\lambda}$



A generalized blow-down with increasing of the acronym “NVAG”. If  $G = I$ , we would have obtained a standard reduction, with all the copies uniformly reduced converging to the centre of the reduction. Here the parameters are

$$G = \begin{pmatrix} 1.3 & -1.3 \\ 0.3 & 0.7 \end{pmatrix}$$

and each successive reduction is by 28%.

# The scale function equation

The basic scale function equation is:

$$\|T_\lambda \underline{r}\| = \lambda^{-1} \|\underline{r}\|$$

With group generator:  $\|\lambda^{-G} \underline{r}\| = \lambda^{-1} \|\underline{r}\|$

In terms of the infinitesimal generator  $\underline{g}(\underline{r}) = \underline{G}\underline{r}$  we have:

$$\left(\underline{g}(\underline{r}) \cdot \nabla\right) \|\underline{r}\| = \|\underline{r}\|$$

Nonlinear GSI: anisotropy = scale and position dependent

In the case of linear GSI,  $\underline{G}$  is a matrix and we have:

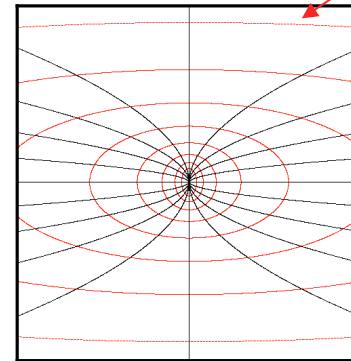
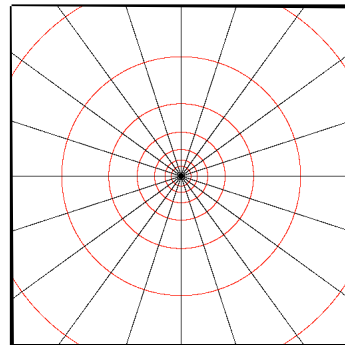
$$\left(\underline{r}^T \cdot \underline{G} \cdot \nabla\right) \|\underline{r}\| = \|\underline{r}\|$$

Linear GSI: anisotropy = scale dependent only

# Scale functions in linear GSI (position independent)

Scale isolines in red

Isotropic  
(self similar)



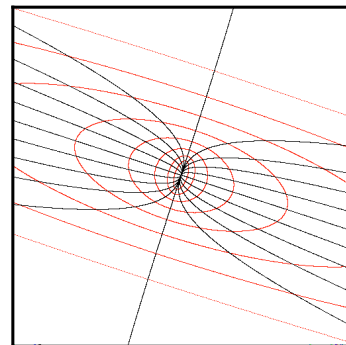
Self-affine

$$T_\lambda = \lambda^{-G}$$

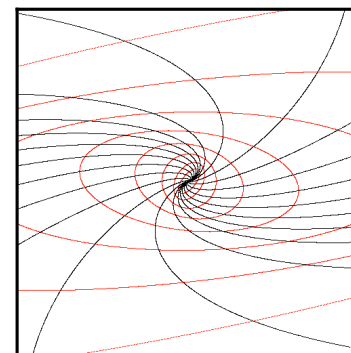
$$G = \begin{pmatrix} 1 & 0 \\ 0 & 1 \end{pmatrix}$$

$$G = \begin{pmatrix} 1.35 & 0 \\ 0 & 0.65 \end{pmatrix}$$

Stratification  
dominant (real  
eigenvalues)



$$G = \begin{pmatrix} 1.35 & 0.25 \\ 0.25 & 0.65 \end{pmatrix}$$



$$G = \begin{pmatrix} 1.35 & -0.45 \\ 0.85 & 0.65 \end{pmatrix}$$

Rotation  
dominant  
(complex  
eigenvalues)

# The physical scale function and differential scaling

$$|\underline{\Delta r}| \rightarrow \|\underline{\Delta r}\|$$

Usual distance  
(=vector norm)

Scale function  
(scale notion)

Scale symmetry  $\|\lambda^{-G} \underline{r}\| = \lambda^{-1} \|\underline{r}\|$

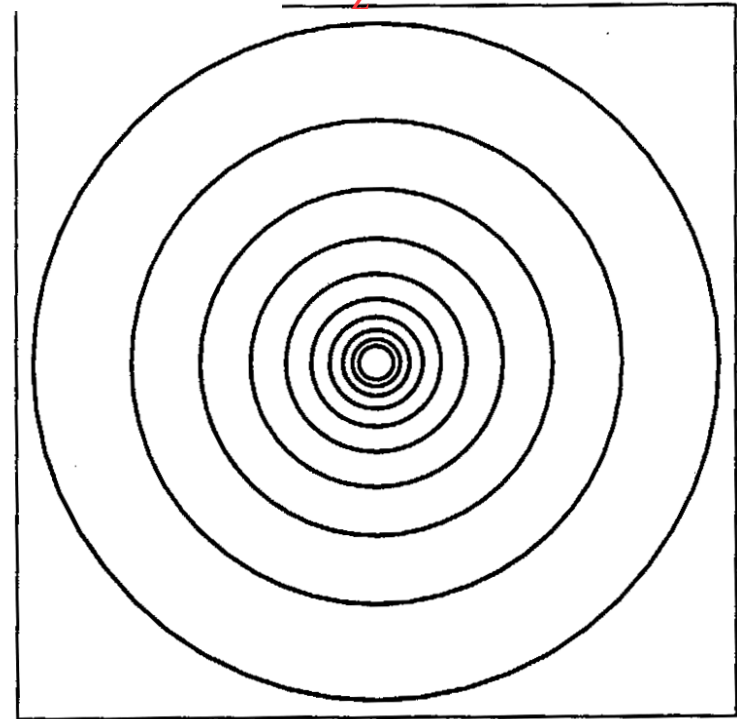
“canonical” scale function:

$$\|(\Delta x, \Delta z)\| = l_s \left( \left( \frac{\Delta x}{l_s} \right)^2 + \left( \frac{\Delta z}{l_s} \right)^{2/H_z} \right)^{1/2}$$

$$G = \begin{pmatrix} 1 & 0 \\ 0 & H_z \end{pmatrix}$$

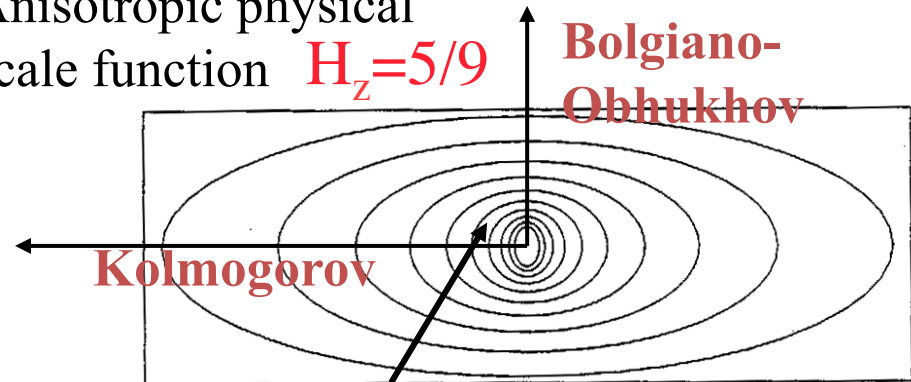
## Vertical sections

Isotropic function  $H_z=1$



Anisotropic physical scale function  $H_z=5/9$

**Bolgiano-Obukhov**

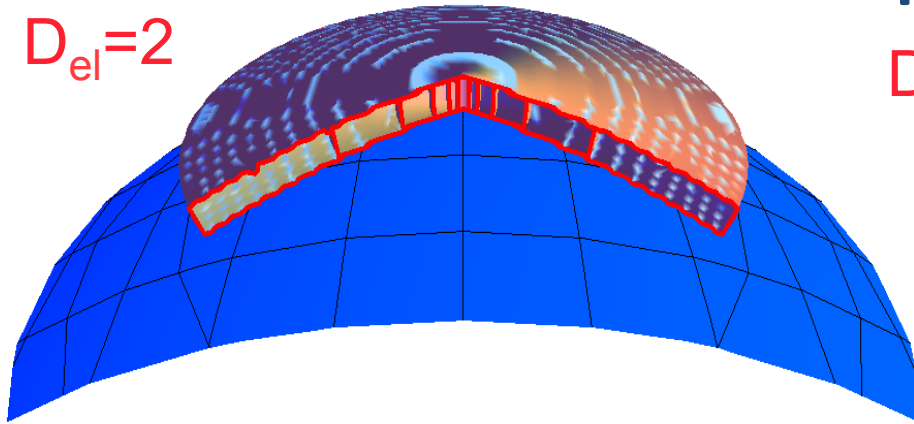


Sphero-scale

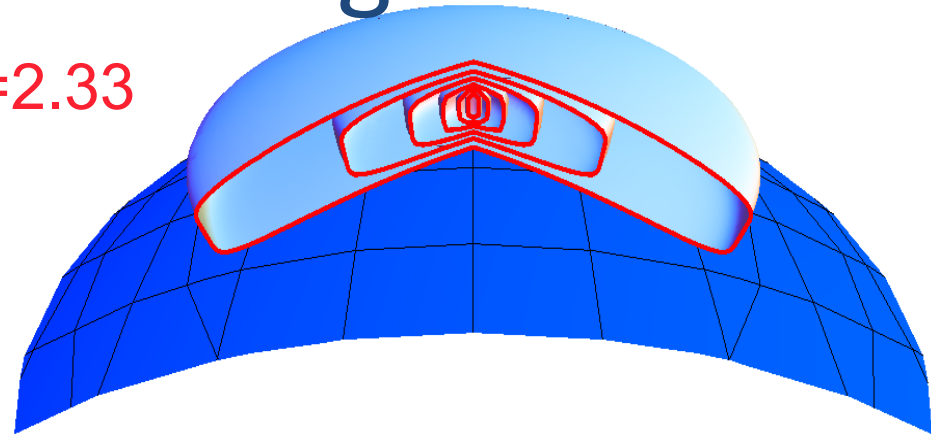


# Anisotropic Scaling

$$D_{el}=2$$

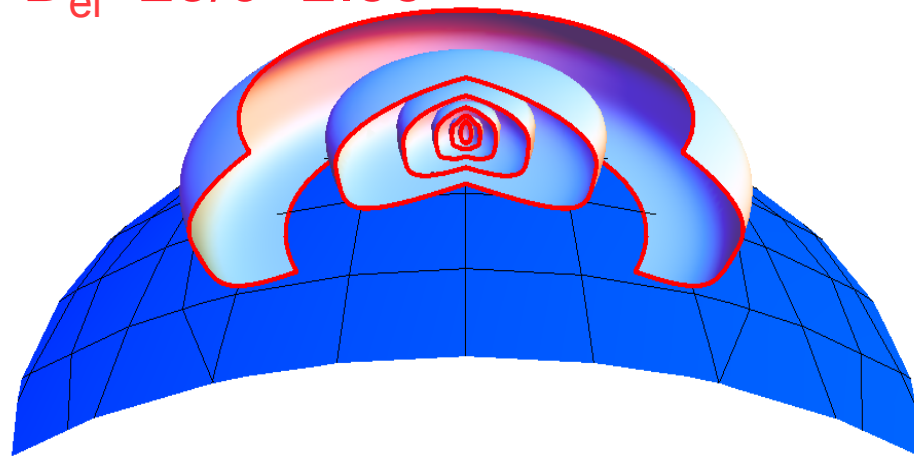


$$D_{el}=2.33$$

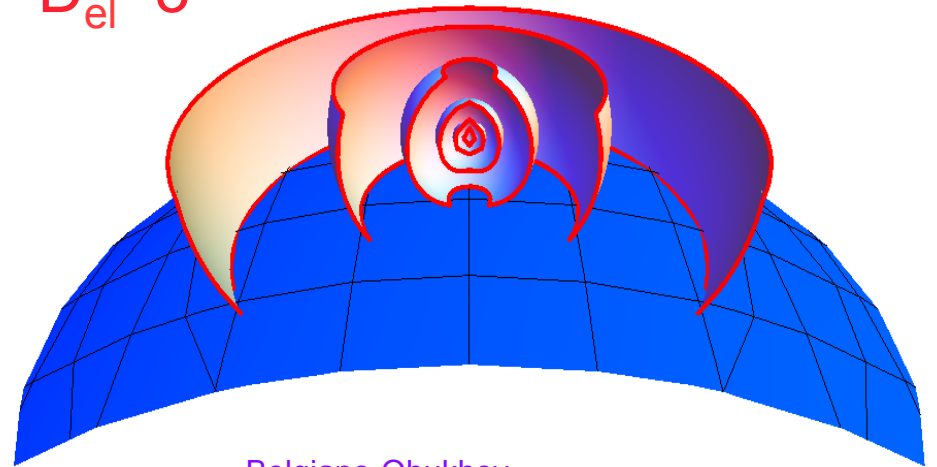


$$D_{el}=23/9=2.55$$

c.f. empirical: 2.57



$$D_{el}=3$$



**The 23/9D model:**

$$\underbrace{\Delta v(\Delta x) = \varepsilon^{1/3} \Delta x^{1/3}}_{\text{Kolmogorov}}; \quad \underbrace{\Delta v(\Delta z) = \phi^{1/5} \Delta z^{3/5}}_{\text{Bolgiano-Obukhov}} \quad H_z = (1/3)/(3/5) = 5/9$$

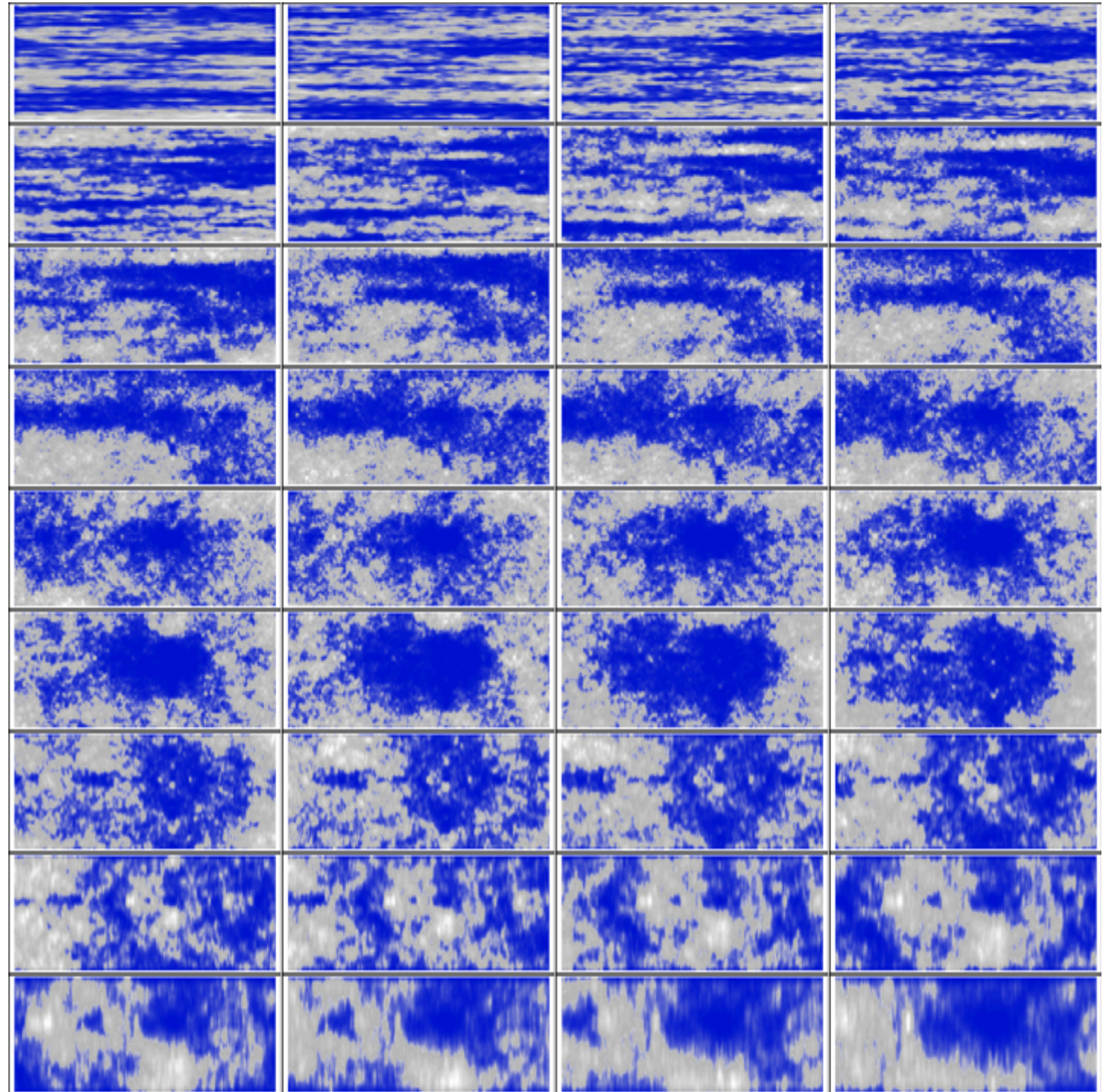
$$\text{Volume} \approx L_x L_y L_z \approx L^{D_{el}} \quad D_{el} = 2 + H_z = 23/9$$

# Overall

**Isotropy**  $\longrightarrow$  **anisotropy**

$$|\underline{x}| \longrightarrow \|\underline{x}\|; \quad D \longrightarrow D_{el}$$

Zoom  
factor  
1000



Vertical cross-  
section



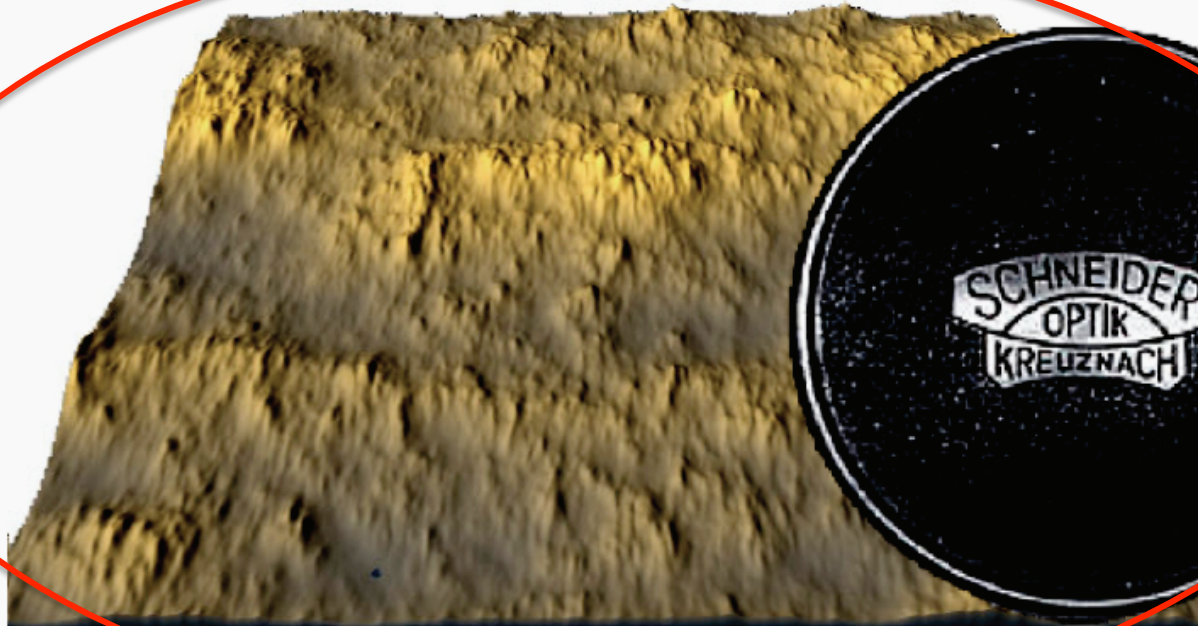
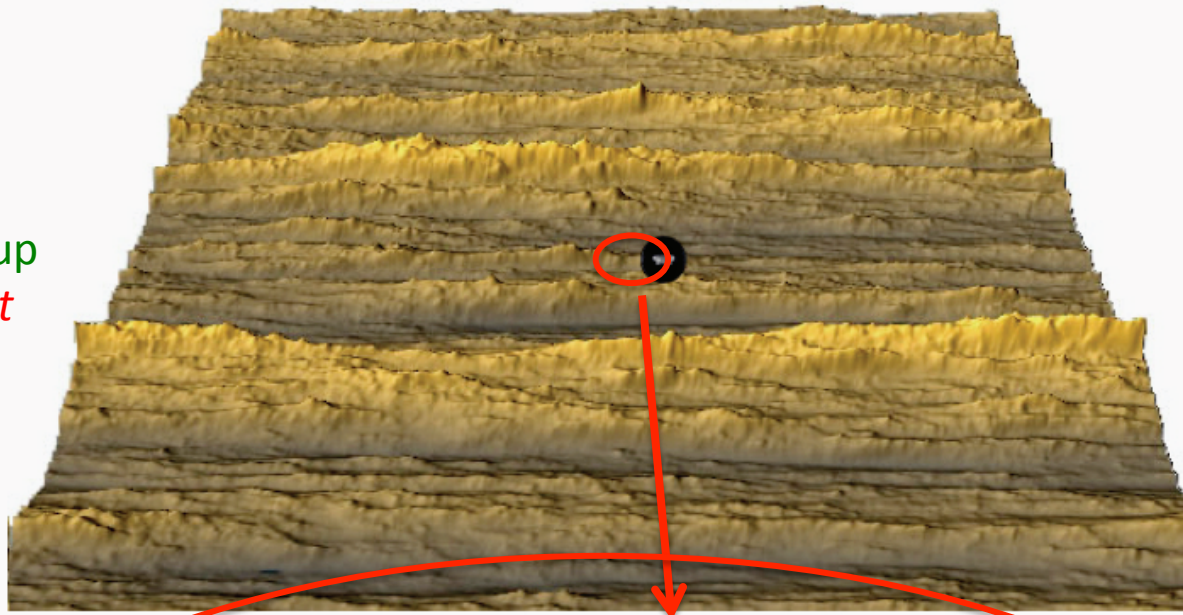
# The unity of clouds and rocks: The Phenomenological Fallacy

1) Morphology not dynamics is taken as fundamental.

2) Scaling is reduced to the isotropic (self-similar) special case.

3) With GSI, morphologies can change with scale even though the dynamical mechanisms are scale invariant.

Isotropic Blow up  
reveals *different*  
morphology



Anisotropic multifractal surface simulation

## Illustrating the effect of varying $G$ and the unit ball with multifractal simulations

The basic morphologies don't depend on the orientation or size; it suffices to consider  $d=1$ ,  $r=f$ ,  $c=0$ , i.e. to only consider matrices of the form:

$$G = \begin{pmatrix} 1 & r - e \\ r + e & 1 \end{pmatrix}$$

In order to explore the possible morphologies, the last element we need is therefore a specification of the unit ball. A convenient one-parameter parametrization is:

Polar coordinate representation  
of the unit ball:

$$r(\theta'') = 1 / \Theta(\theta'')$$

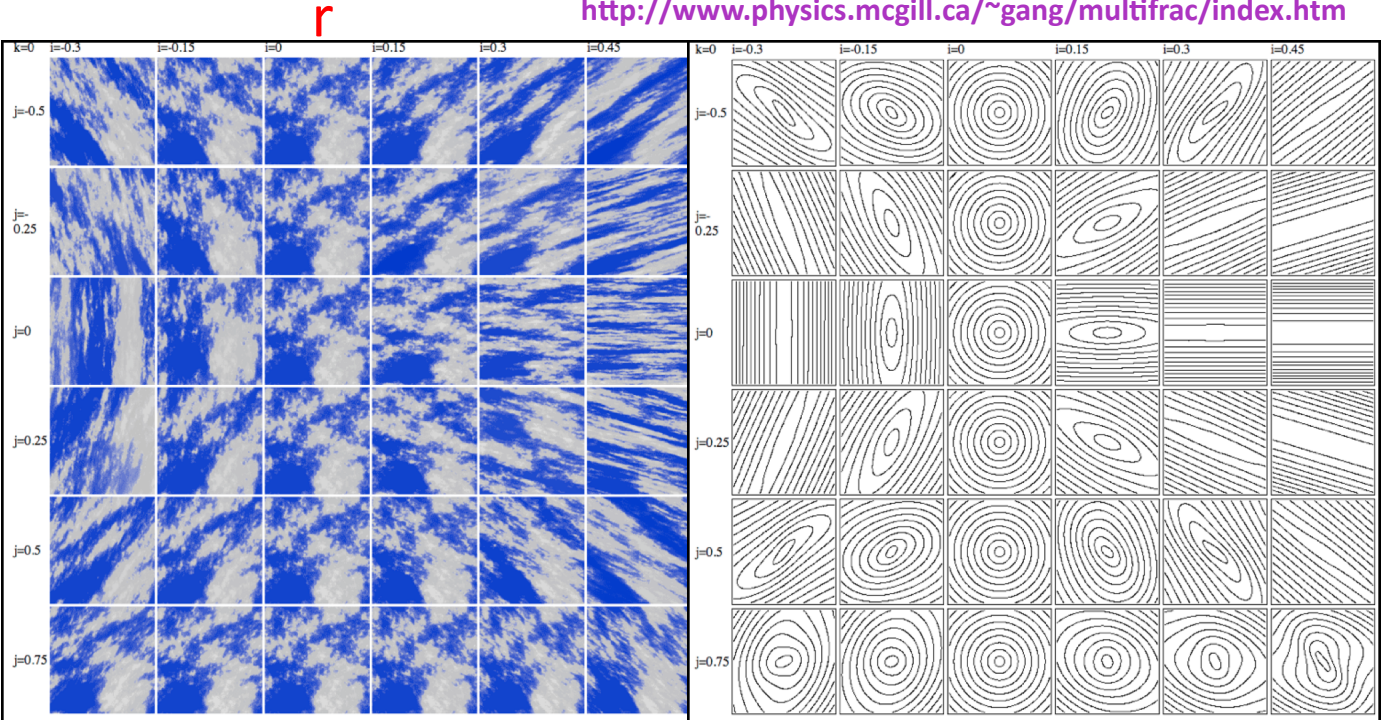
$$\Theta(\theta'') = 1 + \frac{1 - 2^{-k}}{1 + 2^{-k}} \cos \theta''$$

$k$  is the  $\log_2$  of the ratio of  
the largest to smallest scale  
on the unit ball

Roundish unit ball

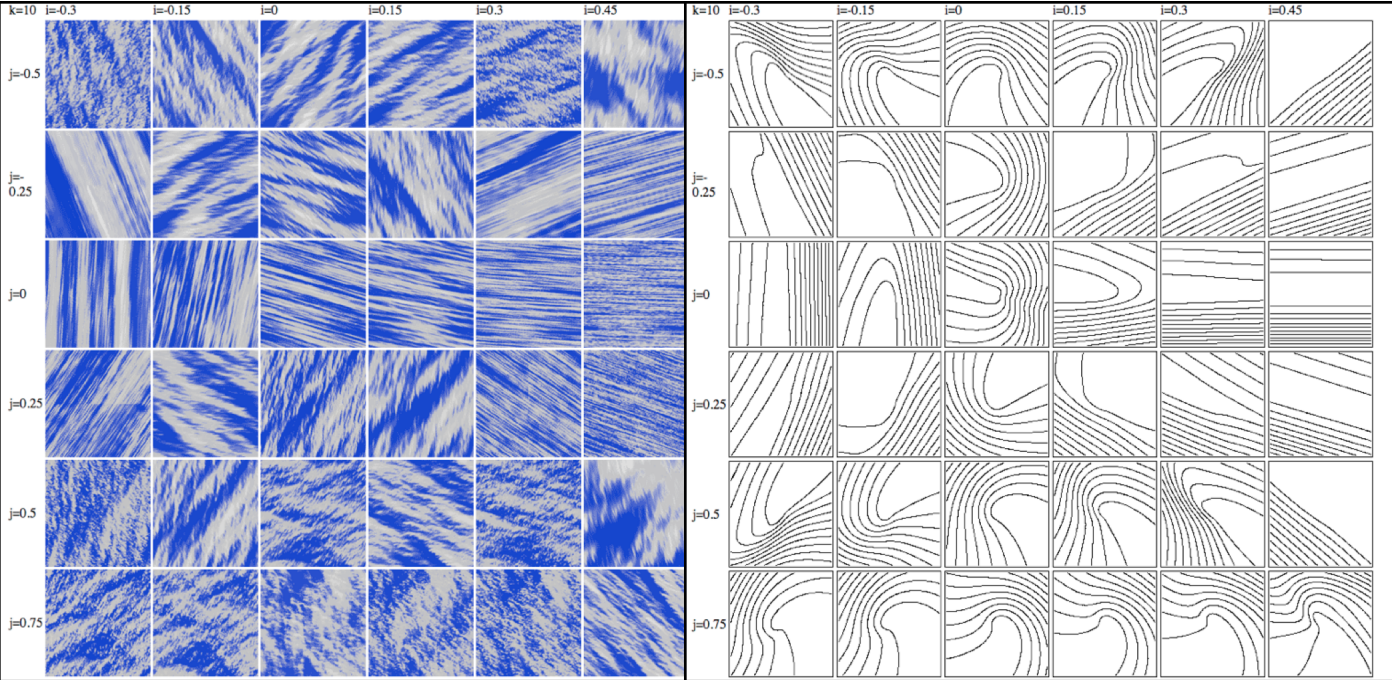
$k = 0$ : we vary  $r$  (denoted  $i$ ) from  $-0.3, -0.15, \dots, 0.45$  left to right and  $e$  (denoted  $j$ ) from  $-0.5, -0.25, \dots, 0.75$  top to bottom. On the right we show the contours of the corresponding scale functions.

$$G = \begin{pmatrix} 1 & r - e \\ r + e & 1 \end{pmatrix} \quad e$$



Highly anisotropic unit ball:  $k = 10$

$$\Theta(\theta'') = 1 + \frac{1 - 2^{-k}}{1 + 2^{-k}} \cos \theta''$$

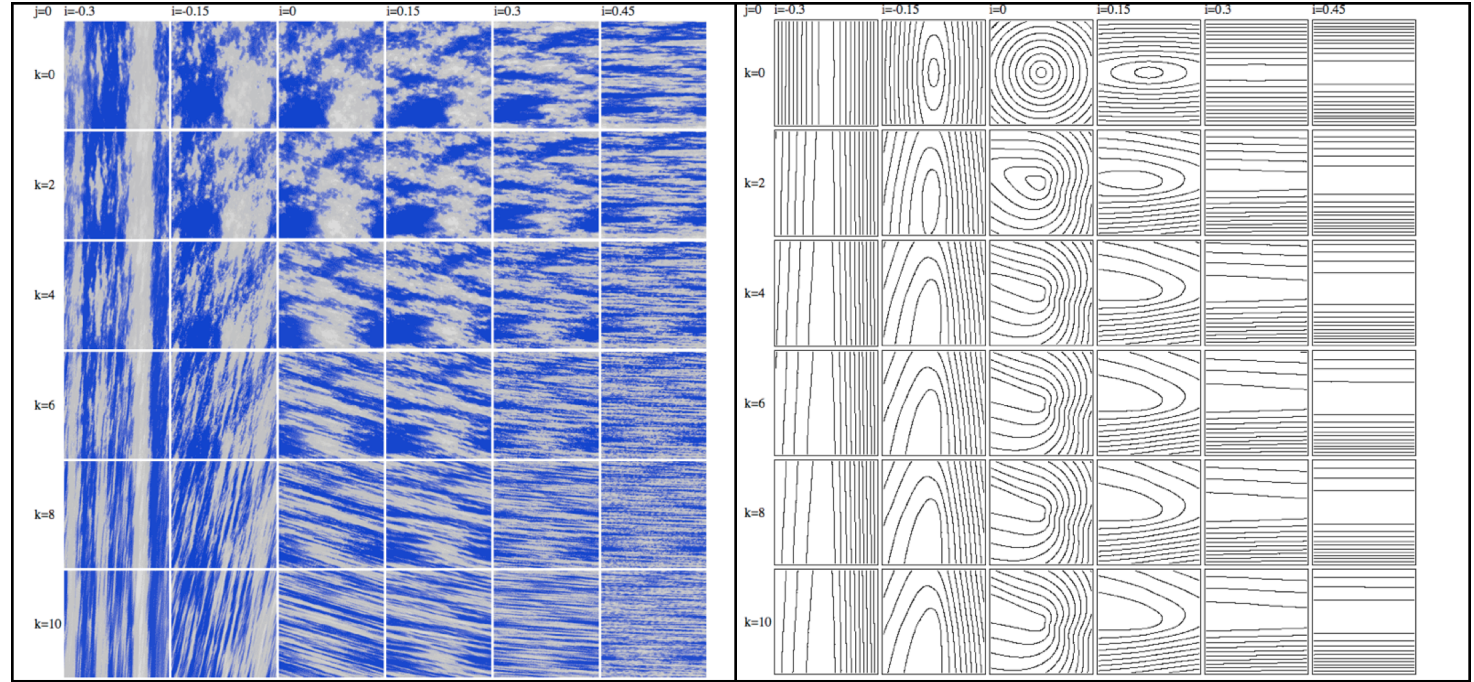


$r$

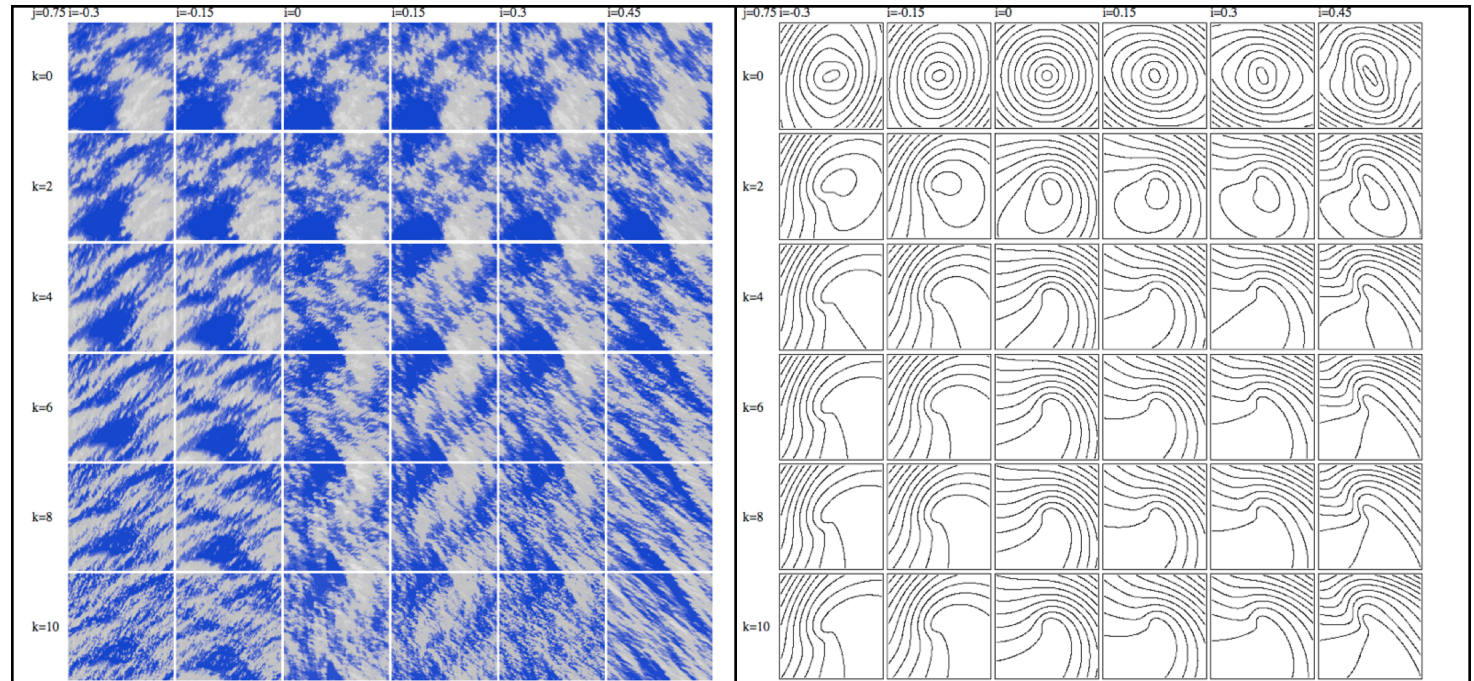
$e = 0$

$r$  is increased from -0.3, -0.15, ...0.45 left to right, from top to bottom,  $k$  is increased from 0, 2, 4, ..10.

$k$



$e = 0.75$



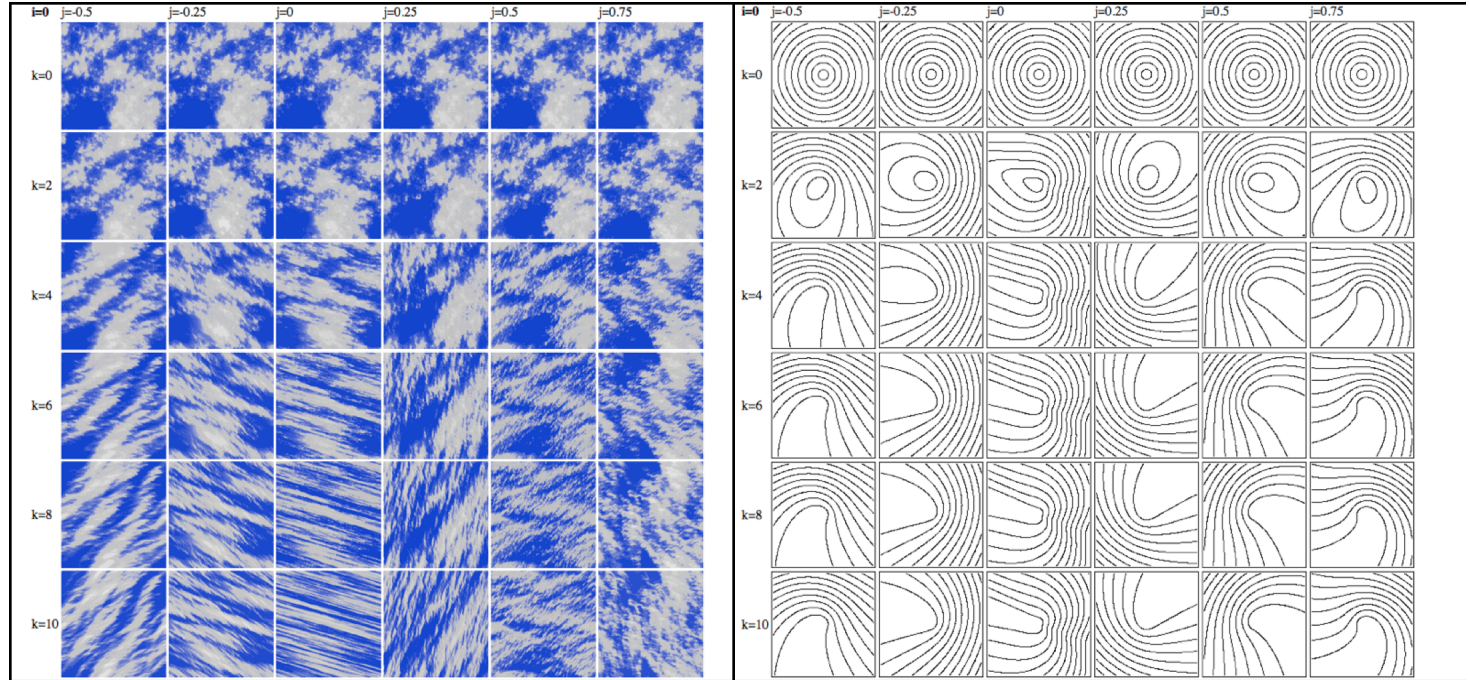


$e$

$r = 0$

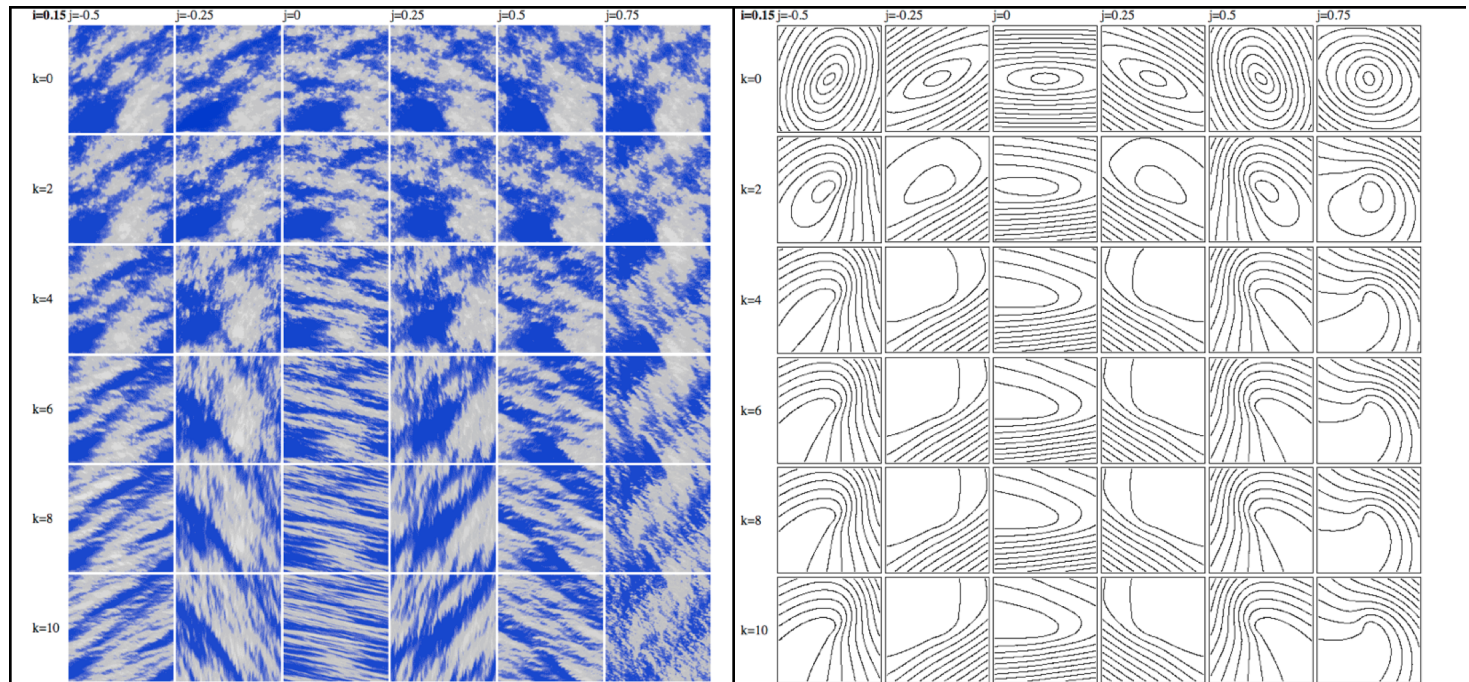
$e$  left to right is:  
-0.5, -0.25, ...0.75.

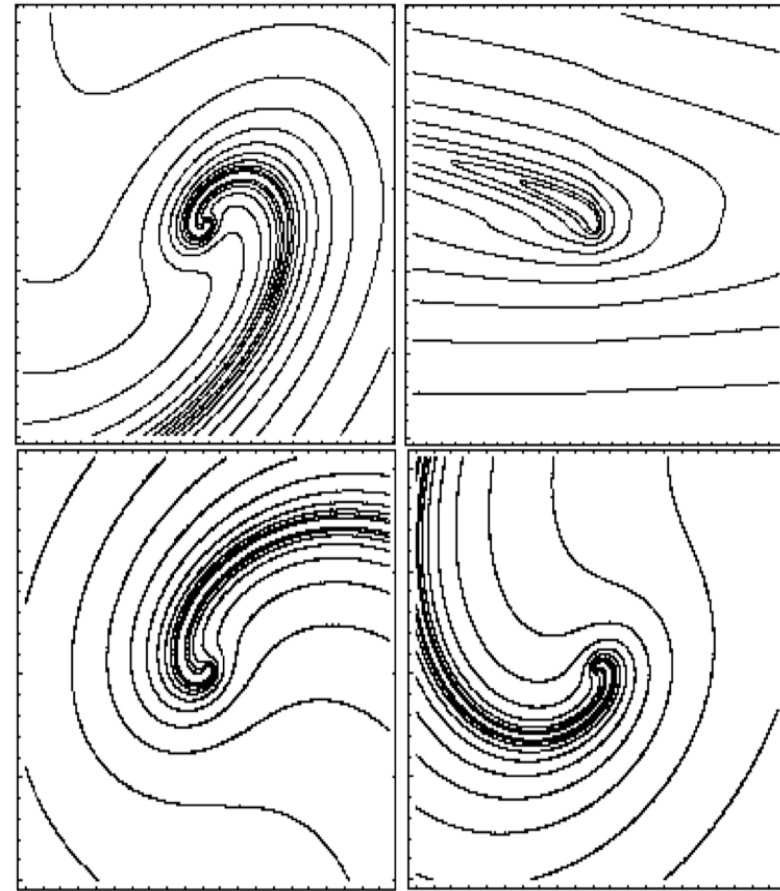
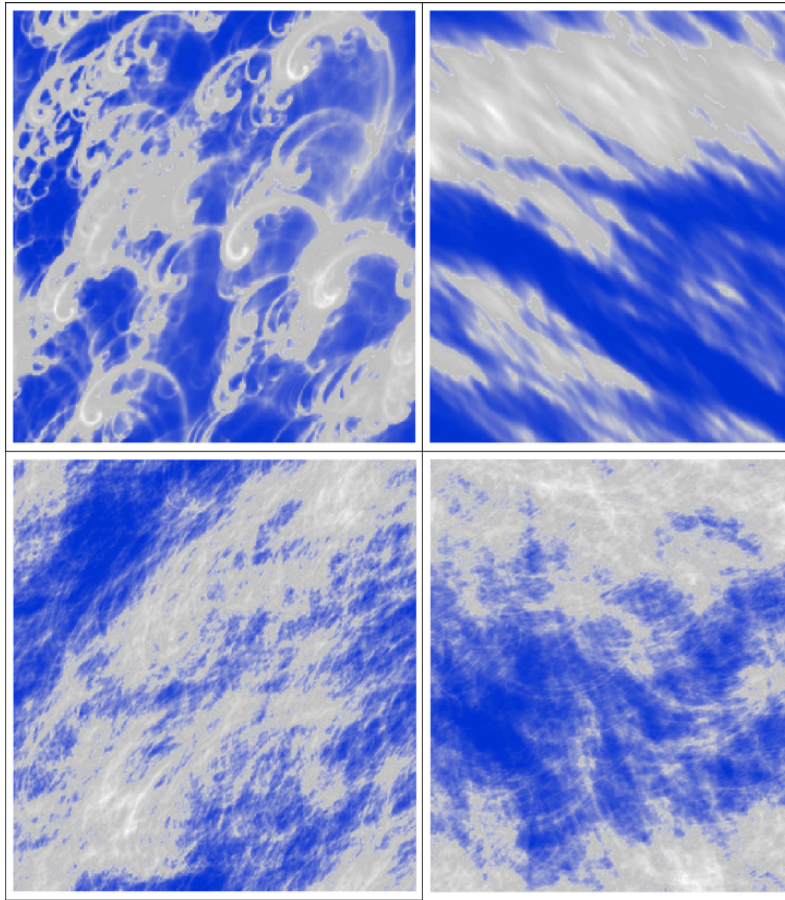
$k$



$r = 0.15$

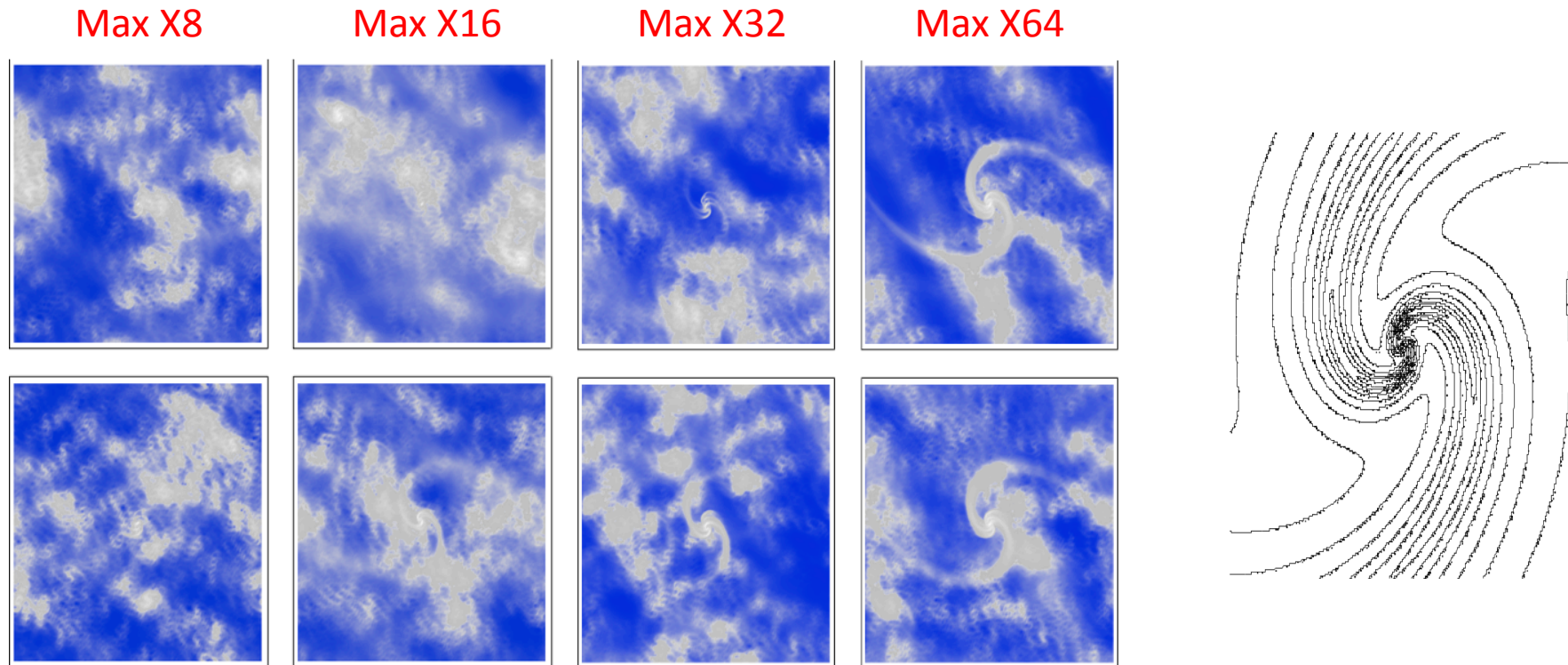
In all rows, from  
top to bottom,  $k$   
is increased (0,  
2, 4,..10),





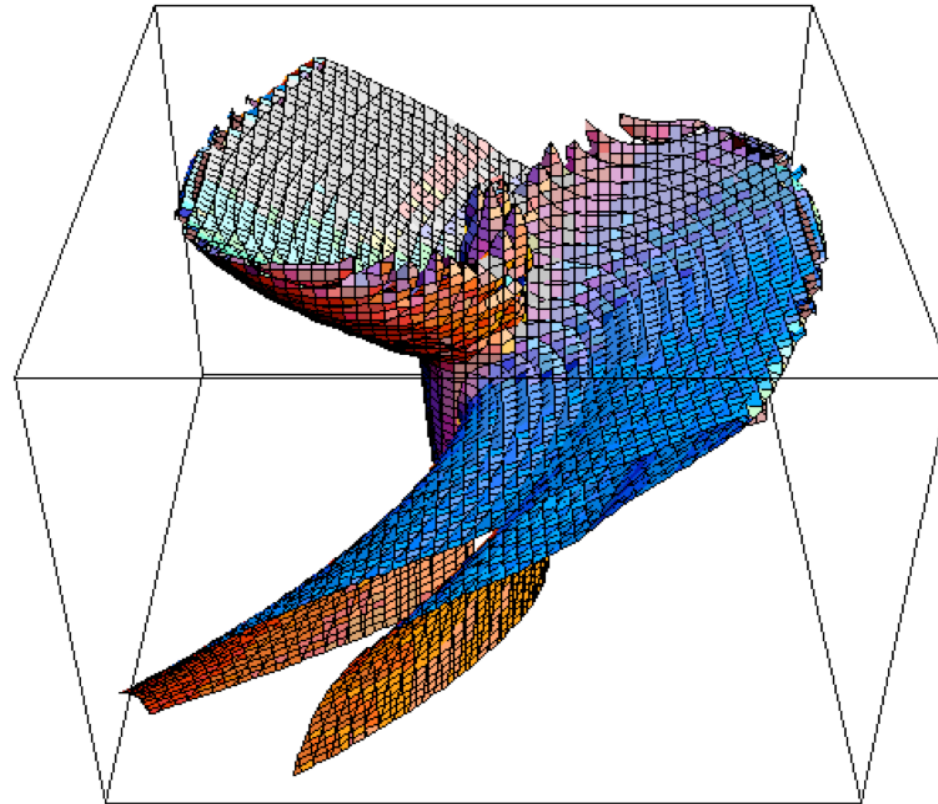
Examples of 2D simulations on 512x512 pixel grids with  $\alpha = 1.8$ ,  $C_1 = 0.1$ ,  $H = 0.333$ ,  $d = 1$ ,  $f = 0$ . Upper left:  $c = 0.8$ ,  $e = 2$ ,  $l_s = 512$ ,  $x = 1.3$  ( $2^k = r_{max}/r_{min} \approx 54$ ), upper right:  $c = -2/7$ ,  $e = 0.1$ ,  $l_s = 32$ ,  $2^k \approx 5$ , lower left:  $c = 0.3$ ,  $e = 1.2$ ,  $l_s = 32$ ,  $2^k \approx 800$ , lower right:  $c = 0.3$ ,  $e = 1.2$ ,  $l_s = 1$ ,  $2^k \approx 800$ .

# Order emerging from chaos



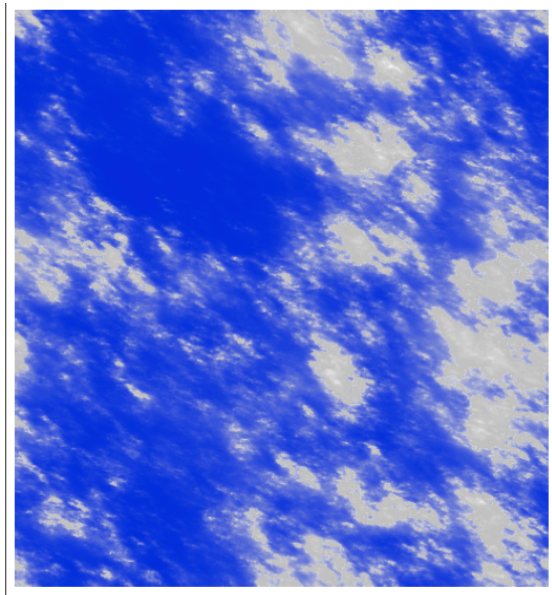
Each row shows a realization of a random multifractal process with a single value of of the subgenerator  $\gamma(\underline{r})$  at the centre of a 512X512 grid replaced by the maximum of  $\gamma(\underline{r})$  over the field boosted by factors of  $N$  increasing by 2 from left to right (from 8 to 64) in order to simulate very rare events ( $\alpha = 1.8$ ,  $C_1 = 0.1$ ,  $H = 0.333$ ). The scaling is anisotropic with complex eigenvalues of  $G$ , the scale function is shown at right.

Simulations in three dimensions, rendering with simulated radiative transfer

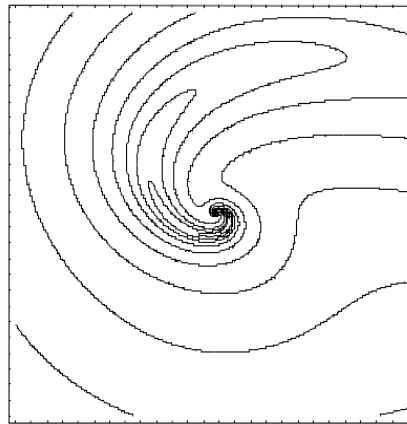


This is a contour of the scale function corresponding to a single scale; this is a strongly rotationally dominant case with  $n = 2$ ,  $x_q = x_f = 1.4$ ,  $d = 1$ ,  $c = 0.5$ ,  $e = 1$ ,  $f = 0$ ,  $H_z = 0.8$ ,  $l_s = 64$ ,

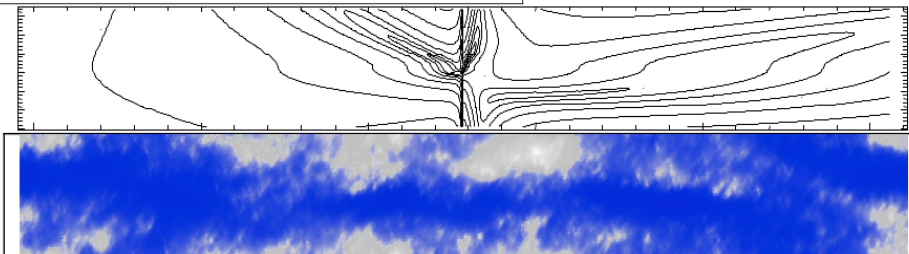
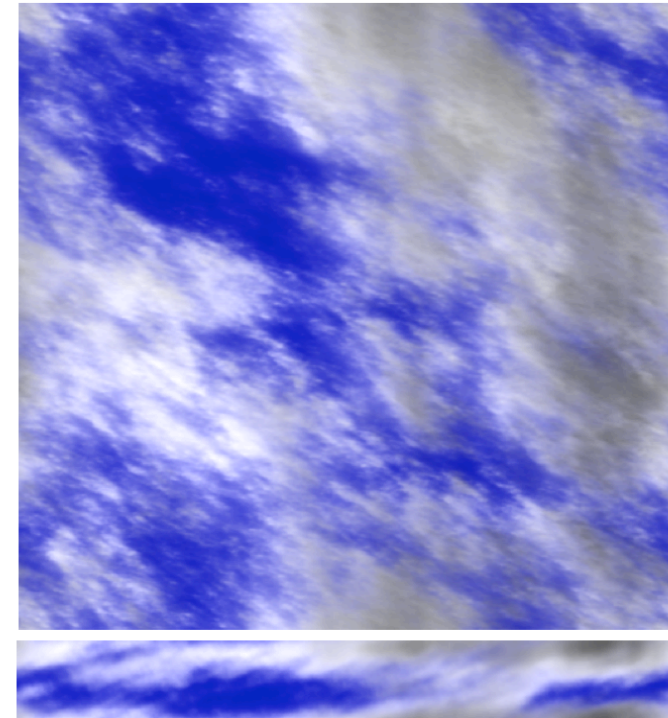
Top horizontal section (density)



Corresponding scale function



Corresponding top radiative transfer

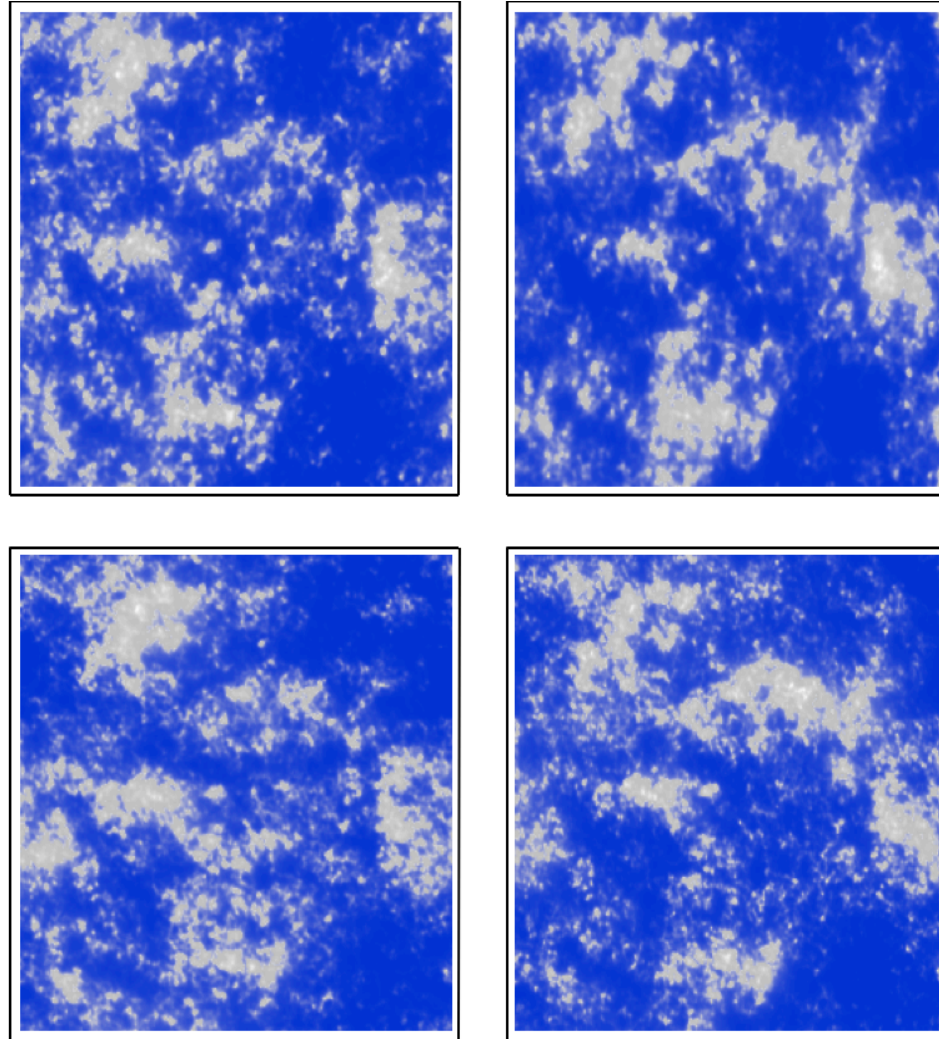


Side (density)

Corresponding side radiative transfer

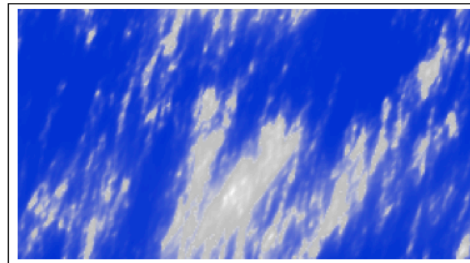
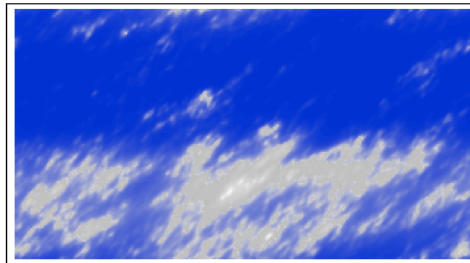
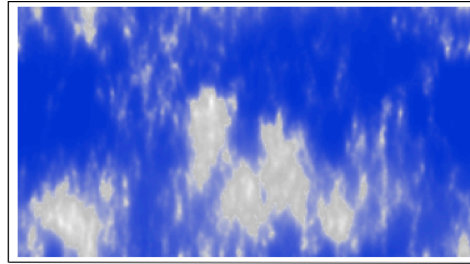
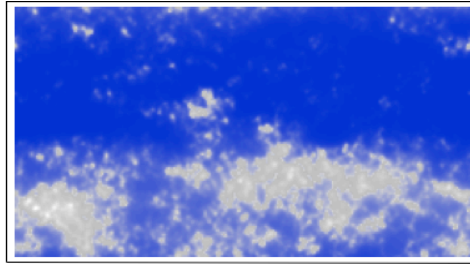
An example with  $a = 1.8$ ,  $C_1 = 0.1$ ,  $H = 0.333$ , on a  $512 \times 512 \times 64$  grid (the latter is the thickness). The parameters are  $n_q = 1$ ,  $n_f = 2$ ,  $x_q = 0.3$ ,  $x_f = 0.8$ ,  $c = 0.2$ ,  $e = 0.5$ ,  $f = 0.2$  (rotation dominant),  $H_z = 0.555$  with  $l_s = 128$ ,  $l_{sz} = 32$ . The upper left is the liquid water density field, top horizontal section, to the right is the corresponding central horizontal cross section of the scale function. The bottom row shows one of the sides ( $512 \times 64$  pixels) with corresponding central part of the vertical cross section.

## Cloud tops (densities)

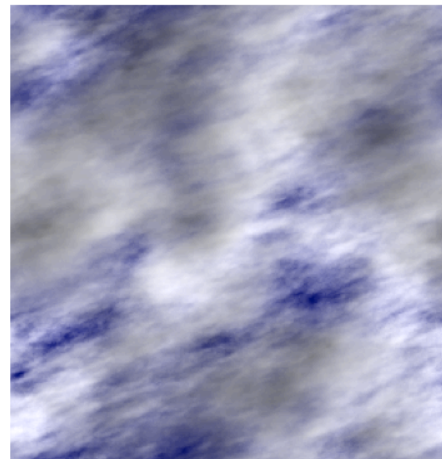
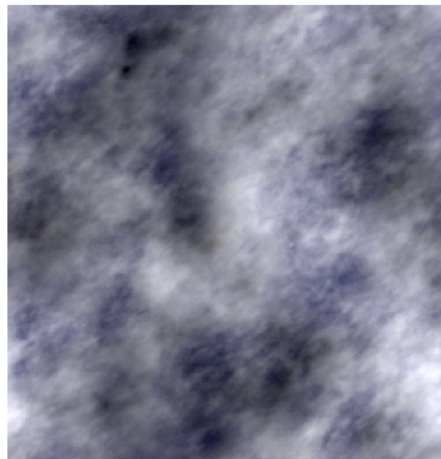
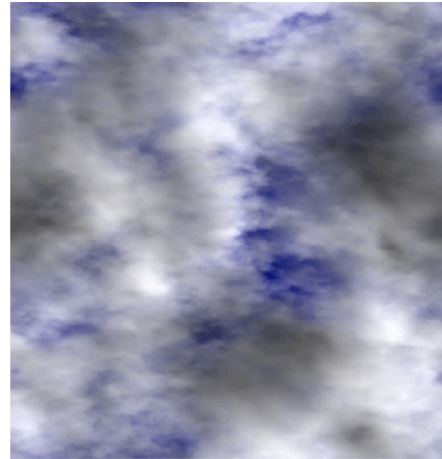
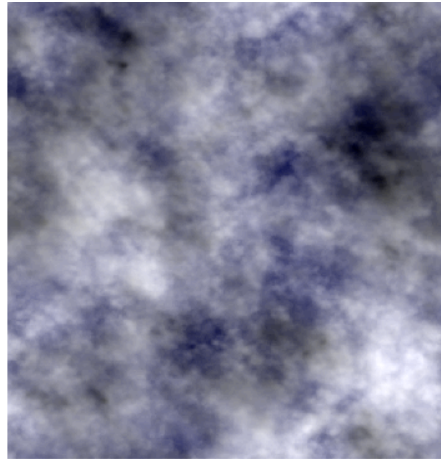


This shows the top layers of three dimensional cloud liquid water density simulations (false colours) all have  $d = 1$ ,  $c = 0.05$ ,  $e = 0.02$ ,  $f = 0$ ,  $H_z = 0.555$ ,  $\alpha = 1.8$ ,  $C_1 = 0.1$ ,  $H = 0.333$  and are simulated on a  $256 \times 256 \times 128$  point grid ( $a^2 > 0$ ; stratification dominant in the horizontal). The simulations in the top row have  $l_s = 8$  pixels, (left column), 64 pixels (right column),  $k=0$ ,  $k=32$  (bottom row). Note that in these simulations, the  $l_s = 8, 64$  applies to both vertical and horizontal cross-sections (i.e.  $l_s = l_{sz}$ ). Show an example with IR scattering?

Sides, same clouds (densities)



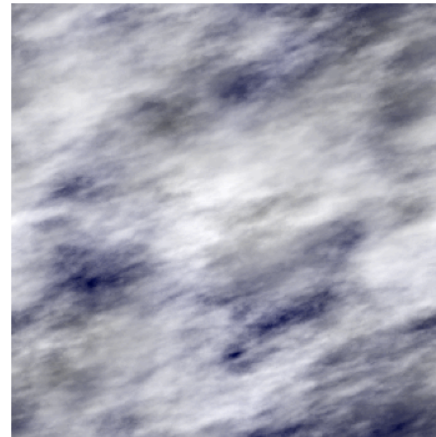
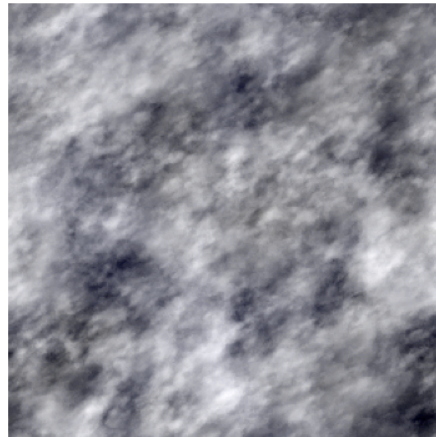
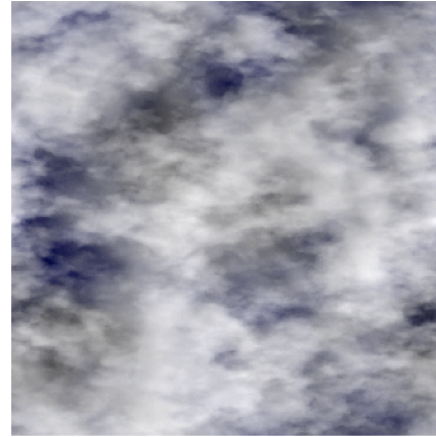
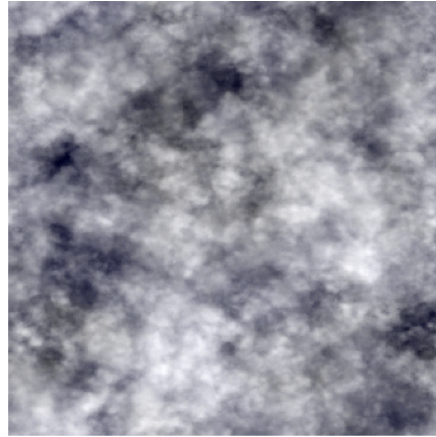
## Same clouds radiative transfer, top view



The top view with single scattering radiative transfer; incident solar radiation at  $45^\circ$  from the right, mean vertical optical thickness = 50



## Same clouds radiative transfer, bottom view



The same except viewed from the bottom.

# Multifractals with wave character

Localized in space, unlocalized in space-time (product of turbulent and wave-like scaling propagators).

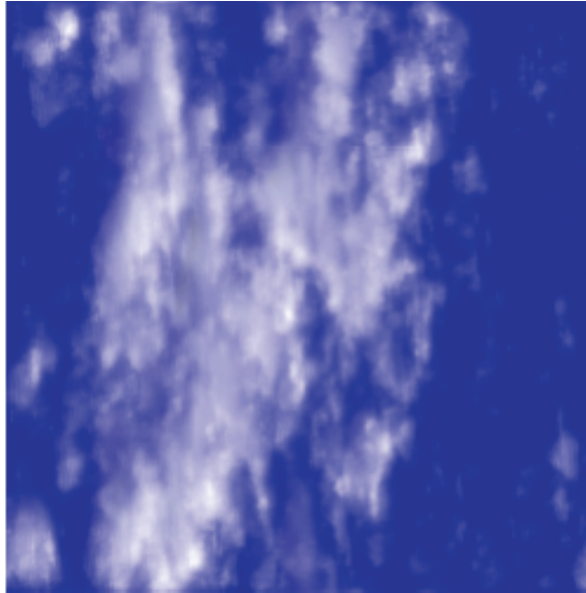
propagator



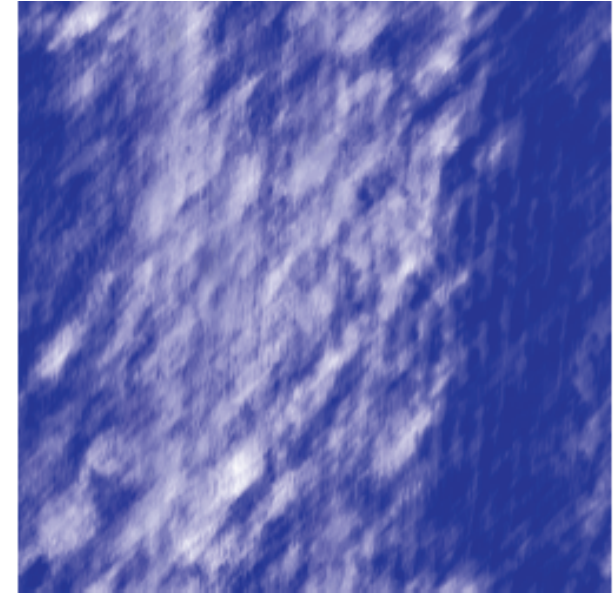
$$\tilde{I}(\underline{k}, \omega) = \tilde{g}(\underline{k}, \omega) \tilde{\epsilon}(\underline{k}, \omega)$$

$$\tilde{g}(\underline{k}, \omega) = (-i\omega + \|\underline{k}\|)^{-H_{tur}} \left( \omega^2 V^{-2} - \|\underline{k}\|^2 \right)^{-H_{wav}/2}$$

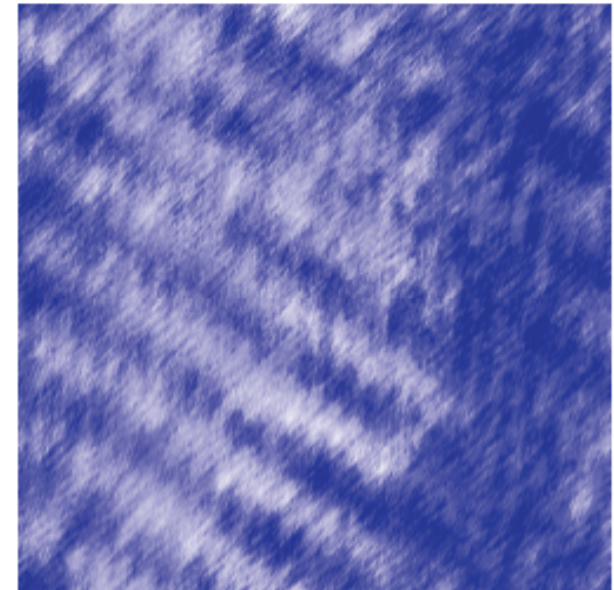
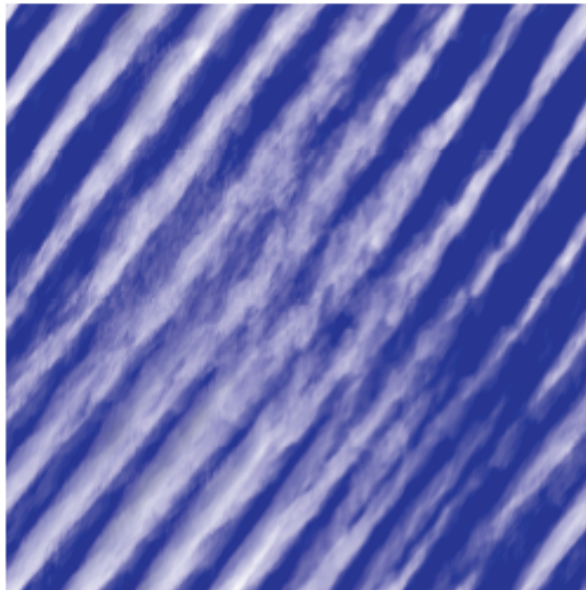
$$H_{wav} = 0$$



$$H_{wav} = 0.33$$



$$H_{wav} + H_{tur} = H = 1/3$$



$$H_{wav} = 0.52$$

$$H_{wav} = 0.38$$

Fly by of anisotropic (multifractal,  
cascade) cloud



# Rocks

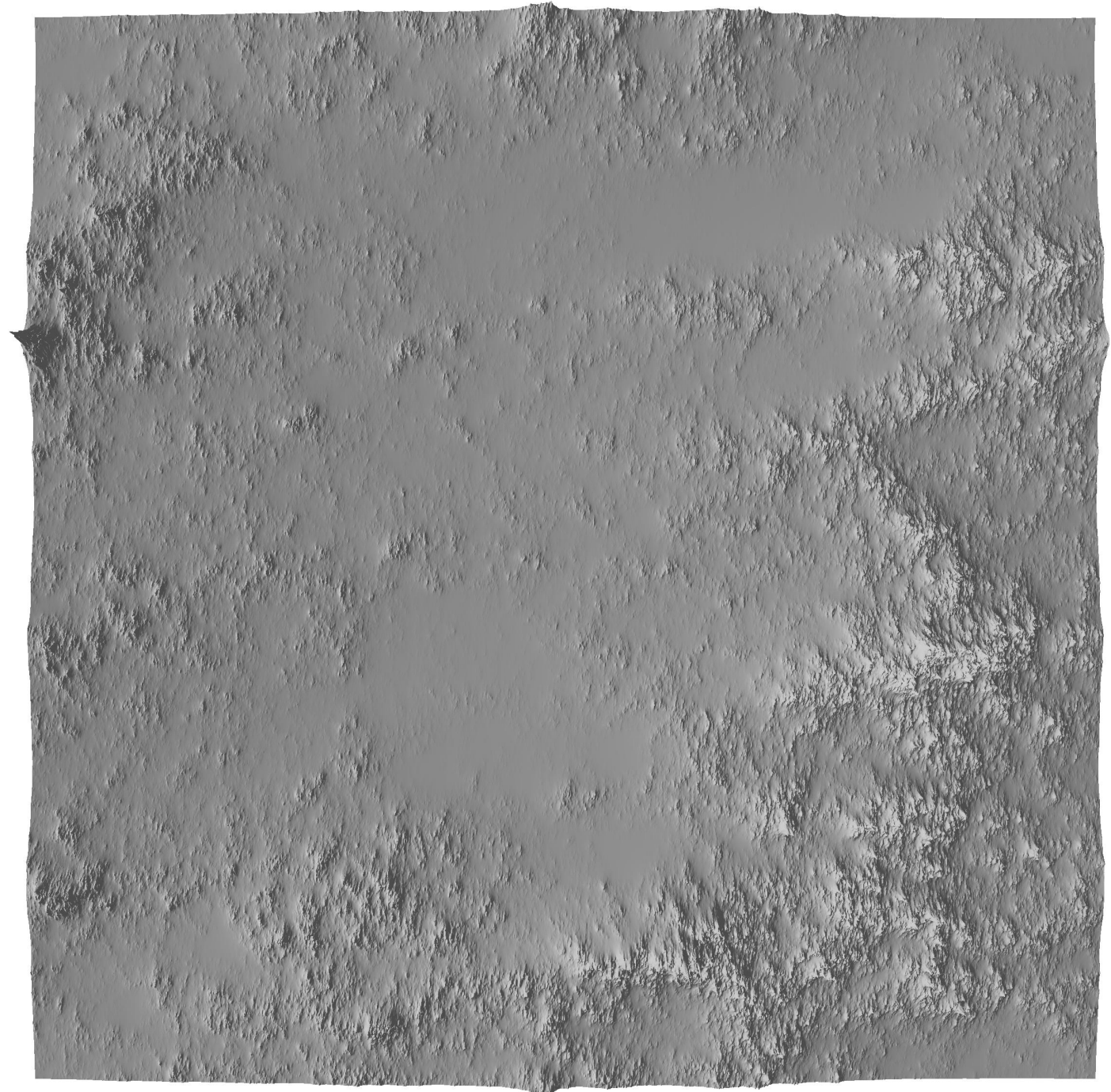
# Flyby 1

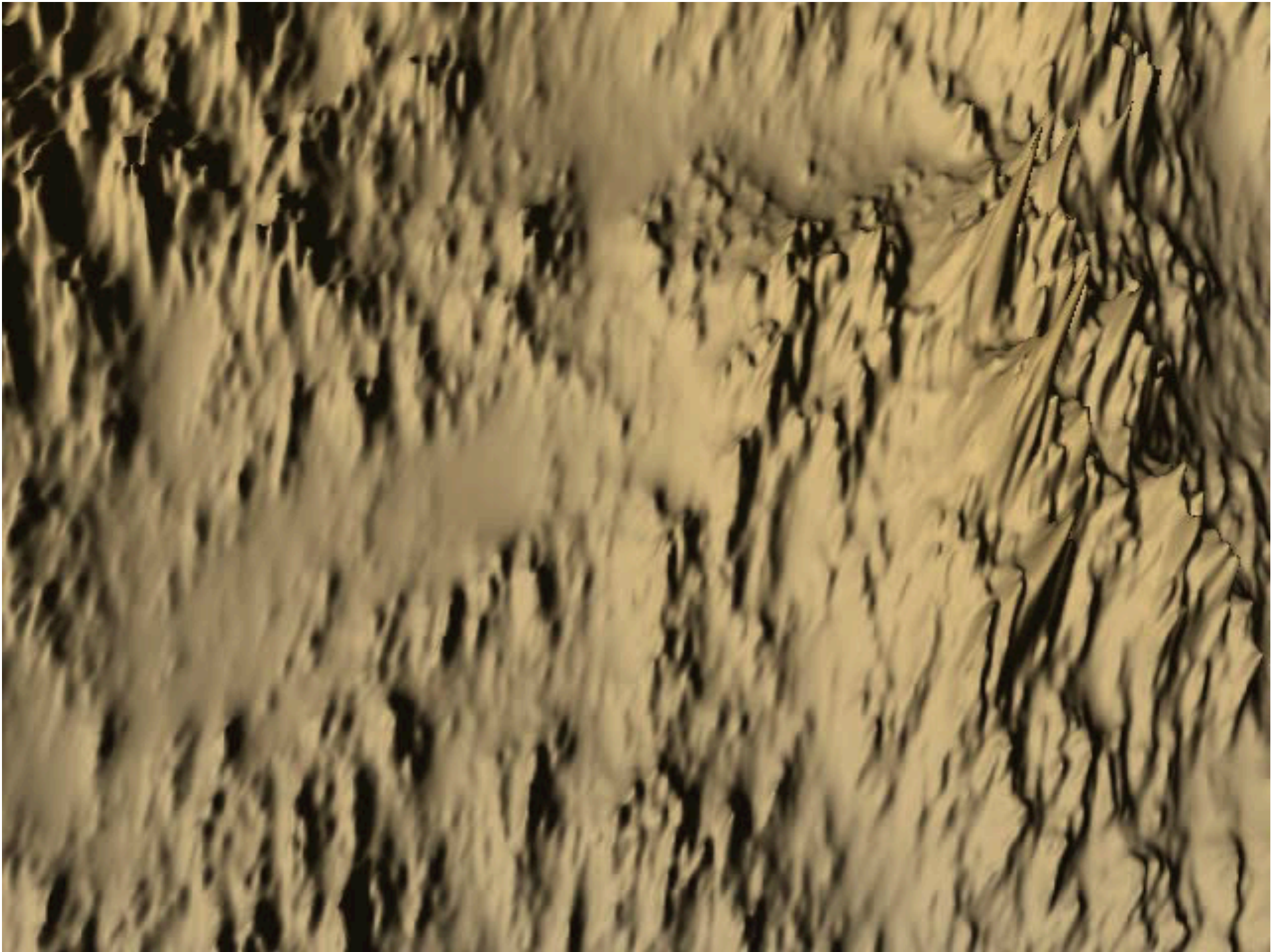
This  
4096X4096  
simulation is  
flown over

$\alpha=1.8$ ,  $C_1=0.12$ ,  $H=0.7$

$$G = \begin{pmatrix} 0.65 & -0.1 \\ 0.1 & 1.35 \end{pmatrix}$$

$l_s=64$  pixels





# Stratified Multifractal Crust, Mantle rock density simulation

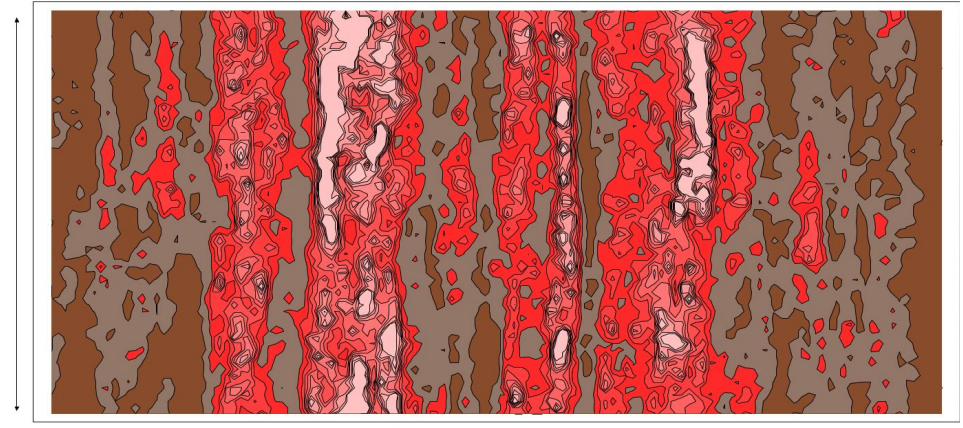
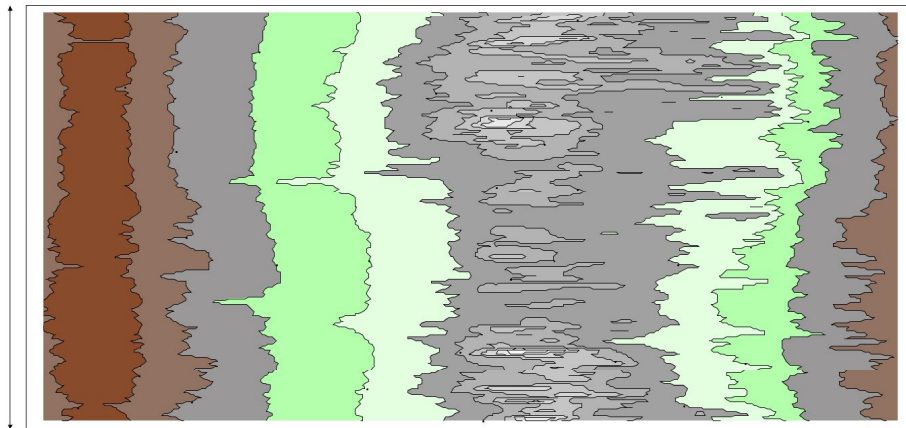
Vertical cross-sections  $D_{el}=3$

Lithospheric rock density

Mantle density

128km

3000km



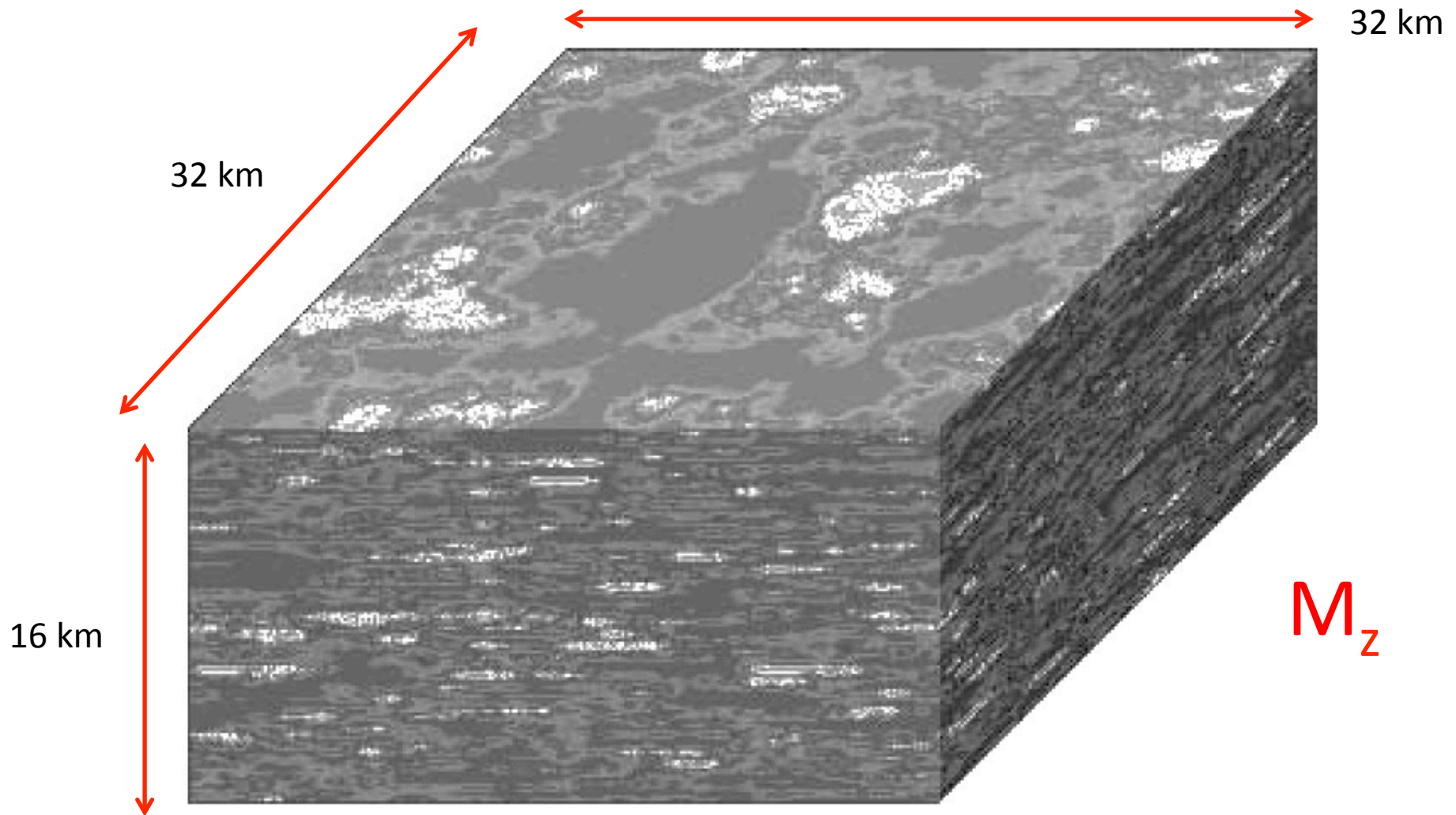
512km

6000km

Sphero-scale  $l_s=256\text{km}$ , with 1 pixel = 1km.

Sphero scale = 1 pixel. Each pixel is 50 km, sphero-scale = 25km. Hot (low density) plumes shown as white/red (this is a model for either density or temperature fluctuations (the two being proportional; we assume constant expansion coefficient). These are for fluctuations with respect to the mean vertical profile

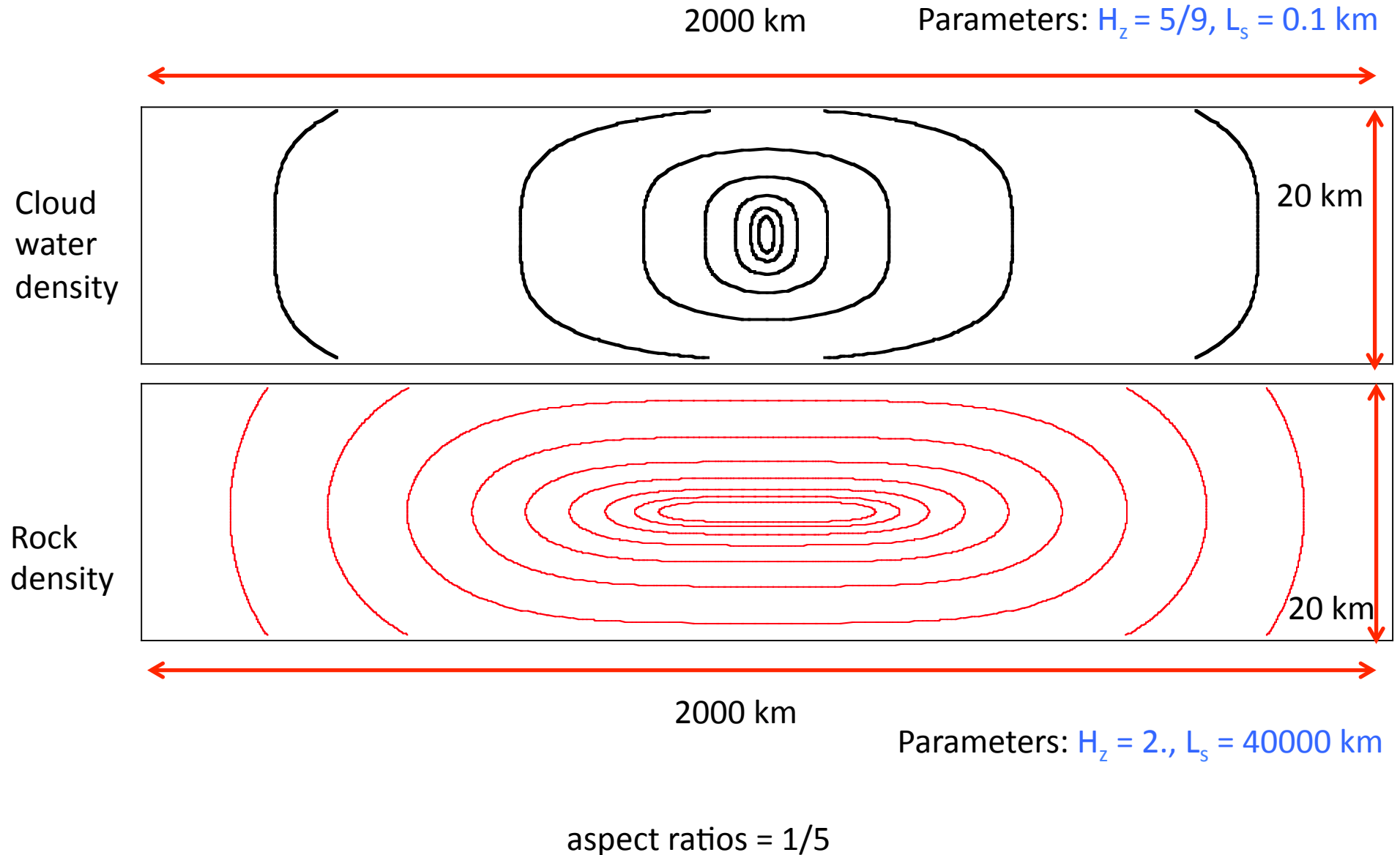
# Simulated magnetization field for horizontally isotropic crustal magnetization



Parameters: are  $H_z = 1.7$ ,  $s = 4$ ,  $H = 0.2$ ,  $\alpha = 1.98$ ,  $C_1 = 0.08$ ,  $l_s = 2500$  km,

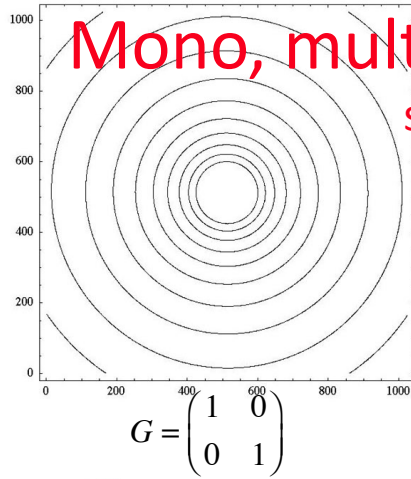


# The unity of geosciences: clouds and rocks

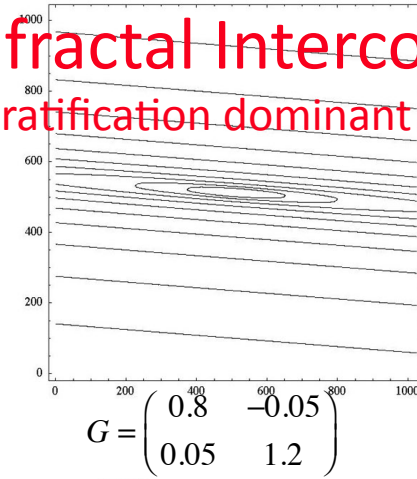


# Mono, multifractal Intercomparison, stratification dominant

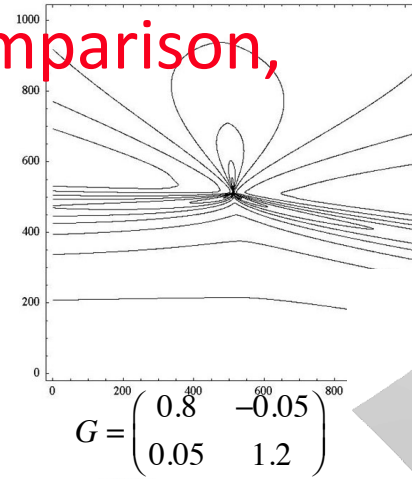
Contours of the  
scale functions



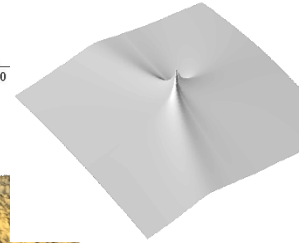
$$G = \begin{pmatrix} 1 & 0 \\ 0 & 1 \end{pmatrix}$$



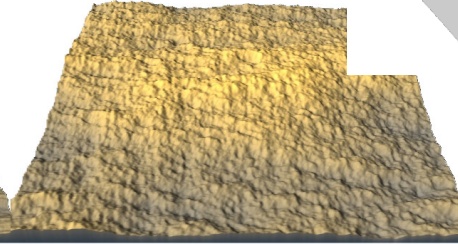
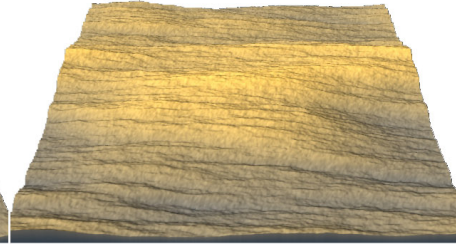
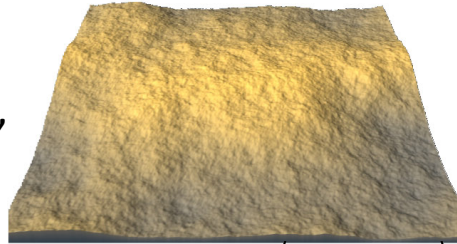
$$G = \begin{pmatrix} 0.8 & -0.05 \\ 0.05 & 1.2 \end{pmatrix}$$



$$G = \begin{pmatrix} 0.8 & -0.05 \\ 0.05 & 1.2 \end{pmatrix}$$



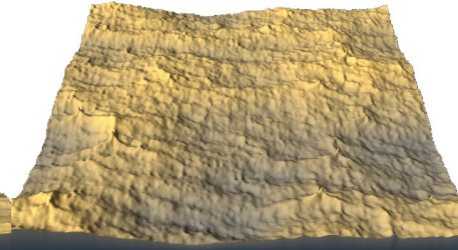
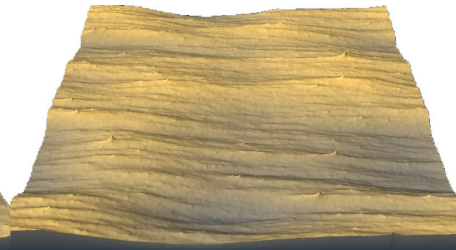
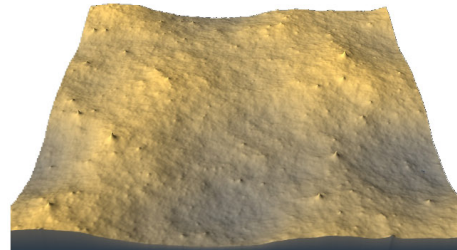
Fractional  
Brownian motion,  
 $H=0.7$



$$\langle \Delta h(\Delta r)^q \rangle \approx \Delta r^{qH-K(q)}$$

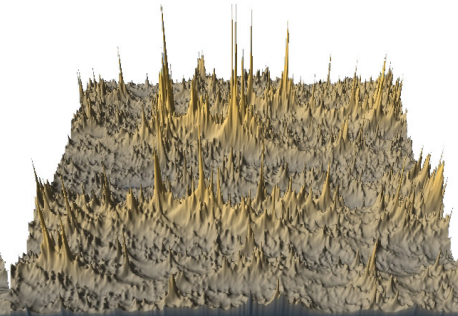
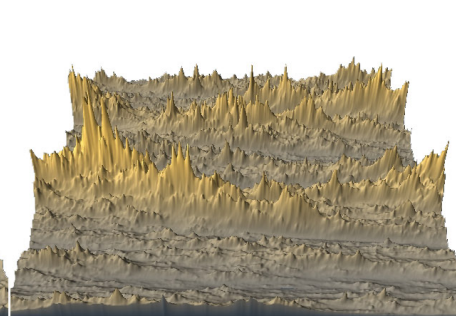
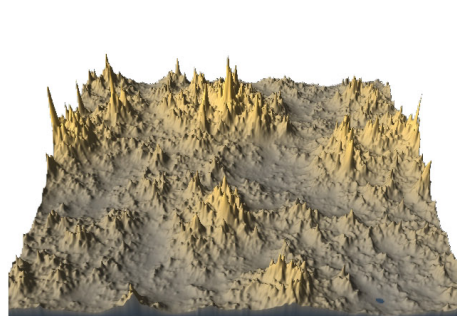
$$K(q) = 0$$

Fractional Levy  
motion,  
 $H=0.7, \alpha = 1.8$



Multifractal FIF  
 $H=0.7, \alpha = 1.8,$   
 $C_1=0.12$

$$K(q) = \frac{C_1}{\alpha-1} (q^\alpha - q)$$



isotropic

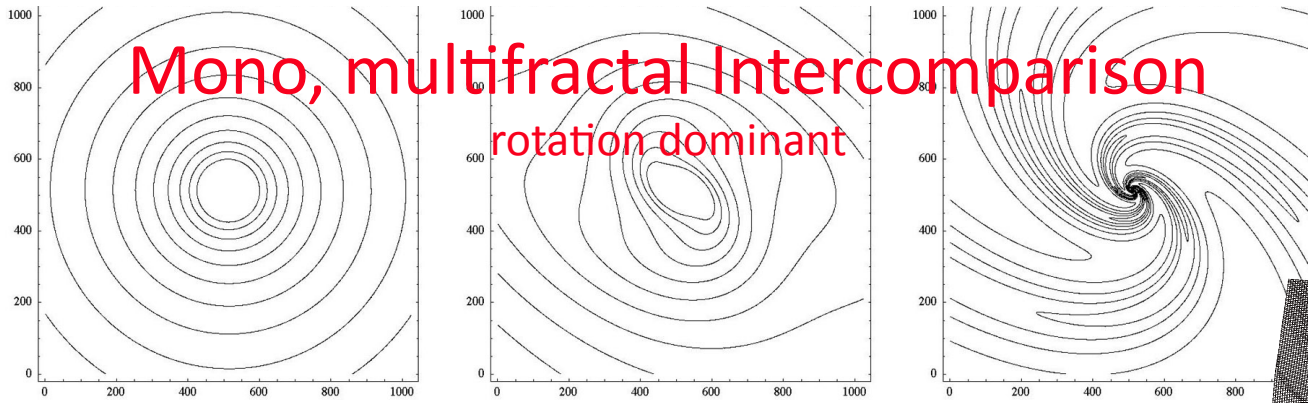
Anisotropic no trivial anisotropy

Anisotropic with trivial anisotropy

# Mono, multifractal Intercomparison

rotation dominant

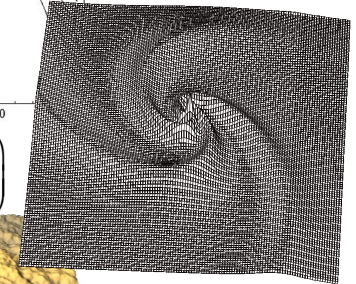
Contours of the scale functions



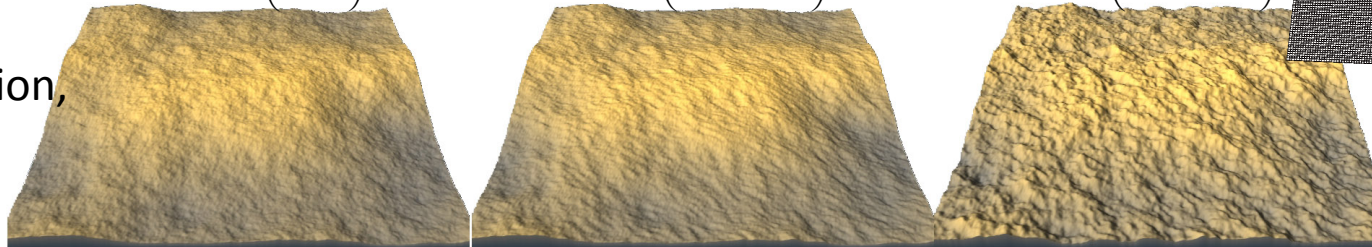
$$G = \begin{pmatrix} 1 & 0 \\ 0 & 1 \end{pmatrix}$$

$$G = \begin{pmatrix} 0.5 & -1.5 \\ 1.5 & 1.5 \end{pmatrix}$$

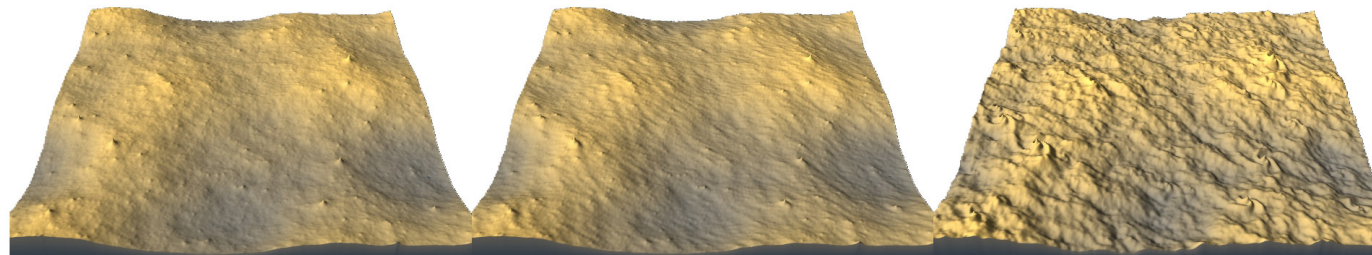
$$G = \begin{pmatrix} 0.5 & -1.5 \\ 1.5 & 1.5 \end{pmatrix}$$



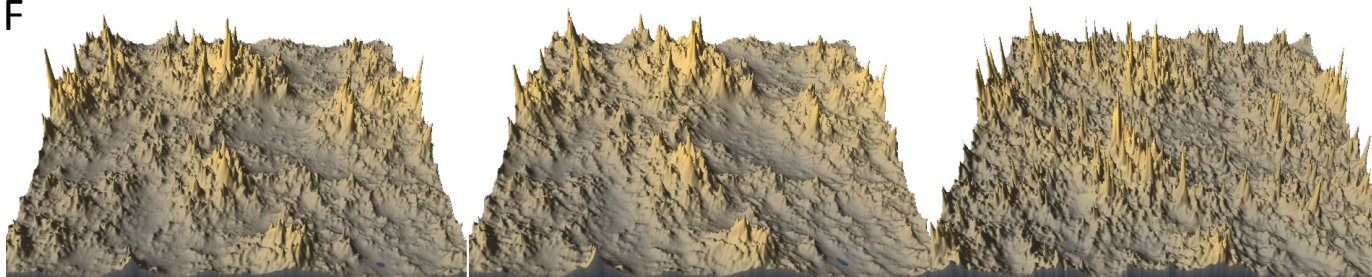
Fractional Brownian motion,  $H=0.7$



Fractional Levy motion,  $H=0.7$ ,  $\alpha=1.8$



Multifractal, FIF  $H=0.7$ ,  $\alpha=1.8$ ,  $C_1=0.12$



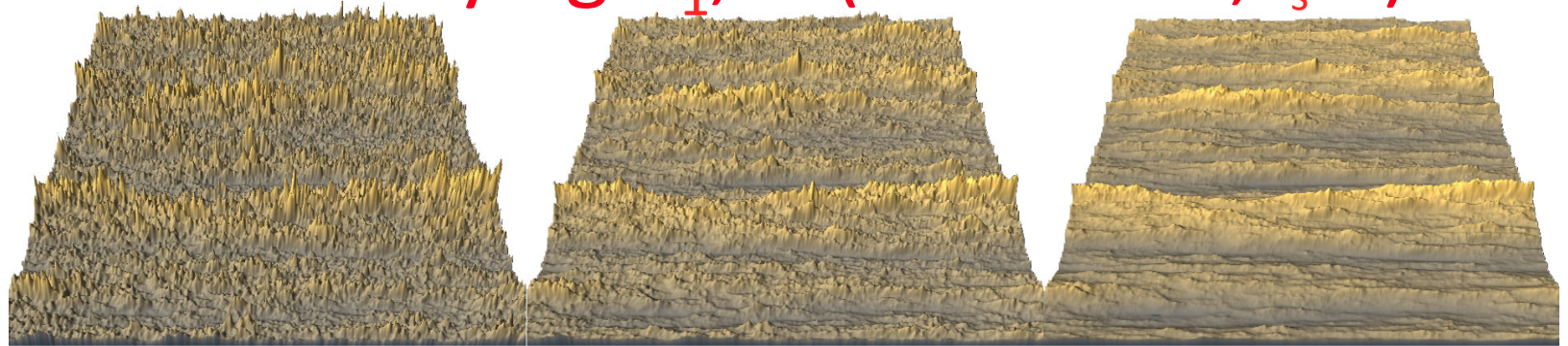
isotropic

Anisotropic no trivial anisotropy

Anisotropic with trivial anisotropy

# Effect of varying $C_1$ , $H$ (self-affine, $l_s=1$ )

$C_1=0.05$   
All:  
 $\alpha=1.8$



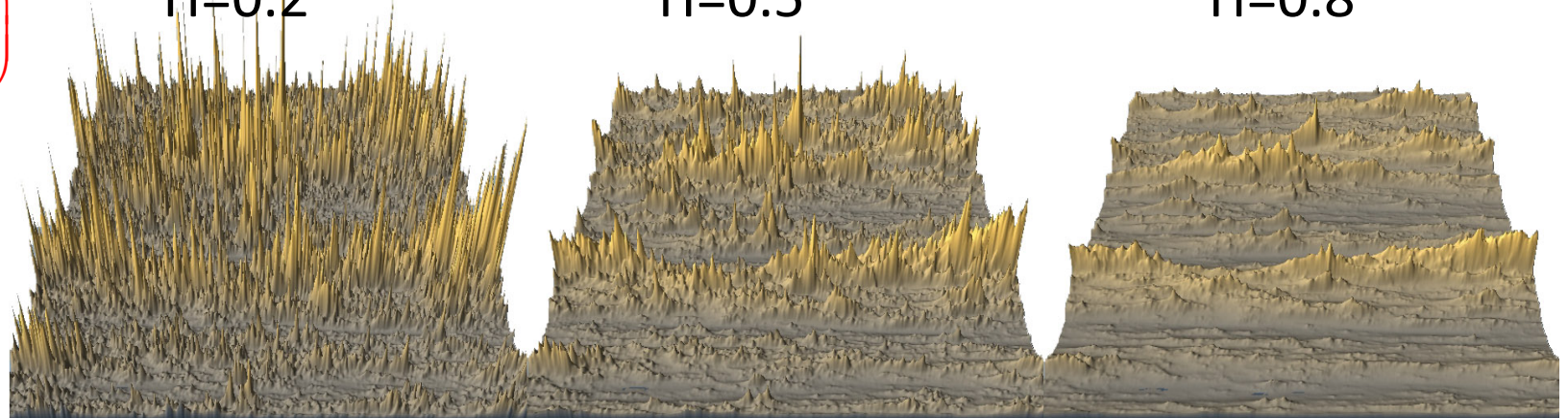
$G = \begin{pmatrix} 0.8 & 0 \\ 0 & 1.2 \end{pmatrix}$

$H=0.2$

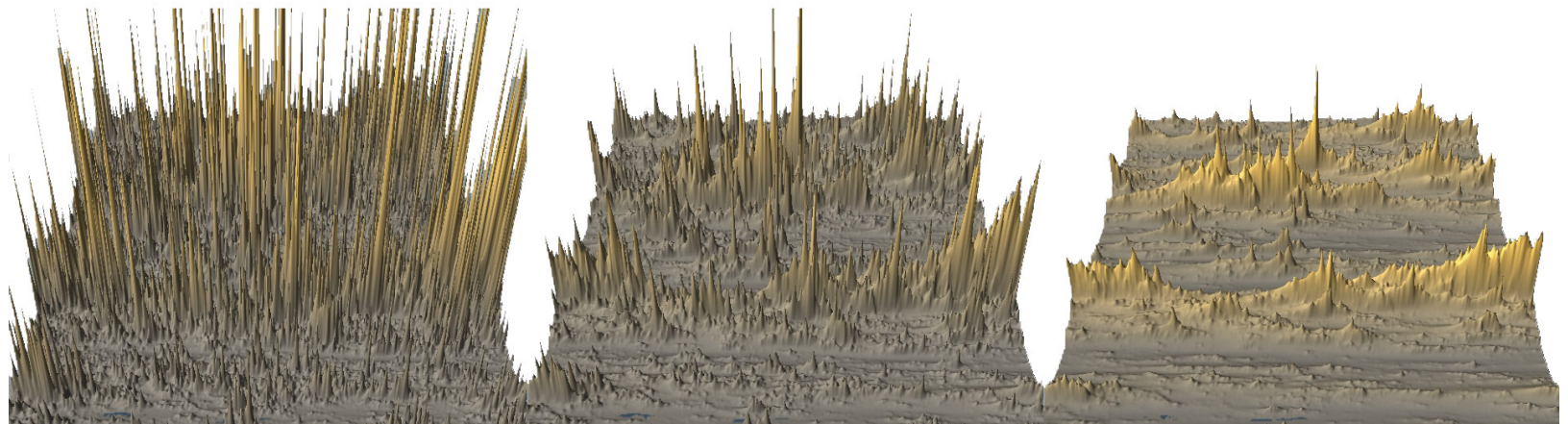
$H=0.5$

$H=0.8$

$C_1=0.15$



$C_1=0.25$

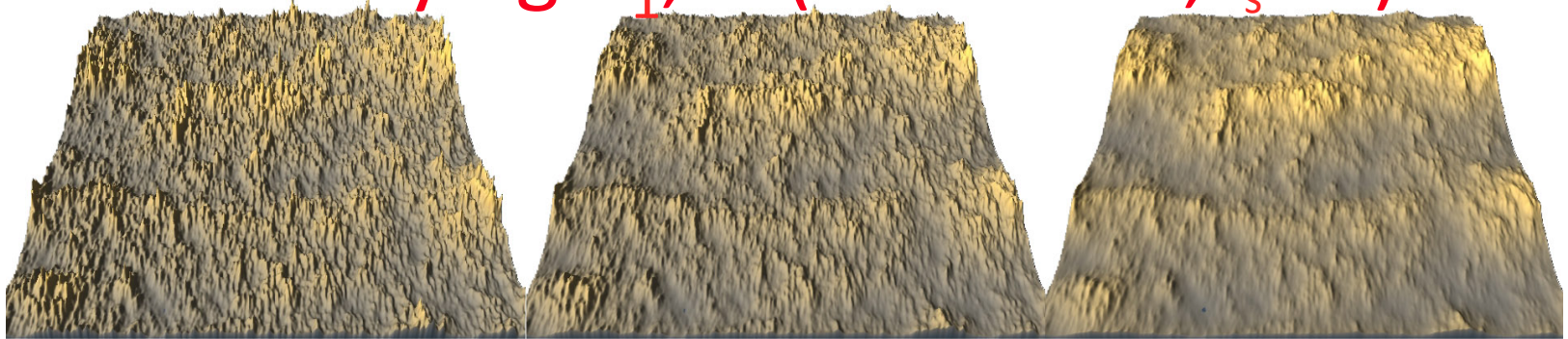


# Effect of varying $C_1$ , H (self-affine, $l_s=64$ )

$C_1=0.05$

All:

$\alpha=1.8$



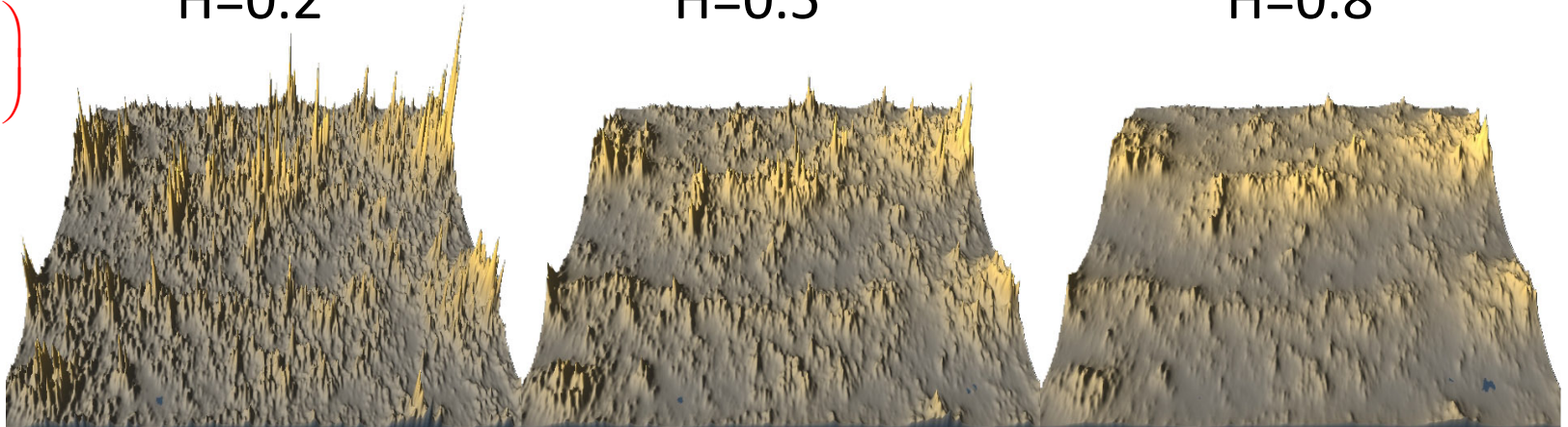
H=0.2

H=0.5

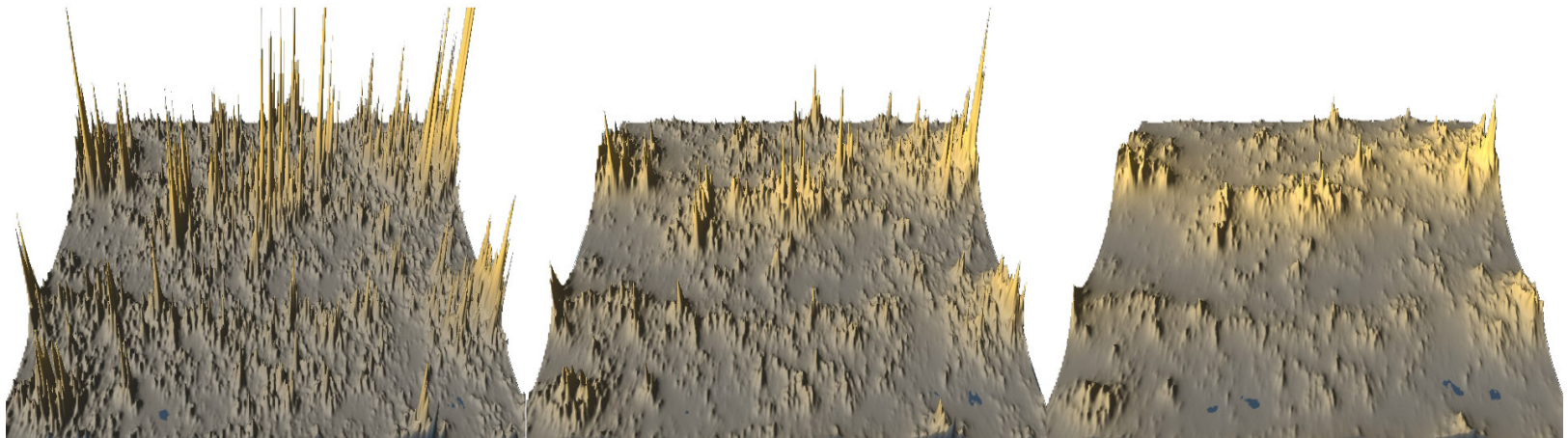
H=0.8

$$G = \begin{pmatrix} 0.8 & 0 \\ 0 & 1.2 \end{pmatrix}$$

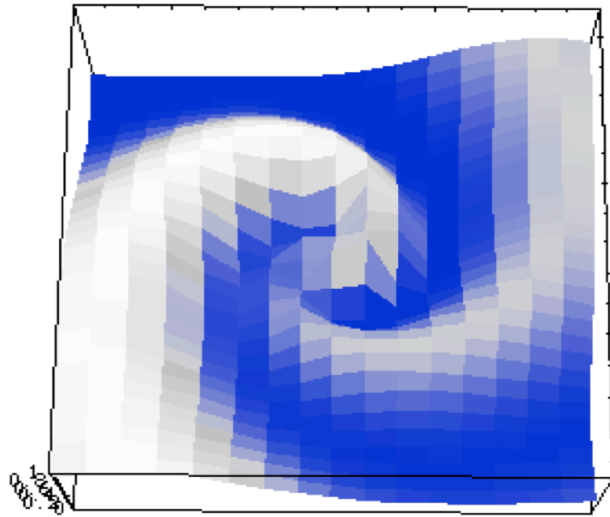
$C_1=0.15$



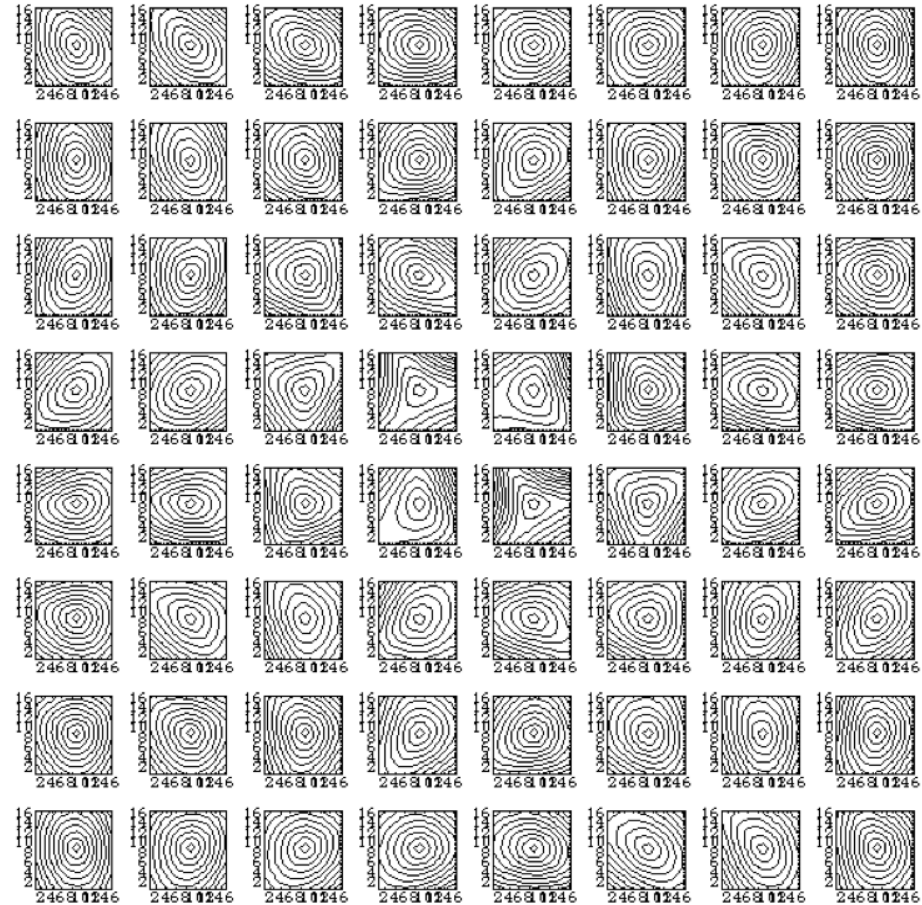
$C_1=0.25$



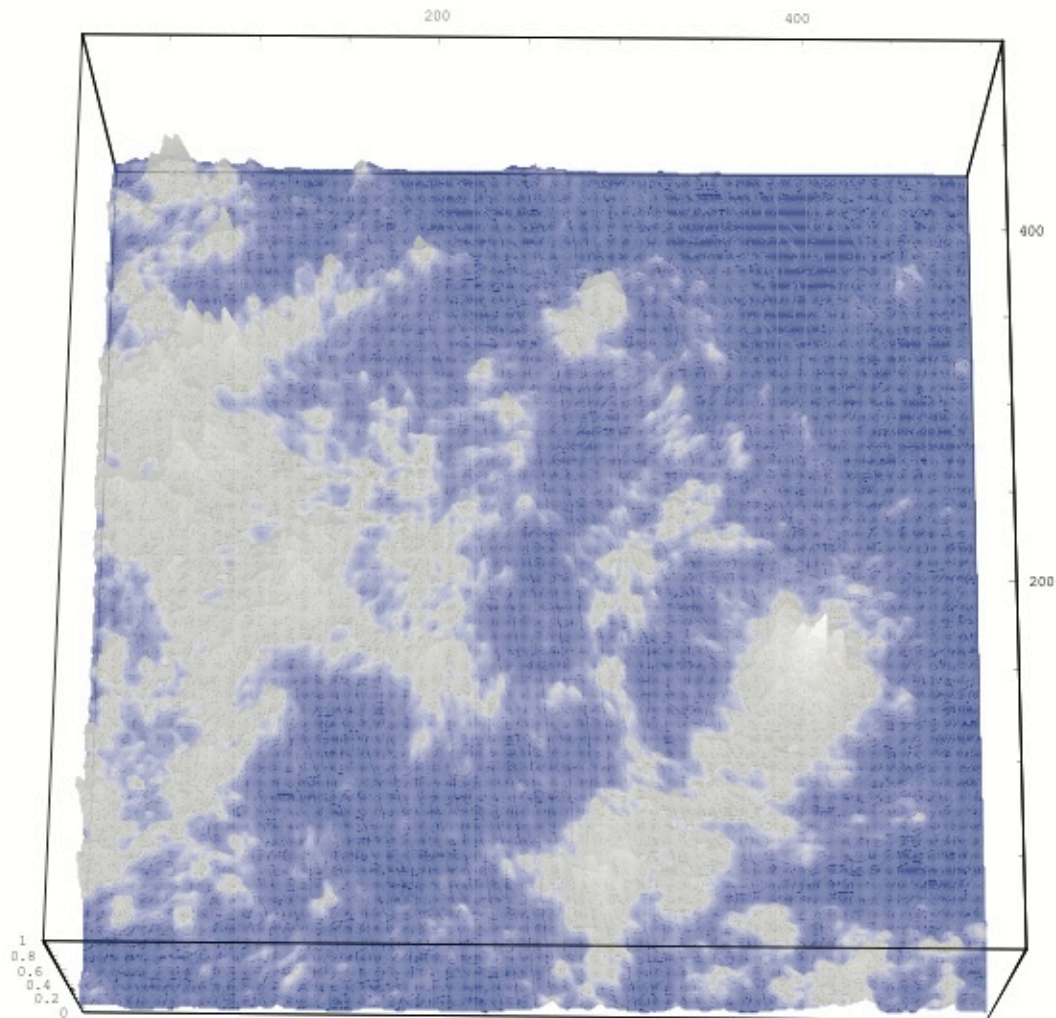
# Examples of Nonlinear GSI



The (spiral shaped) scale scalar  $h$  function used to obtain  $g$ . The false colours indicate the relative values (as does the height).

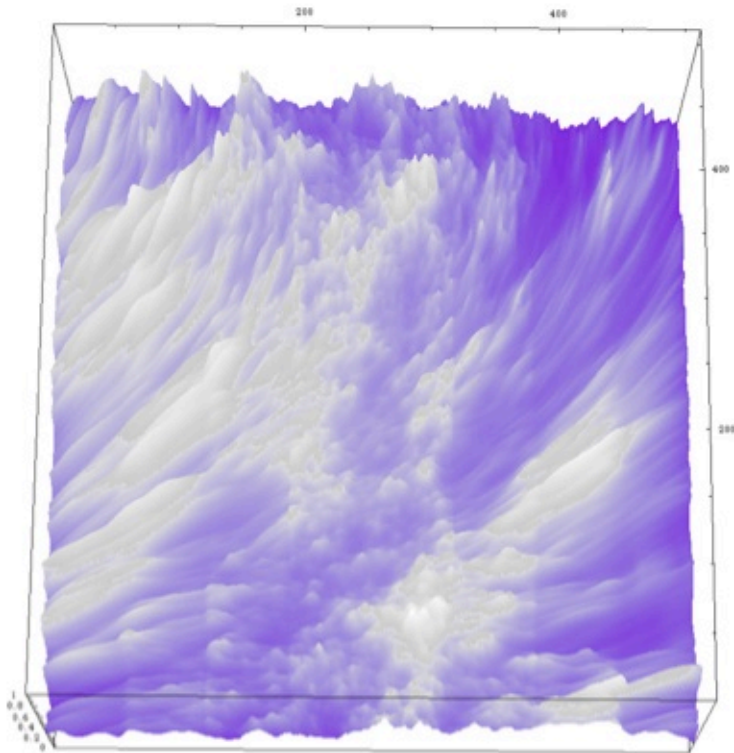


The set of local scale functions displayed according to their relative positions obtained from the spiral shaped scalar  $h$  function at left using a combination of linear GSI with a quadratic transformation of variables to obtain functions accurate to cubic order in scale.



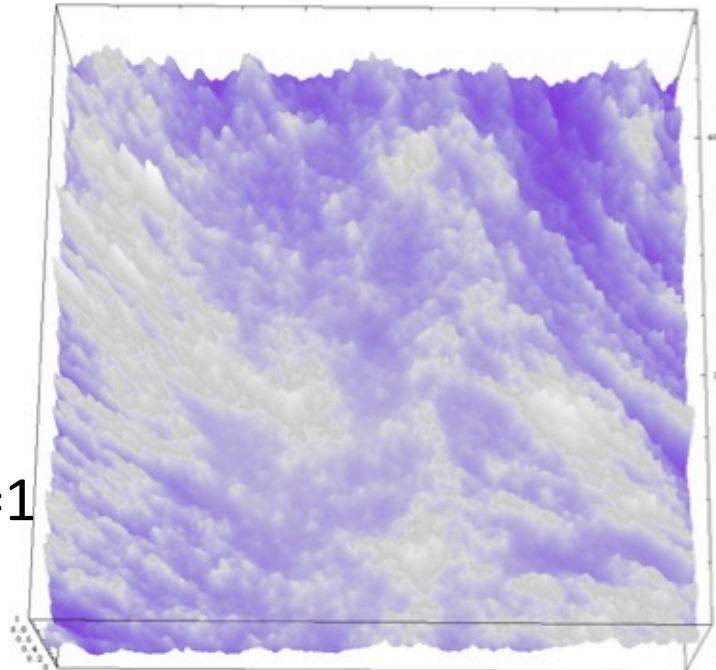
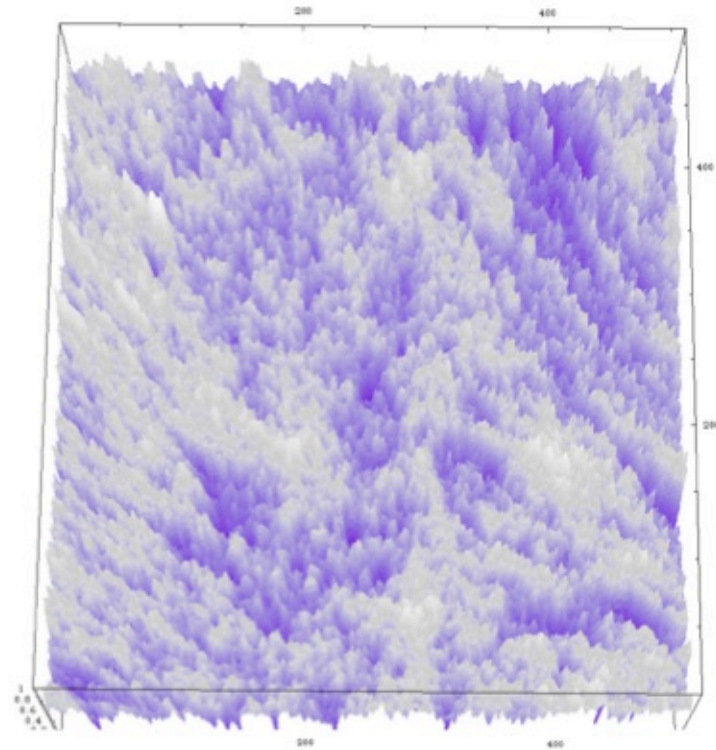
A nonlinear GSI multifractal simulation based on the spiral scale function indicated in the previous slide. The sphero-scale was held constant at 8 pixels,  $C_1 = 0.1$ ,  $a = 1.8$ ,  $H=0$ . It can be seen that the spiral modulates the texture (determined primarily by the linear  $G$  approximation).





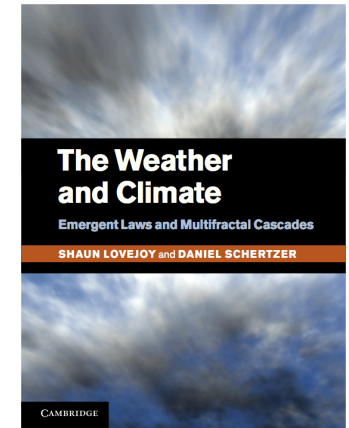
This shows a multifractal simulation of quadratic GSI (with  $\underline{g}$  given by the cubic  $h$ , eq. 107) with  $a=1.8$ ,  $C_1 = 0.1$ ,  $H = 0.33$  and sphero-scale = 256 pixels (the simulation is 512x512 pixels). The effect of the varying  $G$  is quite subtle.

Same  
Left but  
for  $l_s = 1$ ,  
 $H = 0$ .



Same but for  $l_s = 1$

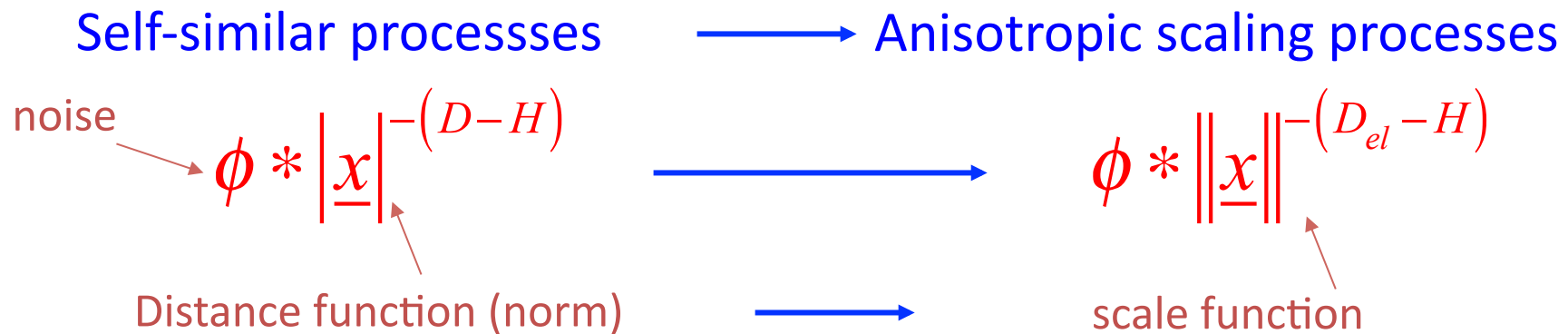
# Conclusions



1. Wide range scaling, multifractals in space, time and space time = unity of geophysics at the level of **processes**.
2. Cascades are the generic multifractal process.
3. Fractionally Integrated Flux (FIF) model for observables.
4. Universality classes make them manageable ( $H$ ,  $C_1$ ,  $\alpha$ ).
5. Wide ranges are possible due to anisotropic scaling: Generalized Scale Invariance:  
  
Linear GSI: scale dependent anisotropy  
Nonlinear GSI: scale and position dependent anisotropy
6. Phenomenological Fallacy.

# Anisotropic singularities, Generalized Scale Invariance

Schertzer and Lovejoy 1987

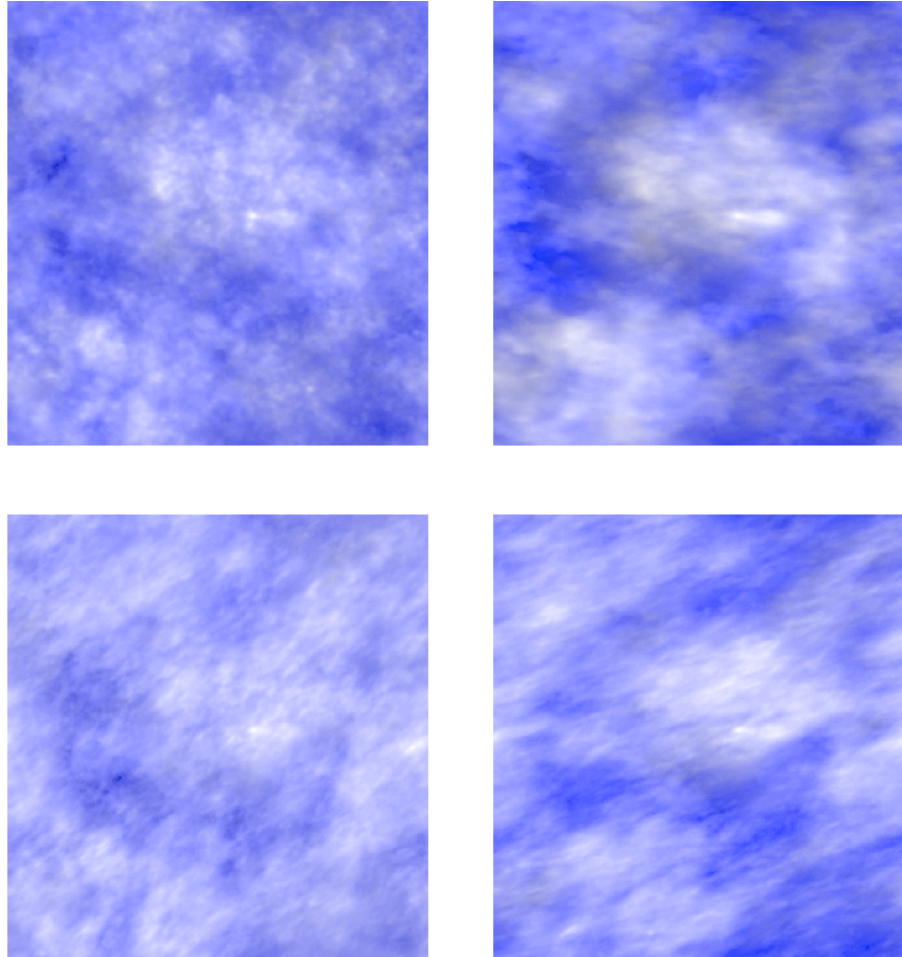


Scale function equation:

$$\|T_\lambda \underline{x}\| = \lambda^{-1} \|\underline{x}\|; \quad T_\lambda = \lambda^{-G}; \quad D_{el} = \text{Trace}G$$

Reduced scale vector  $\longleftarrow$   $\lambda^{-1}$   $\longleftarrow$  generator  $\longleftarrow$  Elliptical dimension

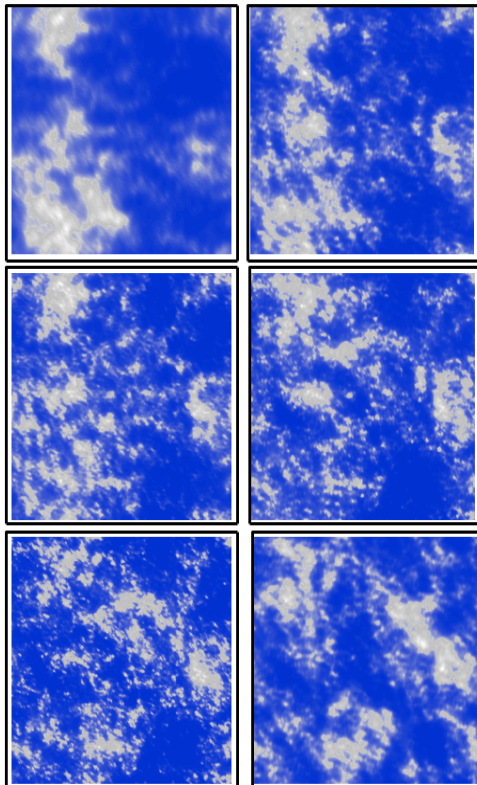
## Same clouds Infra red emission, top view



The same as the previous except for a false colour rendition of a thermal infra red field (assuming a constant extinction coefficient and a linear vertical temperature profile).

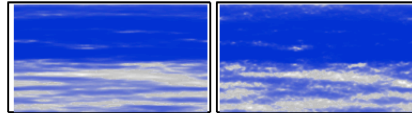
$I_{shor} = 1$

$I_{shor} = 8$

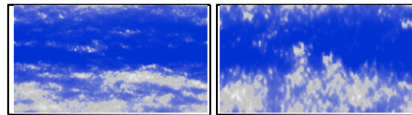


Top  
density

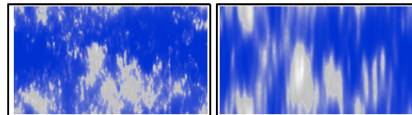
$I_{sver} = I_{shor} / 4$



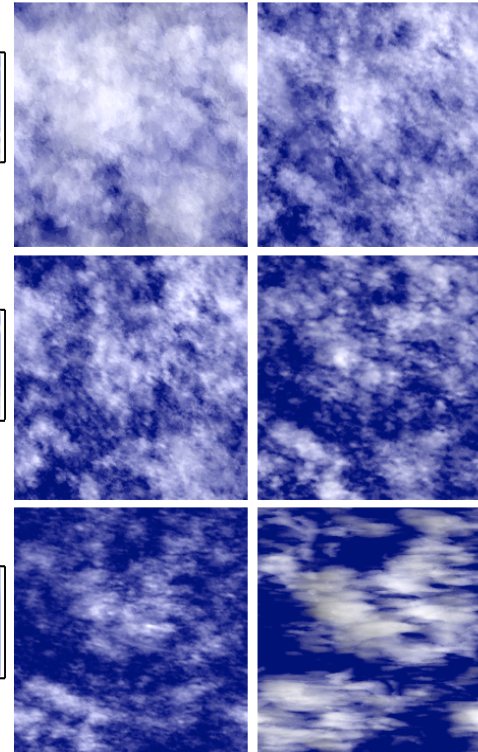
$I_{sver} = I_{shor}$



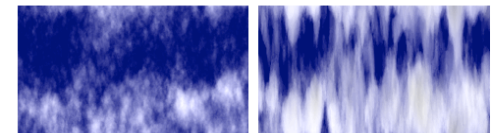
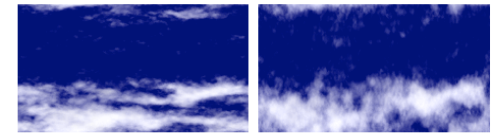
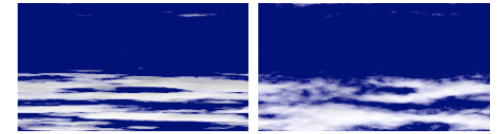
$I_{sver} = 4 I_{shor}$



Side  
density



Top  
Radiative  
transfer



Side  
Radiative  
transfer

$\alpha = 1.8, C_1 = 0.1, H = 0.333, d = 1, c = 0.5, e = 2, f = 0, H_z = 0.555$